Particle Detectors - Part II

Stephan Paul
TU-München
stephan.paul@ph.tum.de

Double course - Novosibirsk Physics School
17-21.9.2018

Particles polarise the medium

- for *v* larger than velocity of light in polarisable medium (ε): *Cherenkov radiation*

$$\varepsilon\beta^2 > 1 \quad \Leftrightarrow \quad \upsilon > \frac{c}{n}$$

$$n = \sqrt{\varepsilon}$$

energy loss: $$\frac{d^2N}{dEdx} = \frac{\alpha z^2}{\hbar c}\sin^2\theta_c$$

$\upsilon << \frac{c}{n}$

symmetric polarisation

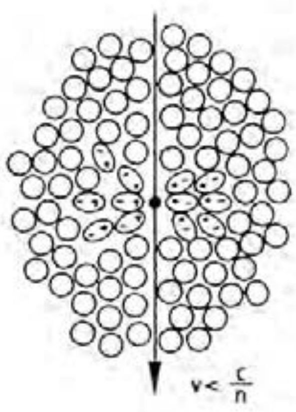

destructive interference (β << 1)

$\upsilon > \frac{c}{n}$

asymmetric polarisation → emission

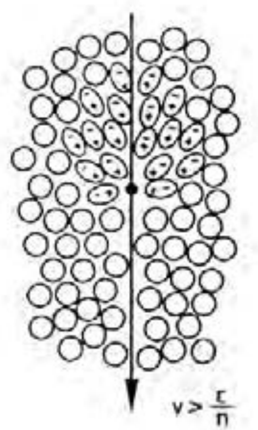

constructive interference β ~1

$$\cos\theta = \frac{1}{\beta n}$$

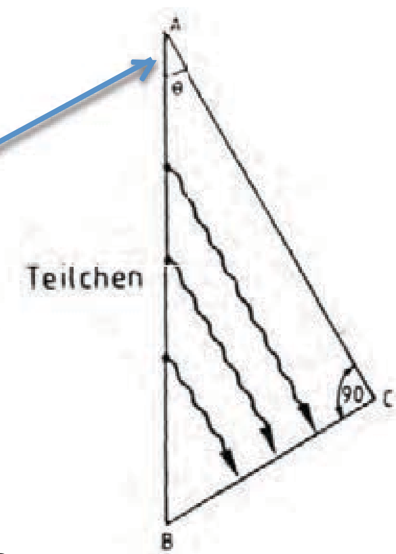

measurement of θ → β

measurement of (p, β) → m → particle ID

3.1 Cherenkov Detectors

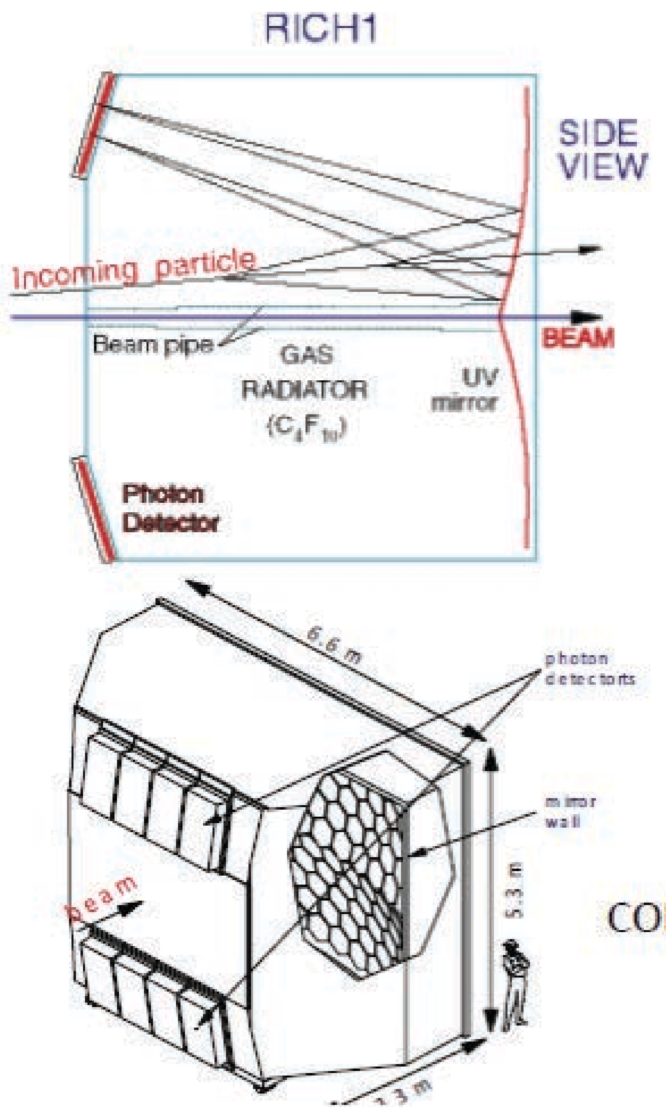

COMPASS@CERN RICH

how to use ?
- threshold (old)
- imaging (modern)

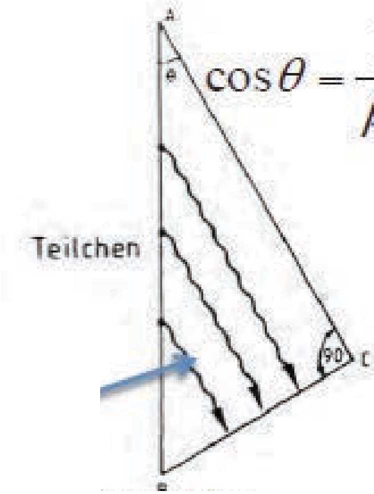

$$\cos\theta = \frac{1}{\beta n}$$

- parallel emission of light under fixed angle along trajectory
- rotational symmetry around trajectory
- imaging with spherical mirror results into ring
- Cherenkov radius $r = f\,\theta$

3.1 Cherenkov Detectors

Light detection:

- Photomultipliers (often UV sensitive - depends on ra
  - e.g. HPD
  - large diameter PM (Kamiokande)
- Gaseous detectors
  - MWPC
  - ThickGEM
  - entrance window (GEM surface) coated with CsI

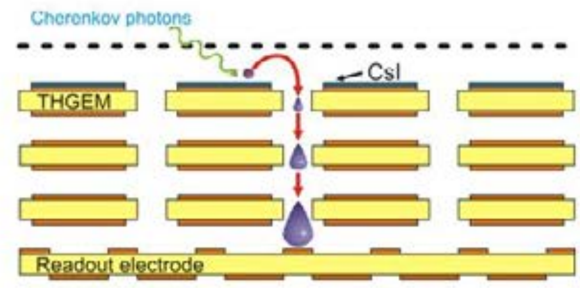

TGEMs/RETGEMs

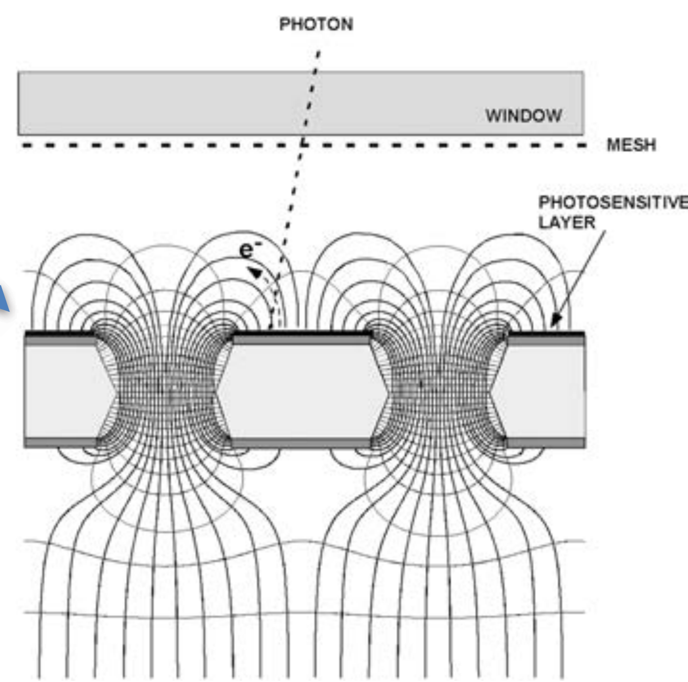

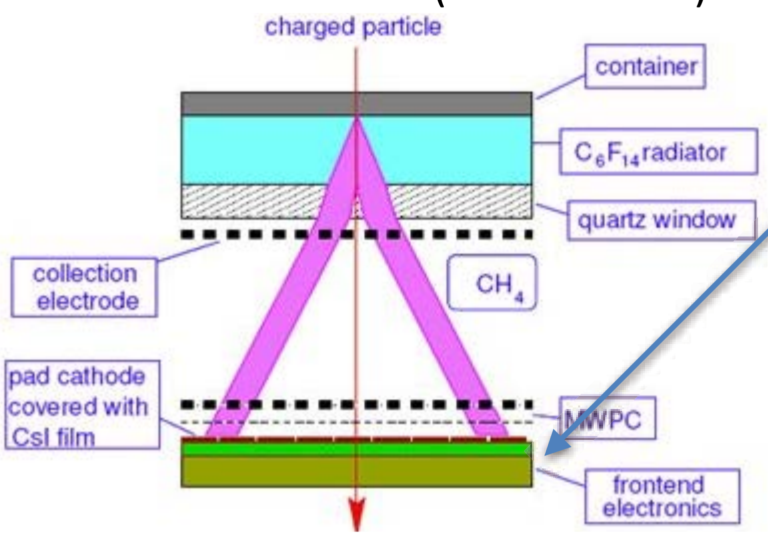

3.1 Cherenkov Detectors

threshold

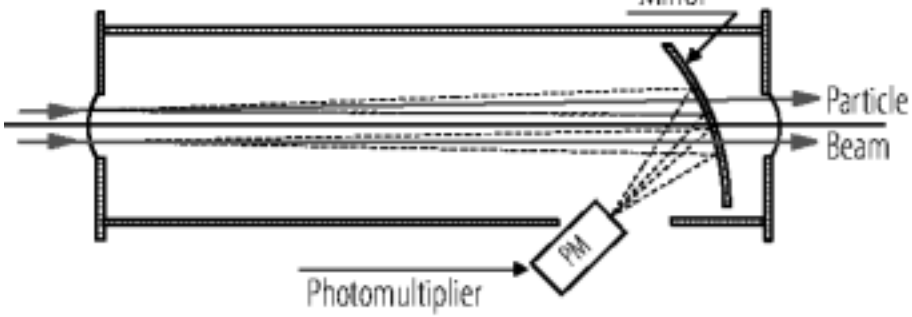

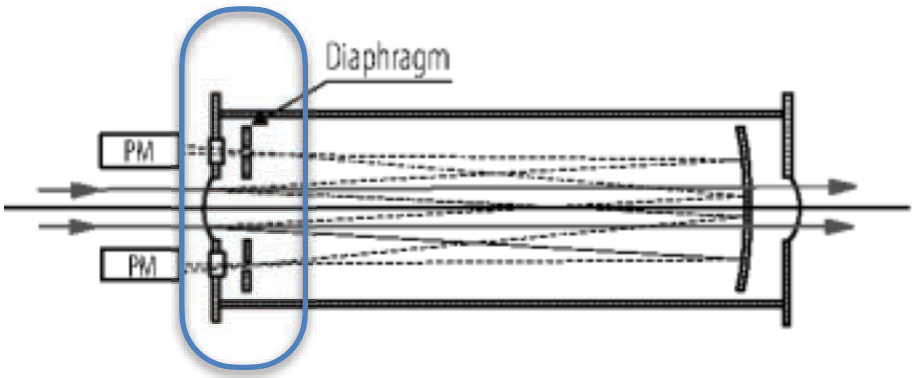

imaging

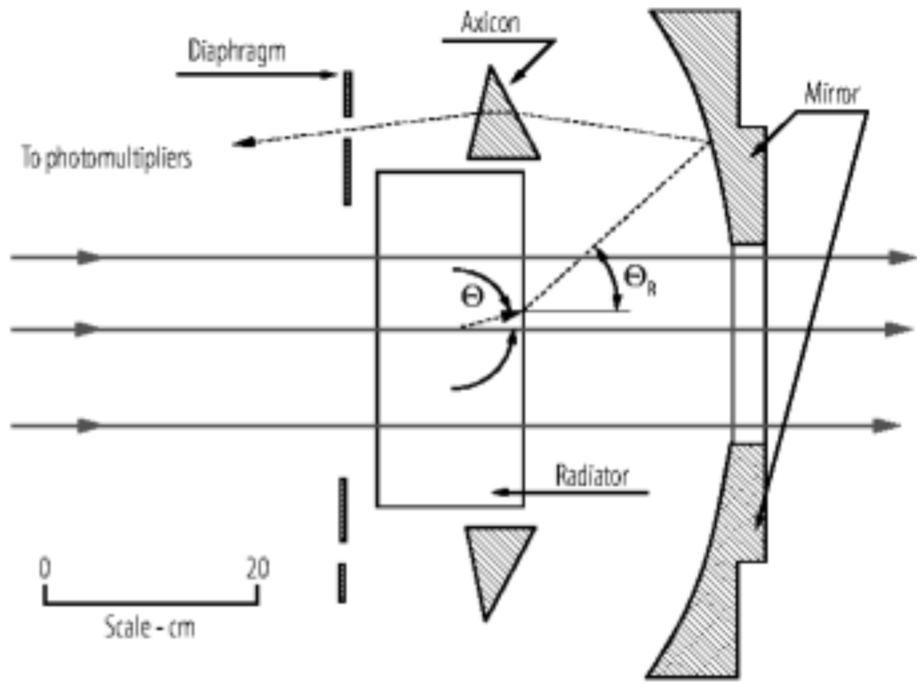

Beam Cherenkov detector: Triggerable Cherenkov counters

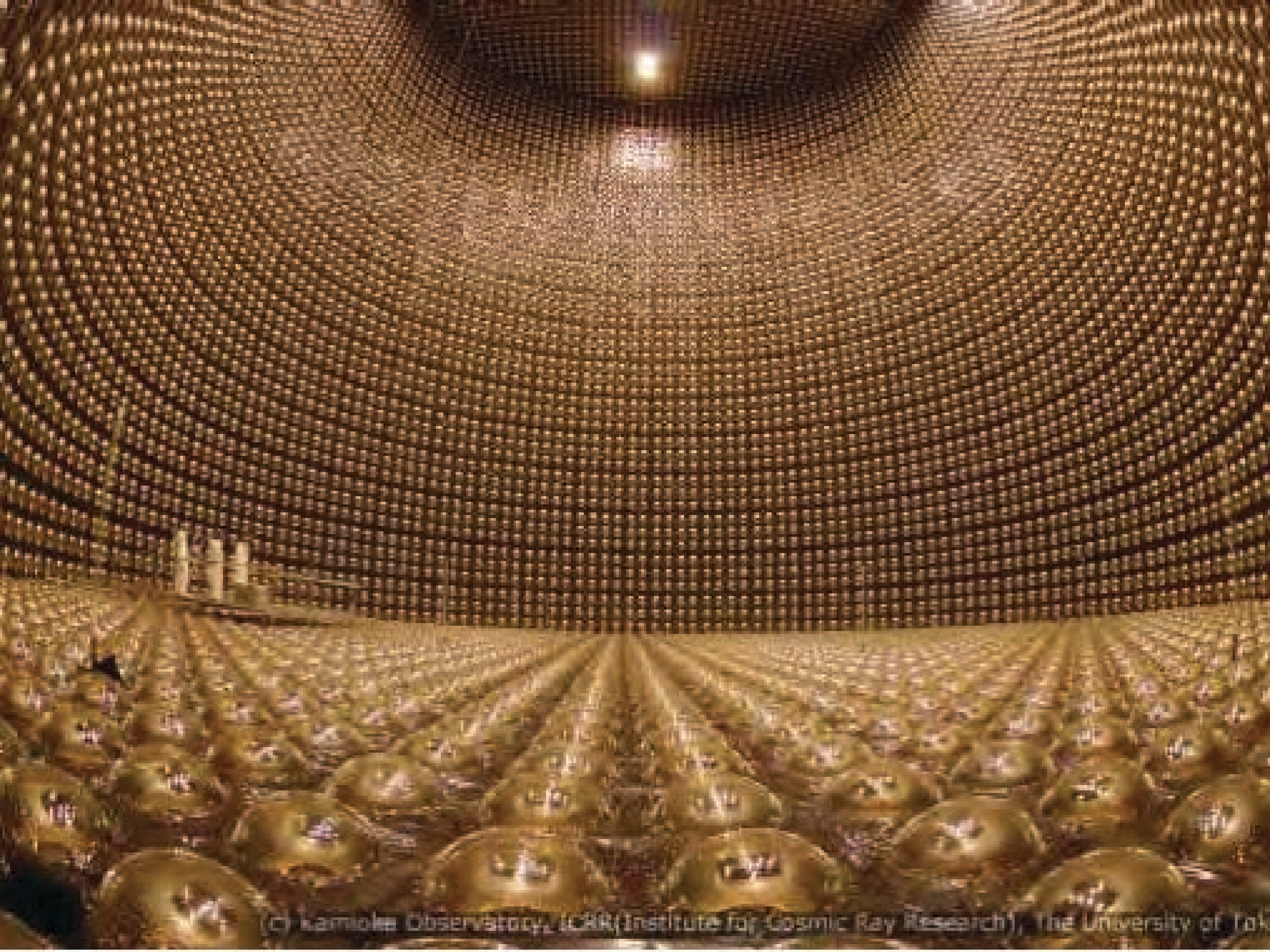
(c) Kamioka Observatory, ICRR(Institute for Cosmic Ray Research), The University of Tok

3.1 Superkamiokande - Japan

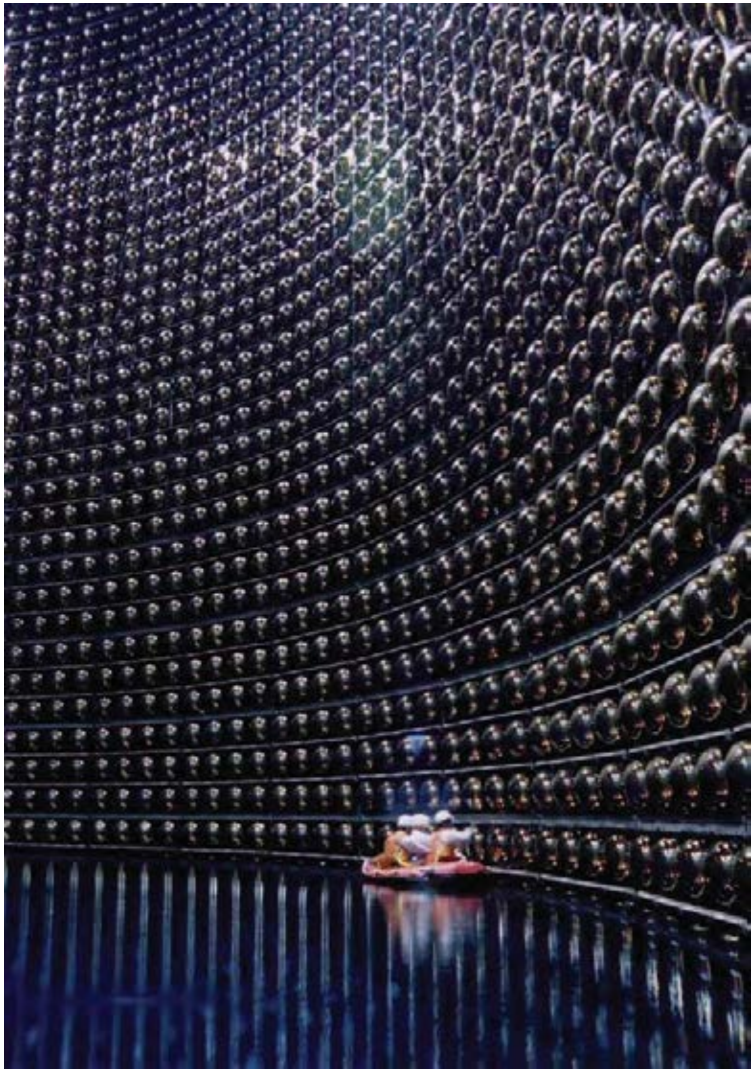

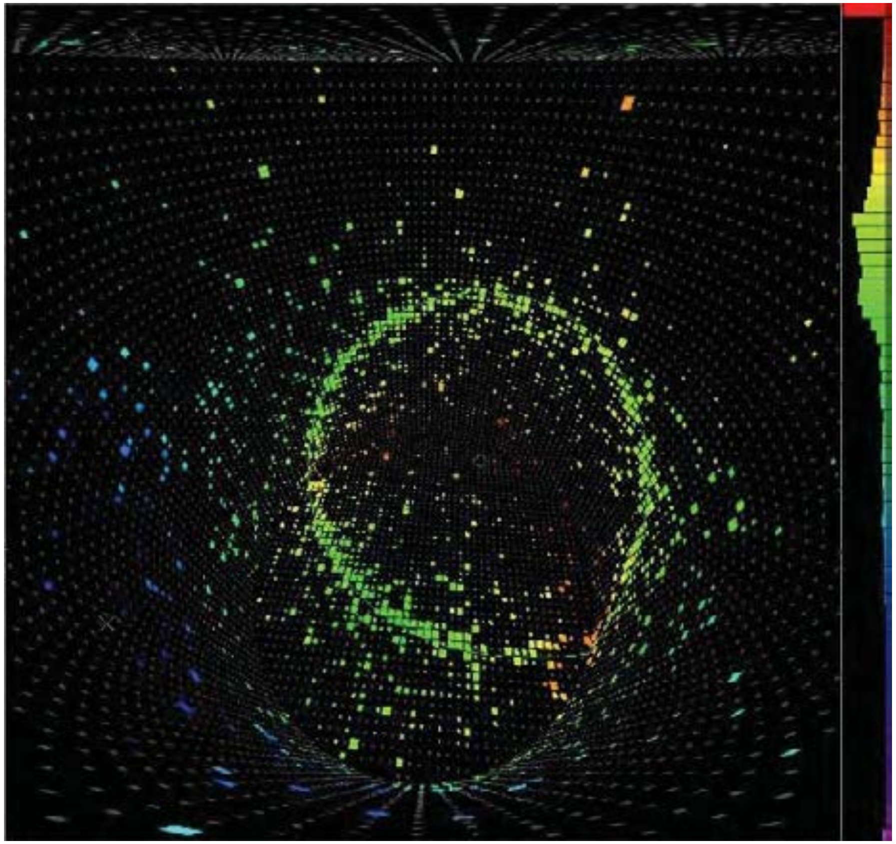

50,000 tons pure water
11,200 photo sensors (45cm diameter each)
41.4m height, 39,4 m diameter
goal: secondary particles from neutrino reactions

Transition radiation:

Generated when a charged particle passes any interface of two dielectrics with different refractive index n_i

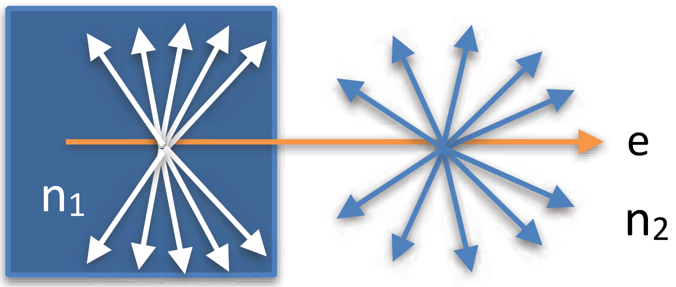

at interface: readjustment of E-field
→ time variation of E-field → radiation

frequency spectrum of radiation depends on $\frac{E}{m} = \gamma$

emission angle α w.r.t particle trajectory: $\alpha \propto \frac{1}{\gamma}$

intensity small $\propto \frac{1}{137}$

many interfaces needed: $n_{Int} >> 100$

intensity depends on plasma frequency

materials: $n_2 = 1$ (air), n_1 = carbon fibres, polyethylene fibres, lithium foils

3.2 Transition Radiation

- Energy spectrum $N(\omega)$ hardens with γ
- soft photons reabsorbed by „radiator“
- effectively: only X-ray part of spectrum emerges from stack of transitions
- Photon flux of X-ray transition radiation for small angles θ_0 and $\beta \sim 1$ ($n_2 = 1$):

$$\frac{d^2 N_\gamma}{d\omega\, d\Omega} = \frac{\alpha}{\pi^2 \omega}\theta_0^2 \cdot 4\sin^2\left[\frac{\omega L}{4c}\left(\frac{\omega_p^2}{\omega} + \theta_0^2 + \frac{1}{\gamma^2}\right)\right] \cdot \left[\frac{1}{1/\gamma^2 + \omega_p^2/\omega^2 + \theta_0^2} - \frac{1}{1/\gamma^2 + \theta_0^2}\right]^2$$

$$\omega_p = \left(\frac{nZe^2}{\varepsilon_0 m}\right)^{1/2}$$

⇨ Maximum at $\theta_0 \sim 1/\gamma$

Neglect interference term, integrate over dΩ:

$$\frac{dN_\gamma}{d\omega} \approx \frac{2\alpha}{\pi\omega}\ln\left(\frac{\gamma\omega_p}{\omega}\right) \quad \text{for} \quad \omega \ll \gamma\omega_p$$

⇨ Total energy flux $\frac{\alpha}{3}\gamma \hbar\omega_p$

[W.W.M.Allison, P.R.S. Wright, in: Experimental Techniques in High-Energy Nuclear and Particle Physics, T. Ferbel ed., 1999]

3.2 Transition Radiation

single interface

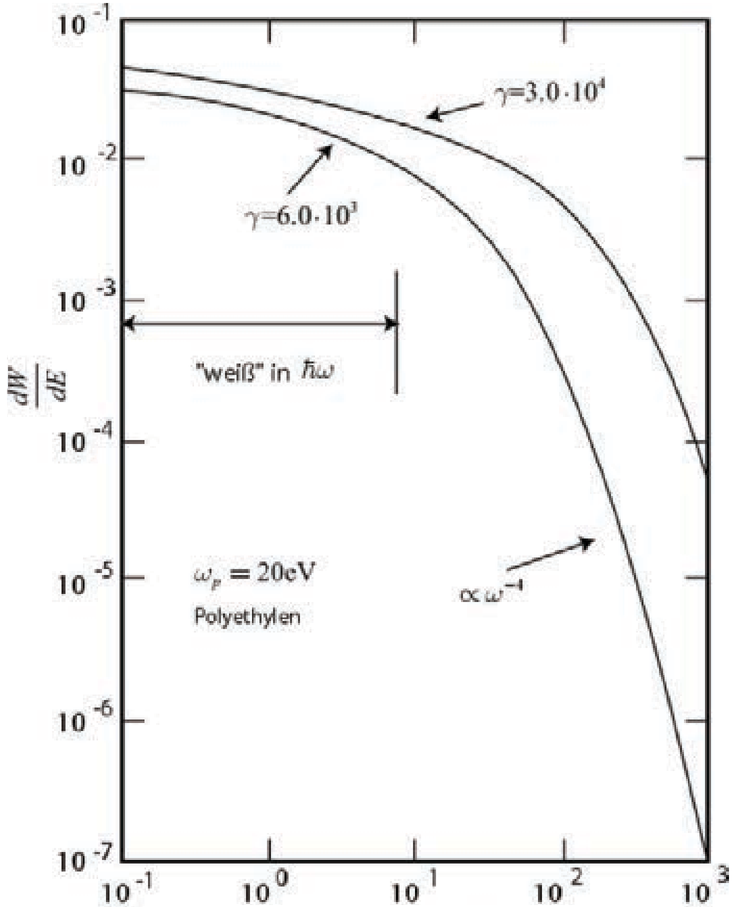

photon energy [KeV]

spectral intensity distribution per foil

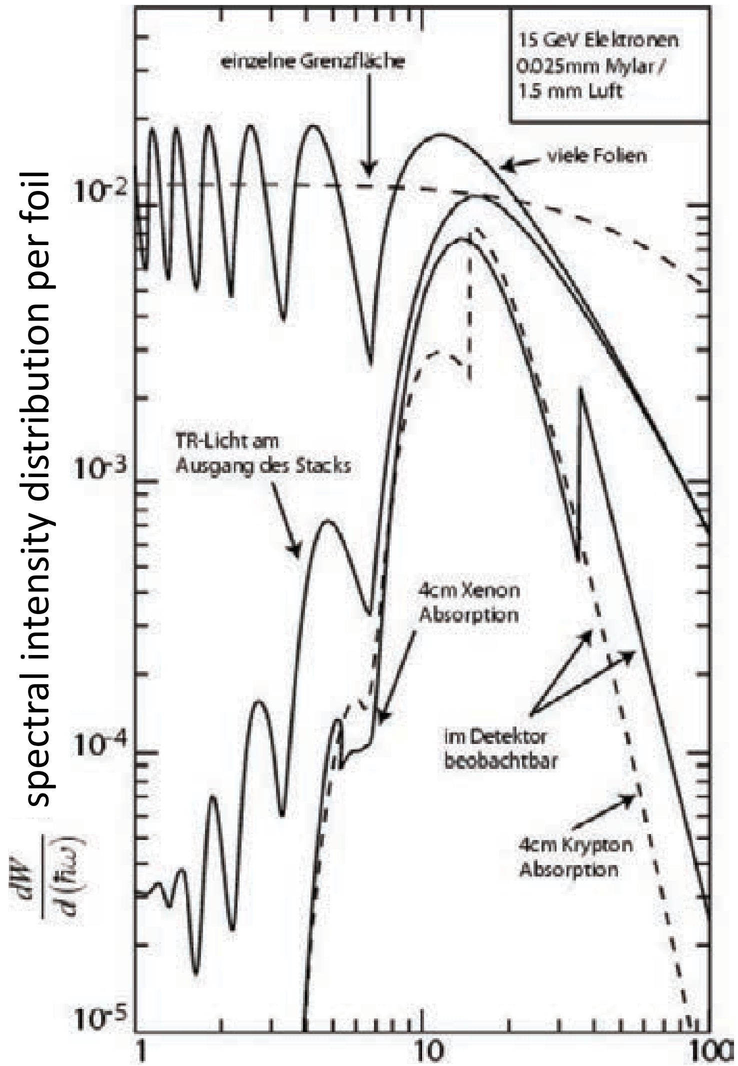

photon energy [KeV]

3.2 Transition Radiation

Energy dependence of detectable transition radiation (X-rays)

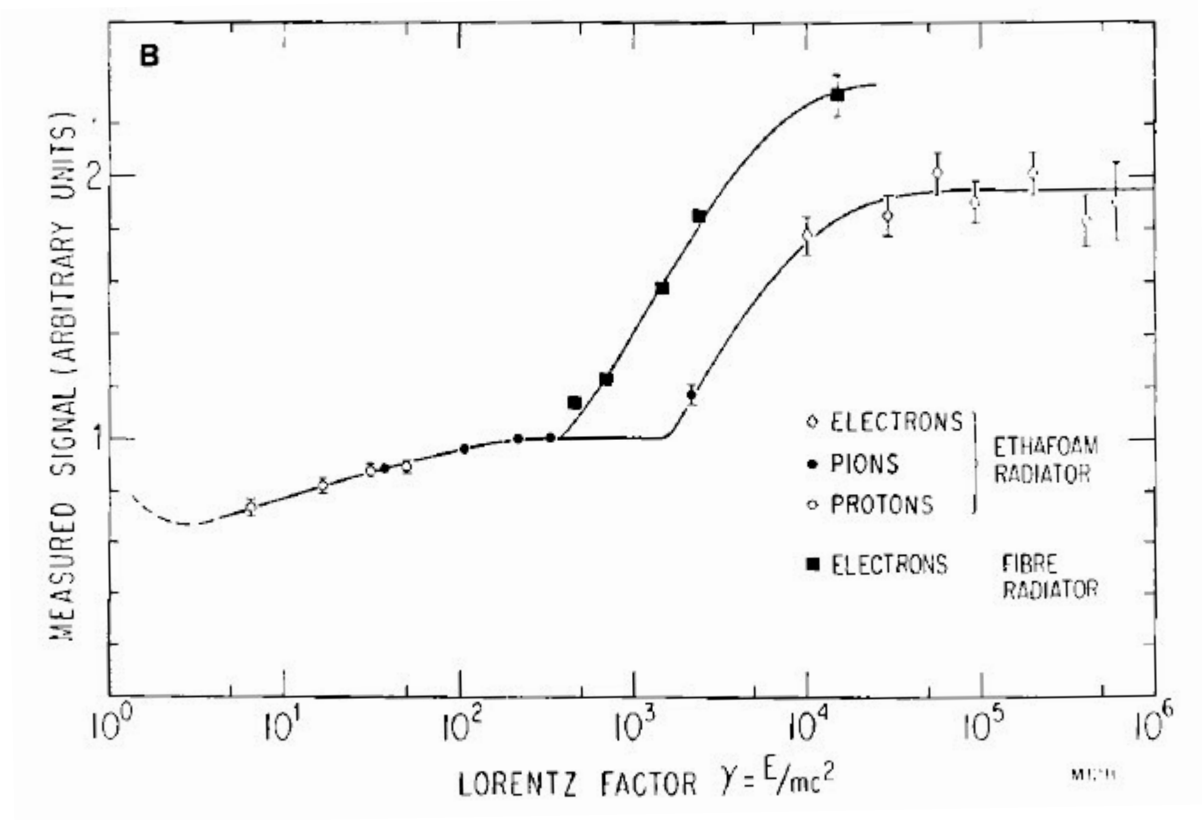

absorption of X-rays in gas:

- use noble gases (Xenon, Krypton)
- absorption edges in X-ray region

energy dependence exhibits effective threshold behaviour

→ typically used for e/π separation

But: π/Σ separation or energy measurements of heavy nuclei in space !!

3.2 Transition Radiation

The last maximum occurs at: $\omega_{max} = \frac{l_1 \omega_{P1}^2}{2\pi\beta c}$ l_1 : thickness of radiator

radiator

TR detection chamber

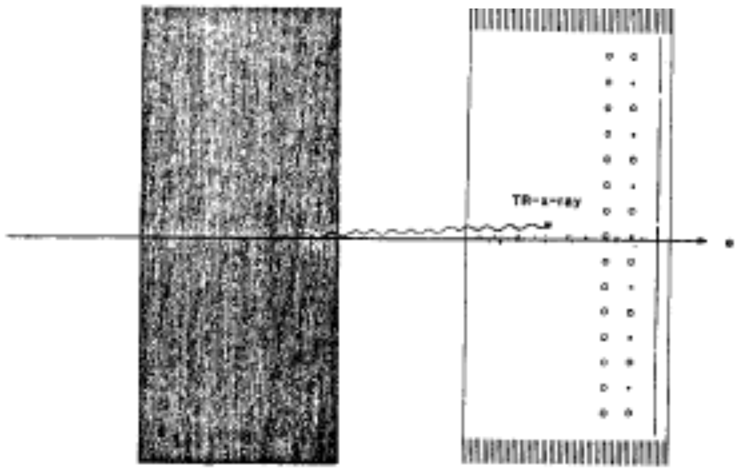

- TR photon typically overlaid with particle track
- KeV photo electron to be detected in the presence of electron clouds from ionization
- use thin detectors (gas)
- integrated method gives small signal over large background (Landau tail !!)
- in differential detection: δ electrons are major background

pulse height

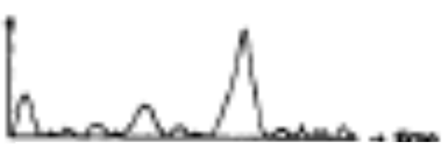

longitudinal charge profile in detector

3.2 Transition Radiation

Owing to Landau fluctuations of electronic energy loss: use many TR sub detectors

- straw tube trackers (filled with Xe) embedded into a foam/matrix structure of radiator
- sets of radiators (set of many interfaces)/ detection modules

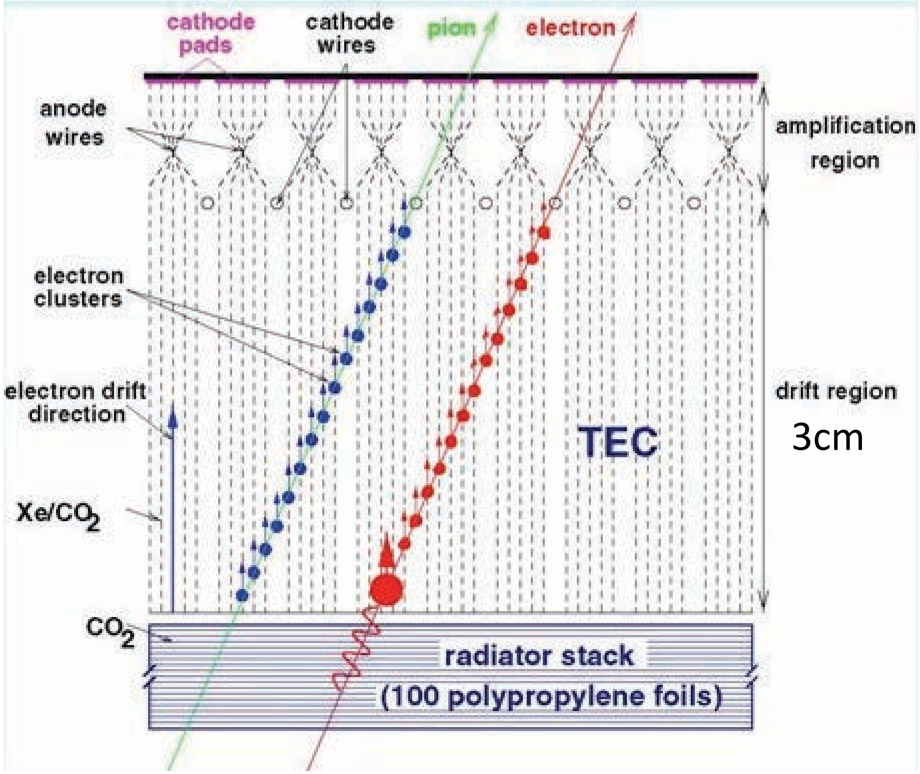

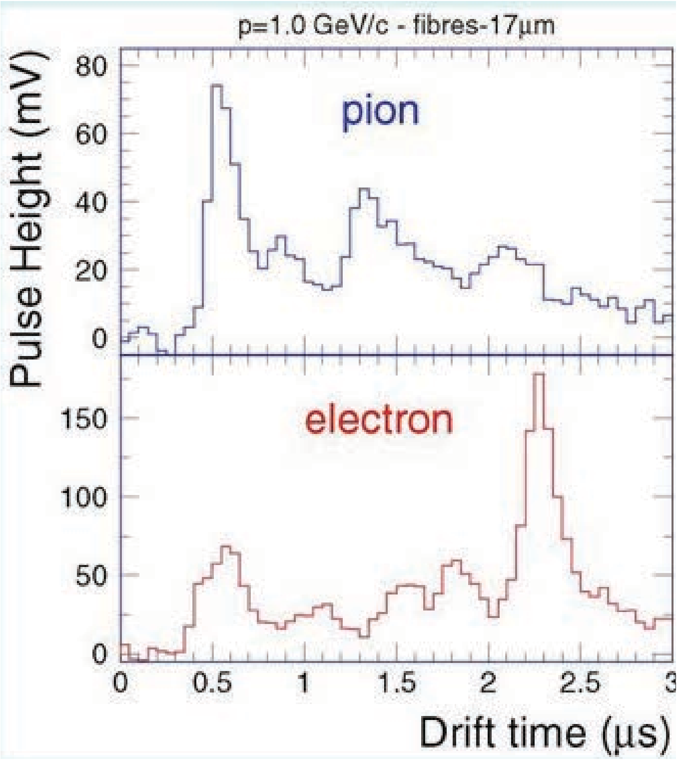

ALICE: pion rejection by factor 100

3.2 Transition Radiation - ALICE

6 modules. radiator / Time Expansion Chamber (TEC)

- rohacell radiator for mechanical stability
- fibre radiator for yield optimisation

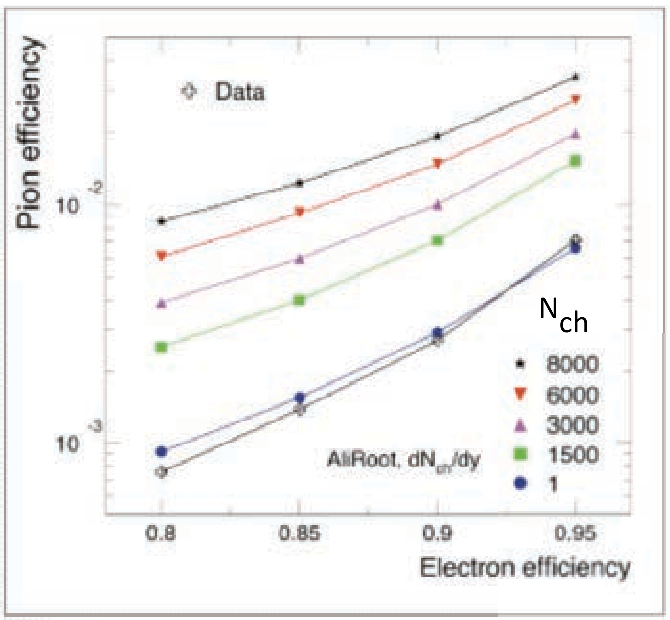

two different radiators

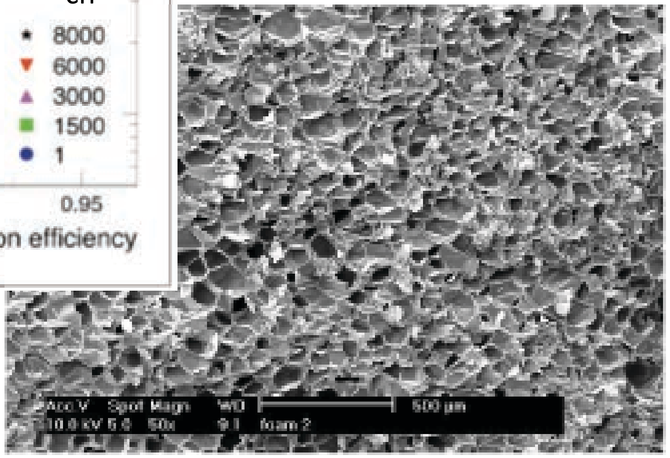

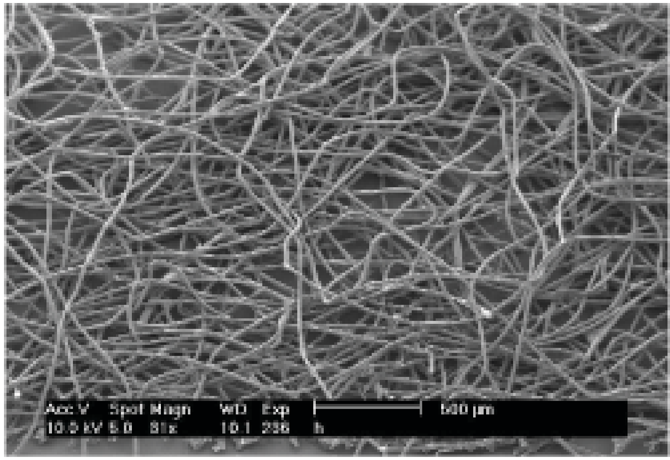

3.2 Transition Radiation

ATLAS TR Tracker (many straw tubes embedded in radiator):

- set low threshold for tracking
- set high threshold for TR signal detection

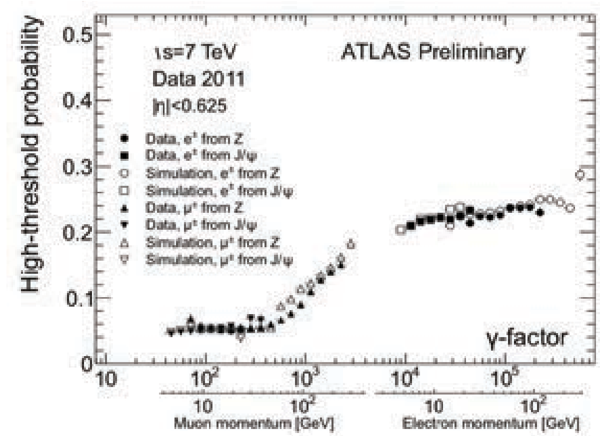

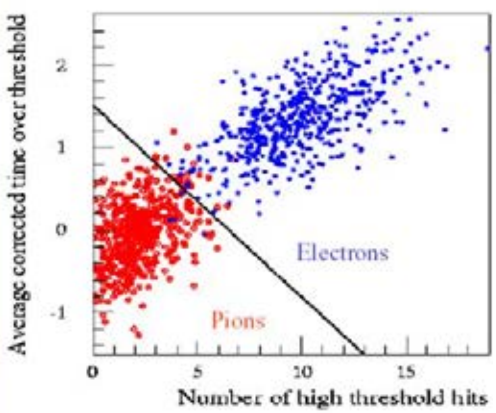

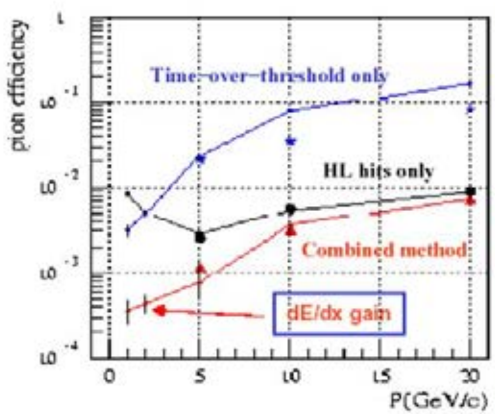

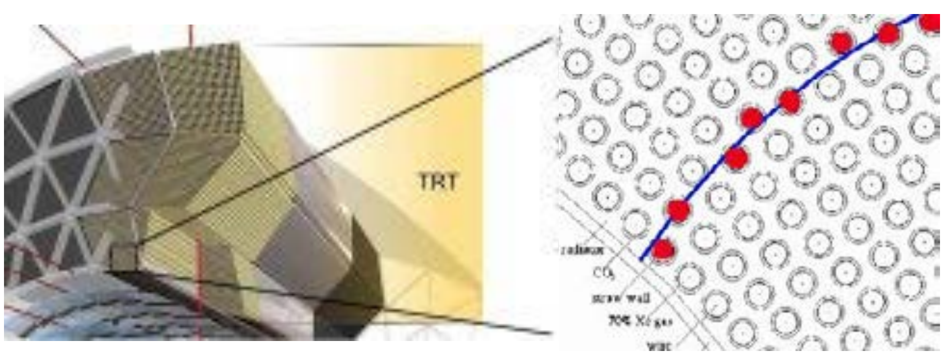

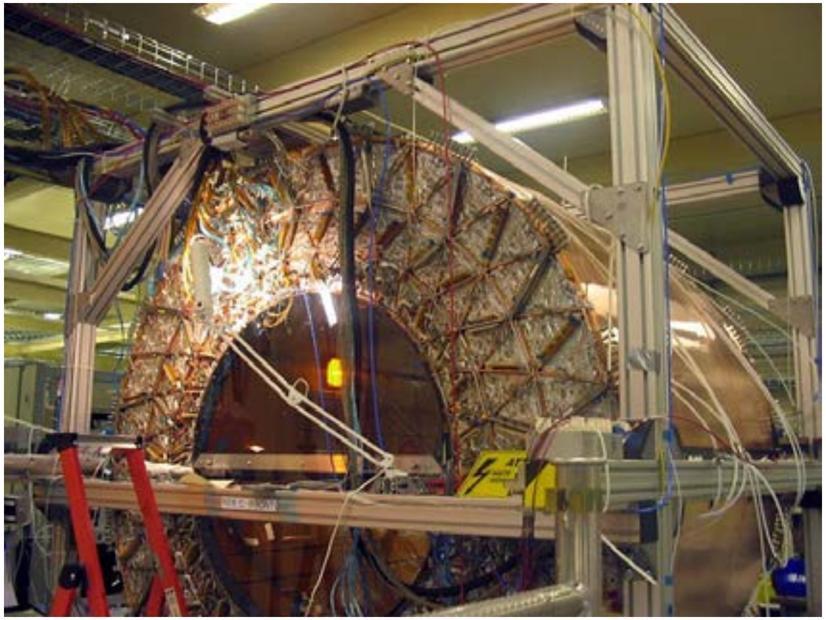

Particle Identification - Summary

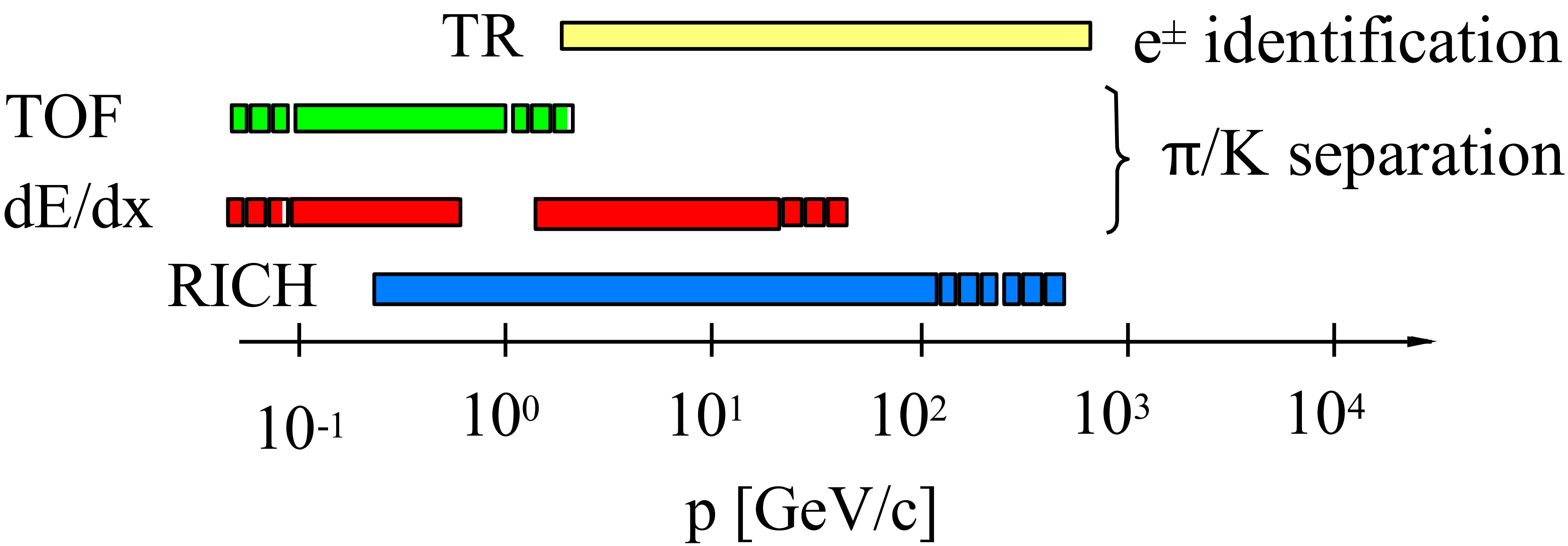

Recapitulation

- What is an MWPC
  - „arrangement of adjacent Geiger counters“
- What is a Driftchamber ?
  - Coarse position information: wire number - fine information: drift time of electrons
- What is a TPC
  - 2 coordinates through a 2D Anode, 3rd coordinate via drift time
- What is the Cherenkov effect
  - emission of dipole radiation through polarisation of medium for $v_{\text{Particles}} > c/n$
- What is Transition Radiation
  - emission of dipole radiation by modulation of medium polarisation at interfaces. Occurs for every value of energy. Practically detectable for for $\gamma_{\text{Particles}} > 1000$
- Which energy are useable TR photons and how to detect them ?
  - X-ray; gaseous counters filled with heavy noble gases

Particle Detectors

Paul TU München
stephan.paul@ph.tum.de

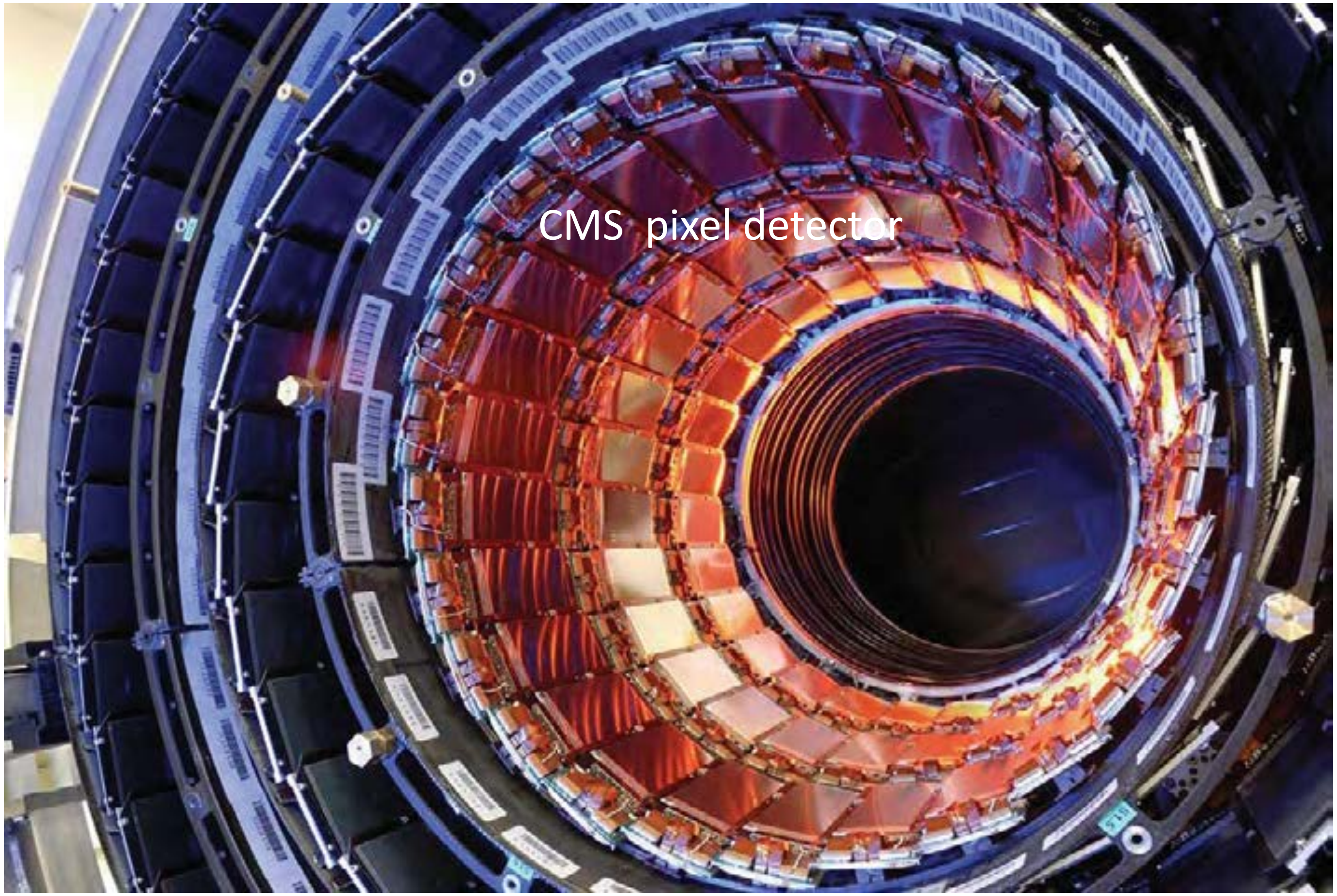

4. Semiconductor Detectors

Größe	Silizium	Germanium
Ladungszahl Z	14.	32.
Atomgewicht A	28.1	72.6
Dichte [g/cm²]	2.33	5.32
innerer Widerstand (300 K) [Ωcm]	230000.	45.
Energielücke (300 K) [eV]	1.1	0.7
Energielücke (0 K) [eV]	1.21	0.785
Elektron-Mobilität (300 K) [cm²/Vs]	1350.	3900.
Loch-Mobilität (300 K) [cm²/Vs]	480.	1900.

Semiconductors:
solid with energy band structure - ~ eV band gap

ionizing particles generate
charge carrier pairs:
can be collected through electric field (as in gaseous detector)

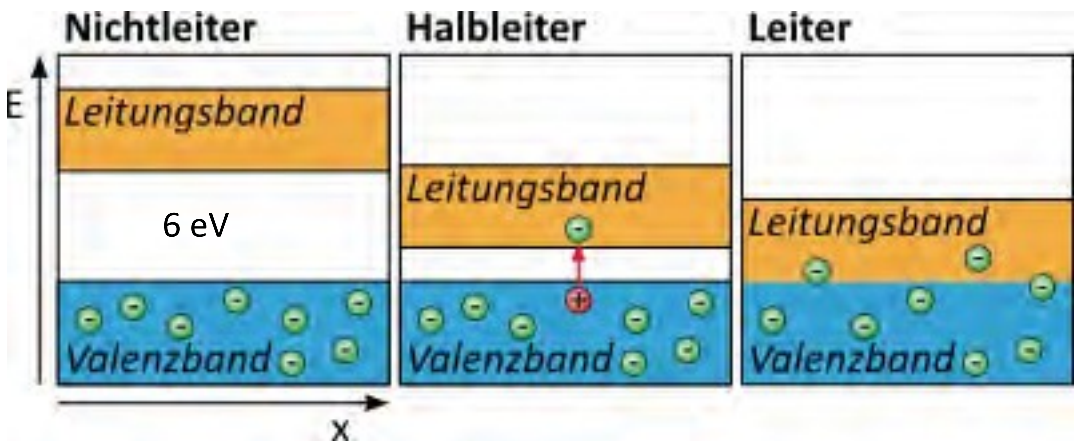

http://lp.uni-goettingen.de/get/bigimage/6798

Energy deposit in semiconductor ~ 3 eV to generate a charge carrier pair
gas detector ~ 30 eV, scintillation detector ~ 100 eV
Problem: at room temperature very many free e^- - hole-pairs: doping or cooling

4. pn-Junction

Si, Ge . 4-valent atoms

Doping of semiconductor: grid positions are occupied through 3 und 5-valent atoms

5-valent : „too many“ electrons „donors“, n-doping

3-valent: ,“too few“ electrons „acceptor“, p-doping

shift of Fermi-levels through ‚impurities’

- normal doping: 10^{13} atoms/cm^3
- heavy doping: 10^{20} atoms/cm^3 (used for contacting layers n^+ or p^+ material)

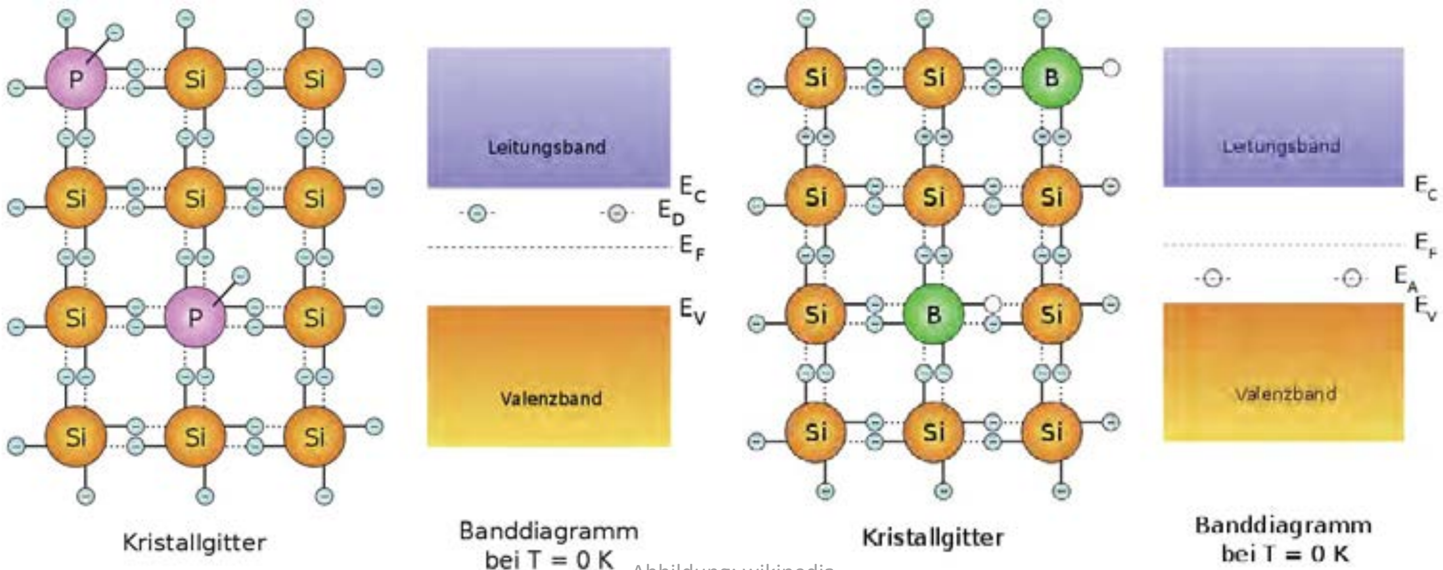

Abbildung: wikipedia

4. pn-Junction

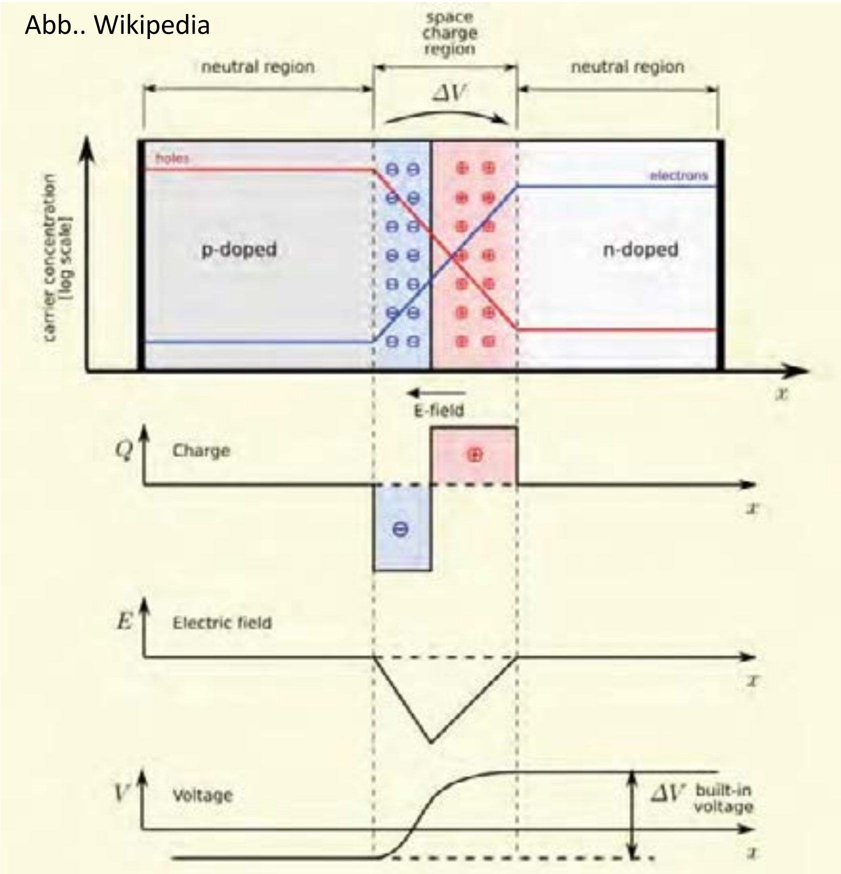

Abb.. Wikipedia

depletion zone ~ 70 µm in Si
at 300 V bias voltage: 5 mm

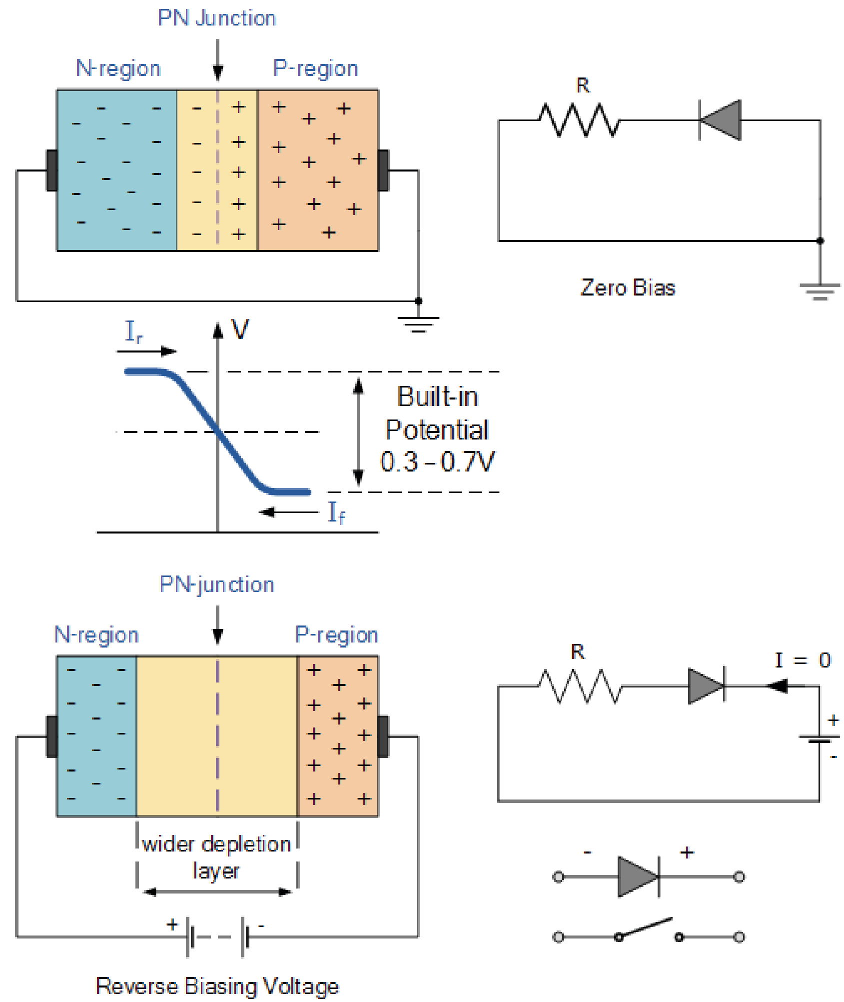

“depletion zone“: no free charge carriers at p-n junction; zone can be enlarged through applying voltage („bias“)

4.1 Strip Detectors

http://hep.fi.infn.it/CMS/sensors/Silicon_Detector.gif

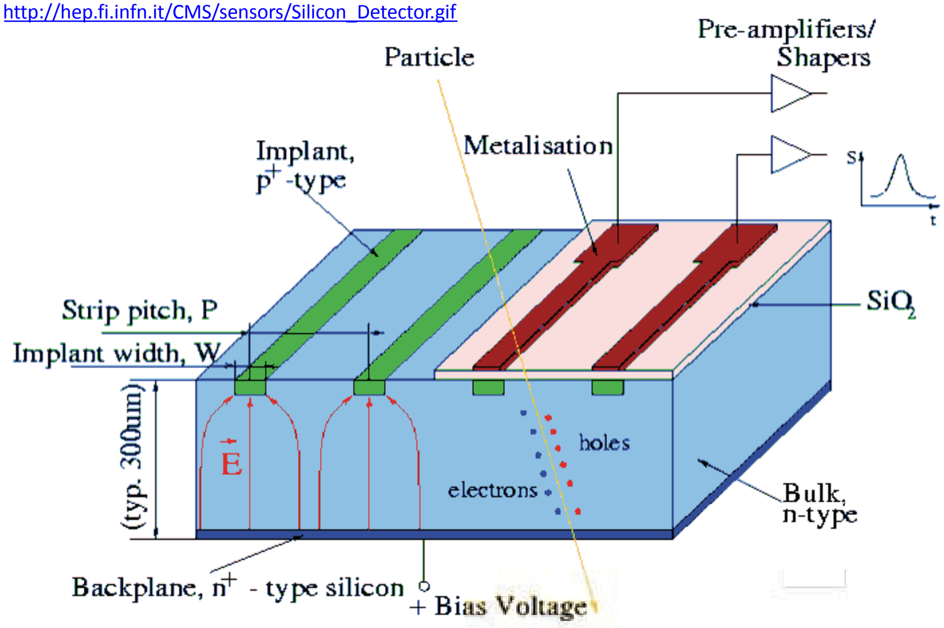

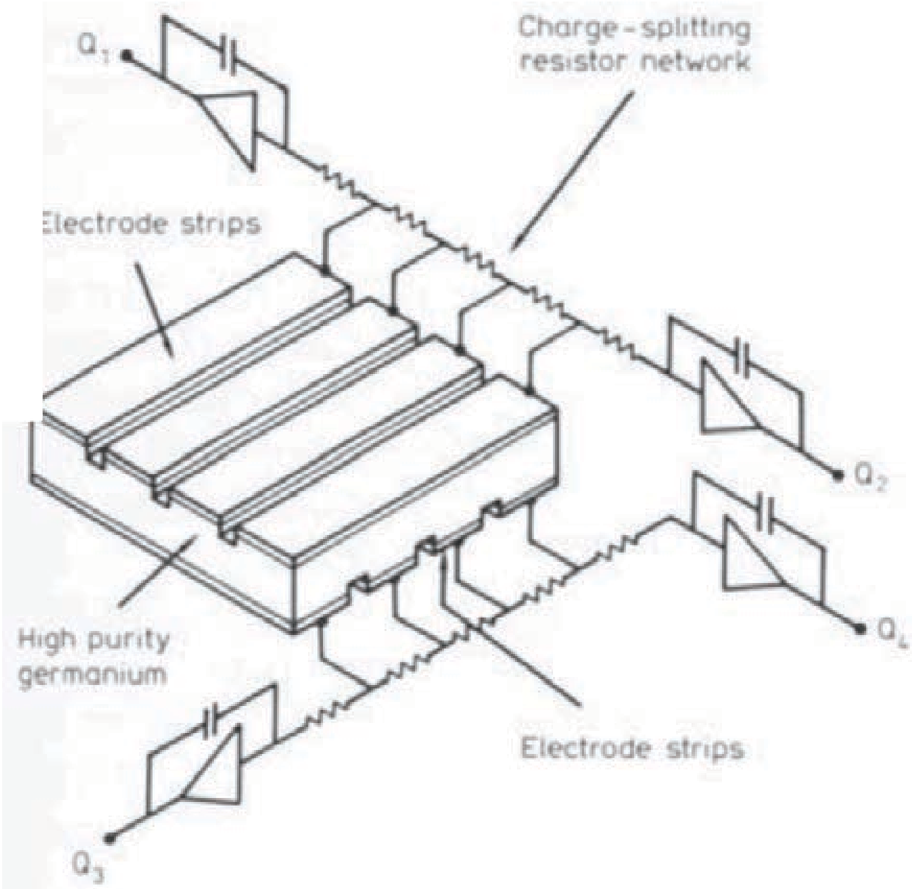

σ ~ 10μm

Continuous development:

Pixel detectors, e.g. ATLAS detector ~ 80.000.000 read-out channels

Problems:

radiation exposure,

read-out speed

4.1 Strip Detectors

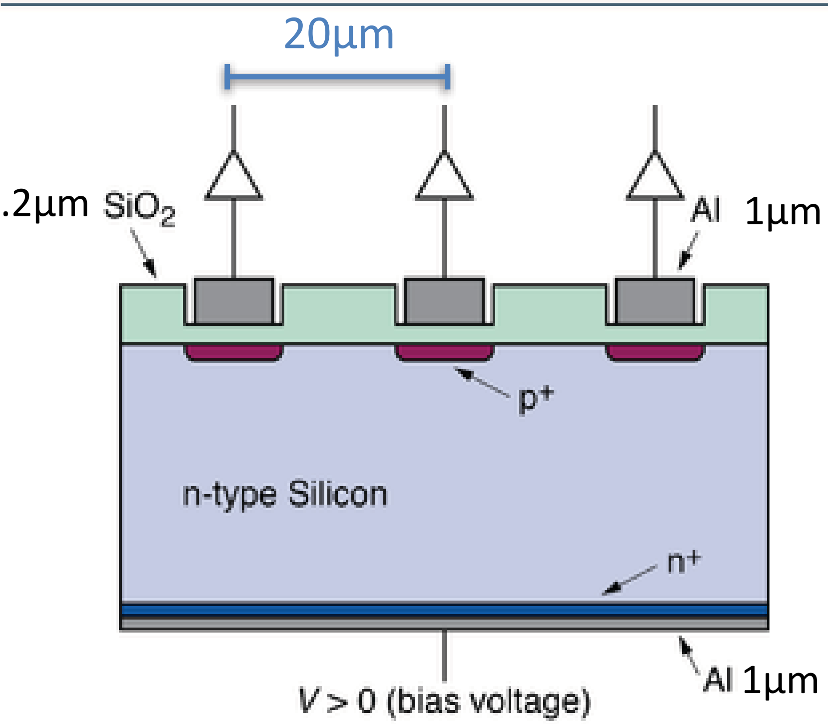

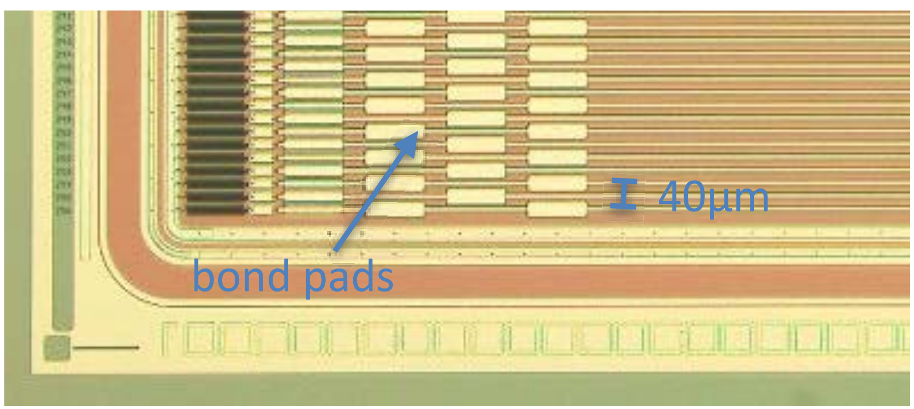

two possibilities: AC and DC coupled strips

double sided segmentation: requires more elaborate structure owing to space charge effects

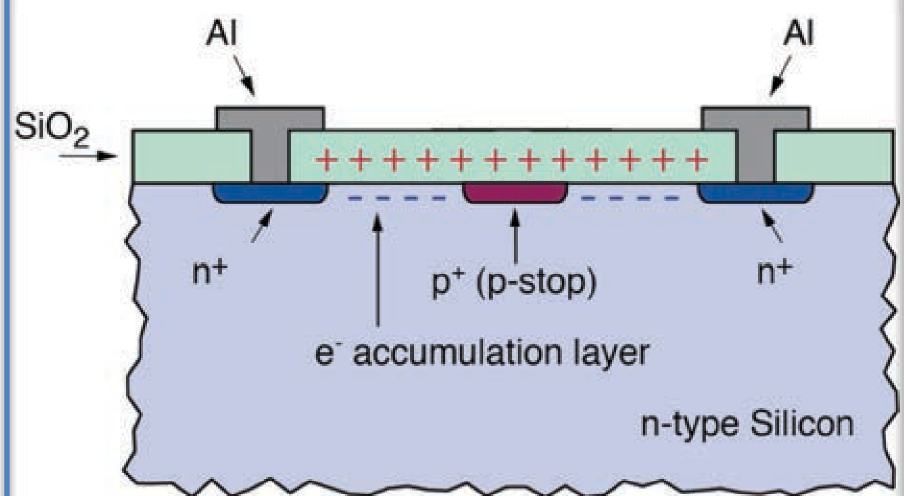

4.2 Pixel Detectors

‚Flip-Chip' Technologie:

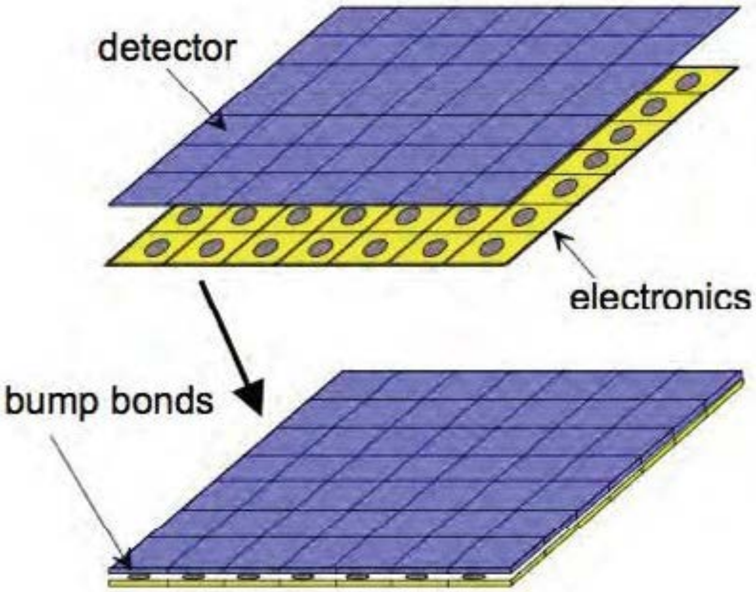

RD 19, E. Heijne et al., NIM A 384 (1994) 399

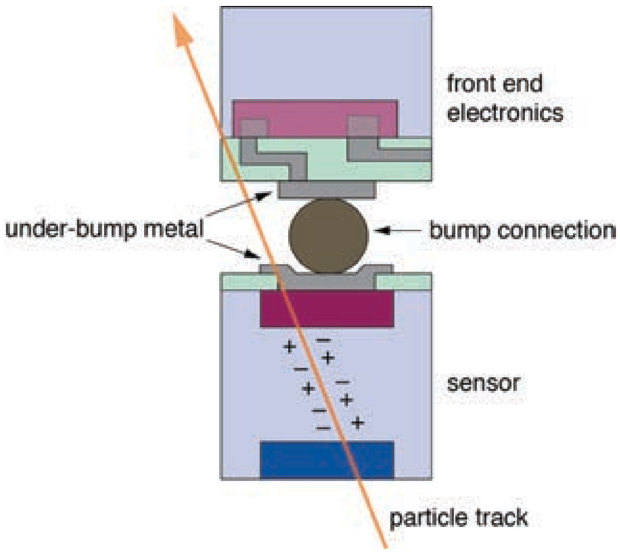

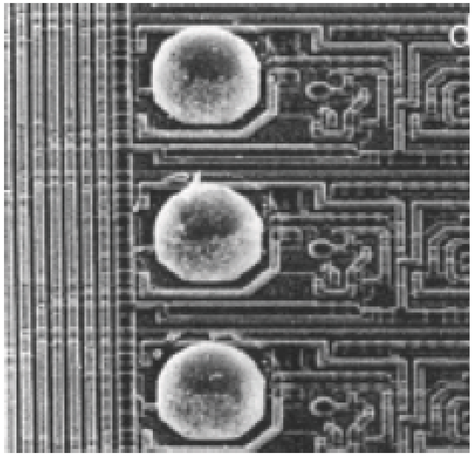

4.2 Example Pixel Detector - ATLAS

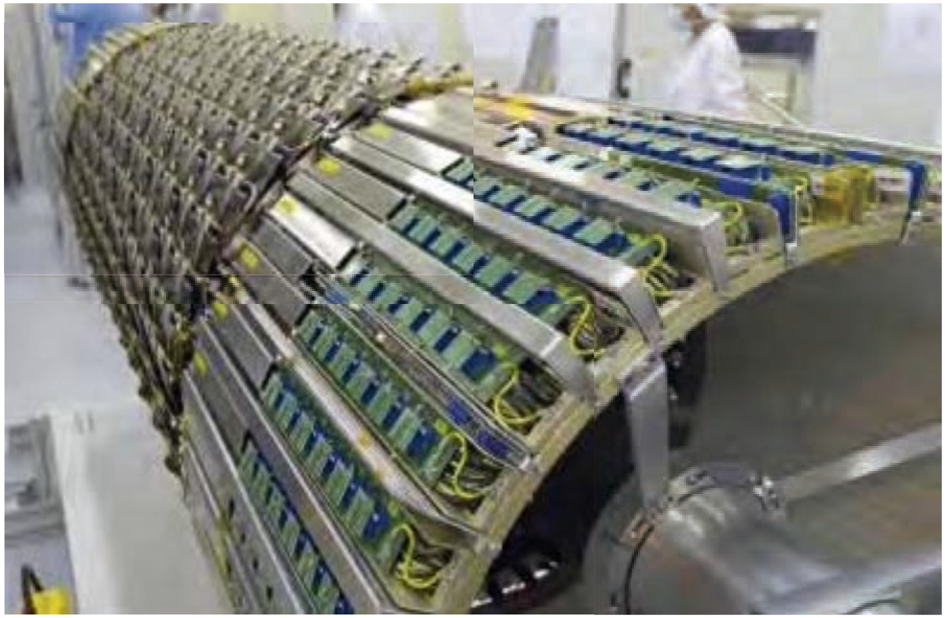

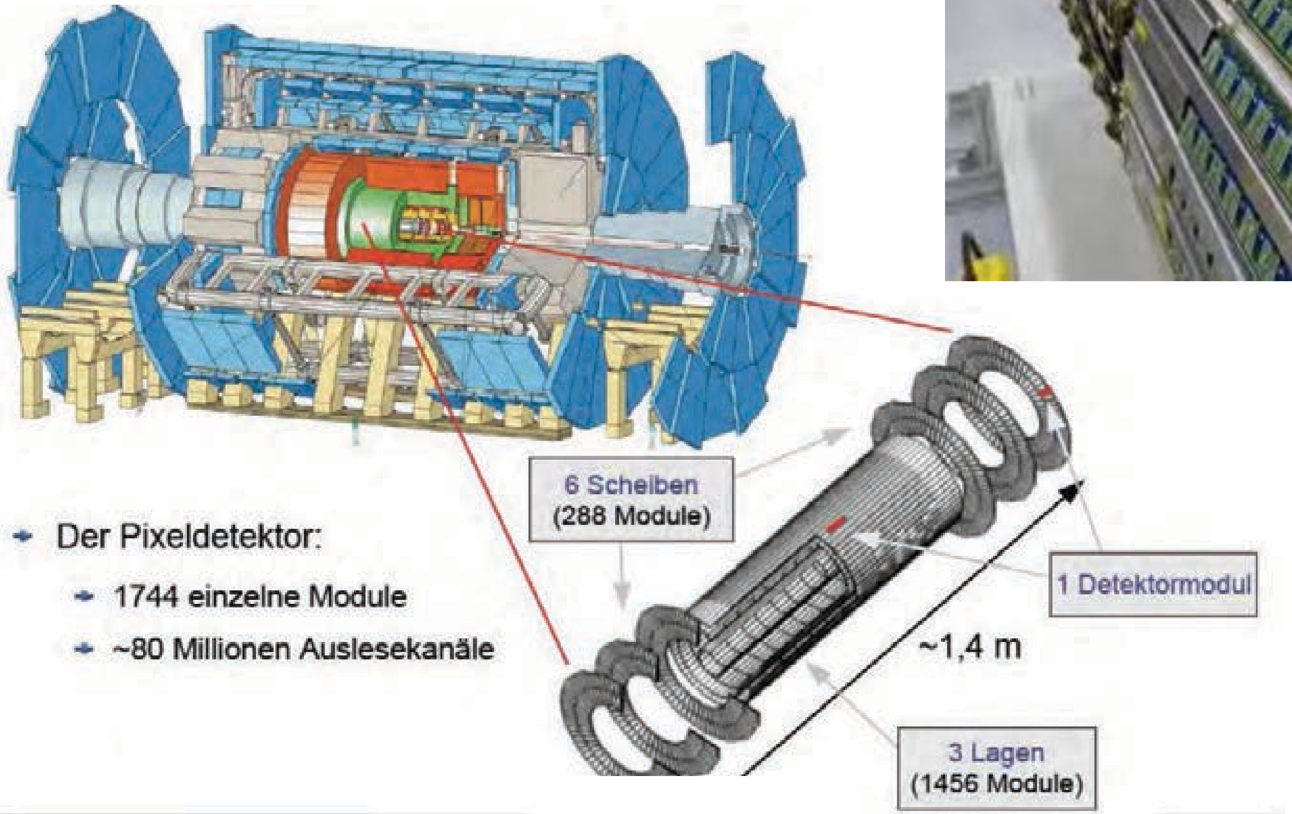

4.2 Example Pixel Detector - CMS

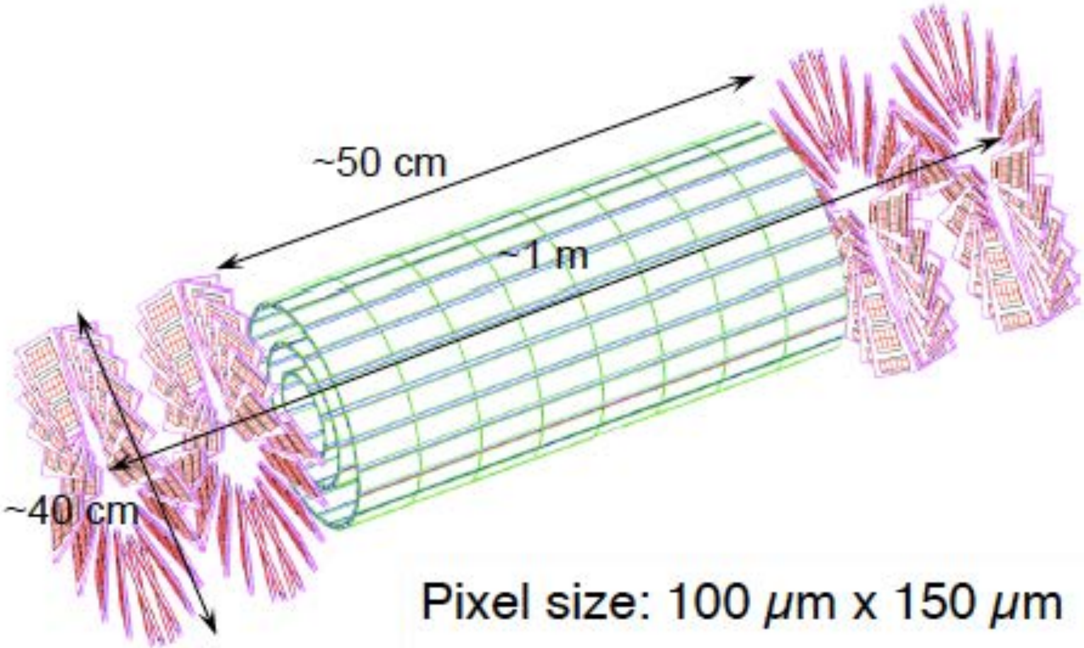

Pixel size: 100 μm x 150 μm

Barrel Pixel:
- 3 barrel layers at *r* of 4.3, 7.3, 10.4 cm
- 11520 chips (48 million pixels)

Forward Pixel:
- 4 disks at *z* of ±35.5 and ±46.5 cm
- 4320 chips (18 million pixels)
- Modules dilted by 20º for better charge sharing

4.3 New Developments

Issues:

- sensor thickness (reduction multiple scattering)
- low noise
- monolithic (built in amplification)

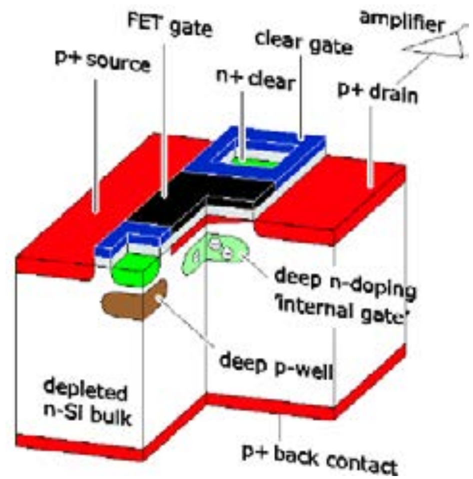

Solutions:

- DEPFET detectors (Depleted P-channel Field Effect Transistor) - Belle 2
  accumulated electrons drift underneath the gate of a FET
  → modification of the source drain current → built-in amplification

- Monolithic Active Pixel Sensors (MAPS) A
  standard IC CMOS technology Fabricated
  - Active volume: thin p-epitaxial layer
    - ⇨ charge collection by diffusion
    - ⇨ small signal charge: ~ 1000 e-
    - ⇨ long collection time: ~ 100 ns
    - ⇨ small depletion voltages

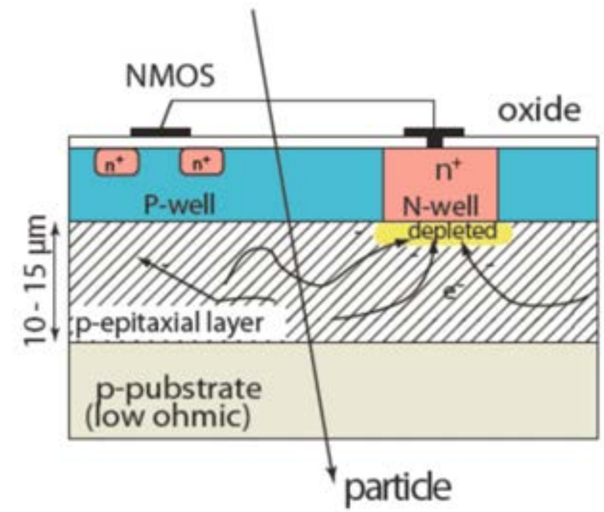

4.3 New Developments

- High Voltage Monolithic Active Pixel Sensors (MAPS) (Peric)
  - fabricated in standard IC CMOS technology
  - very low noise (small capacitance)
  - amplification on chip (transistors)
  - high voltage (15 µm depletion zone) 60-100 V
  - fast charge collection (200 ps)
  - thin substrate
  - high radiation tolerance

deep n-well:
- separates transistors from bulk HV
- collection region for electrons

- Usage foreseen
  - Mu3e
  - ATLAS upgrade

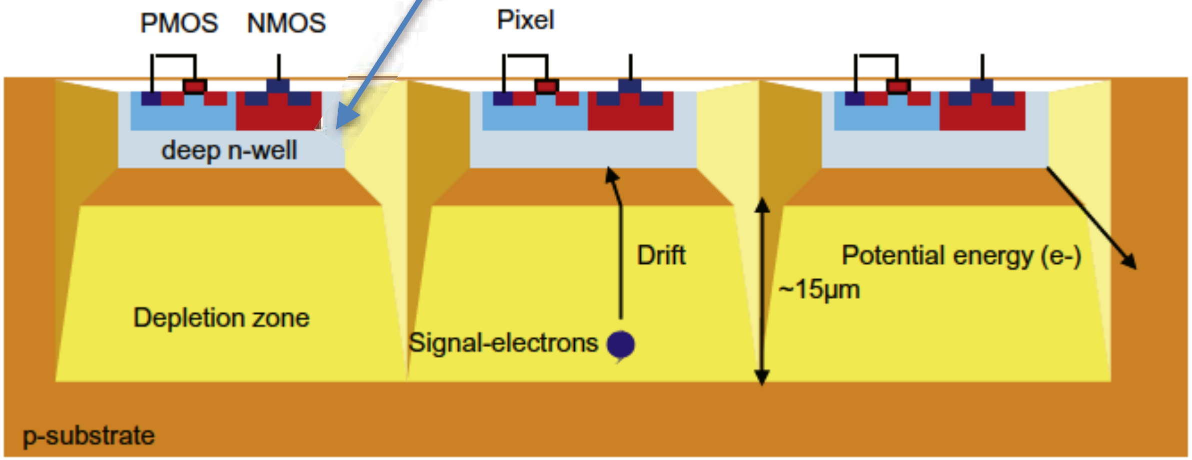

I. Peric´, *A novel monolithic pixelated particle detector implemented in high-voltage CMOS technology*, Nucl. Instrum. Meth. A 582 (2007) 876

Interaction of photons (UV, visible) with matter
detection of scintillation, Cherenkov, astronomy etc..

Effects:

photoelectric effect: small energies : $E_\gamma \geq E^e_{Bindung} (K, L, M - Schale)$

Compton scattering: medium energies $E^e_{Bindung} << E_\gamma < 2 m_e c^2$

Pair creation: high energies : $E_\gamma > 2 m_e c^2$

Photon spectrum stays unaltered with straight transmission through matter !
But: reduced intensity

$I(x) = I_0 \cdot e^{-\mu x}$ extinction law extinction
extinction coefficient $\mu = \frac{N_A}{A} \sum \sigma_i$

5.1 Mass Absorption Coefficient

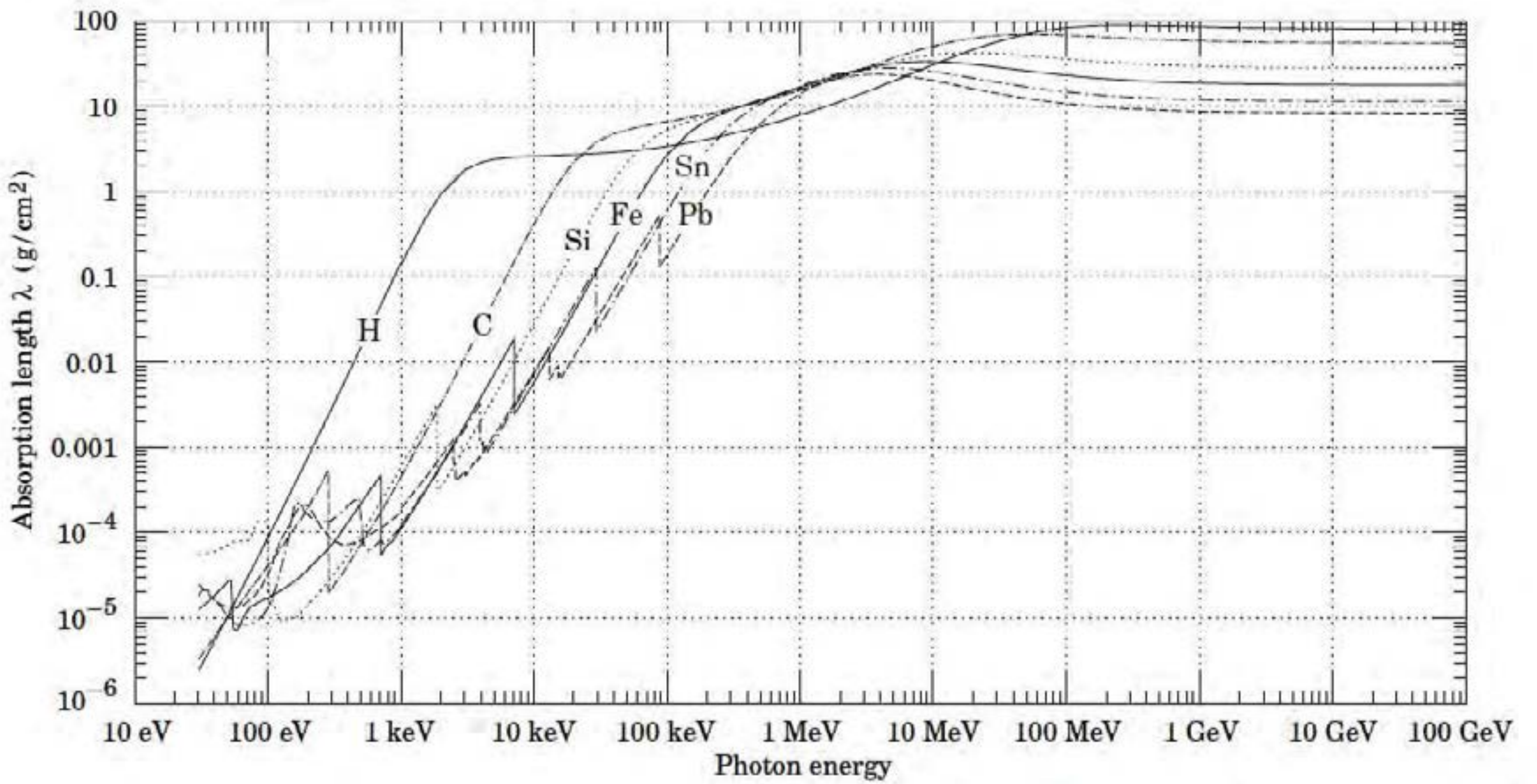

$\lambda = 1/(\mu/\rho)$

Fig.: PDG 2012

Photoelectric effect $\gamma + Atom \rightarrow e^- + Ion^*$

- kinetic energy of outgoing electron $T_{e^-} = E_\gamma - E_{Bindung}$
- cross section $\sigma_{ph} \propto \frac{Z^{4.5}}{E}$
- maxima at ionisation threshold (K, L, M - edges)

low energy (atomic shell)

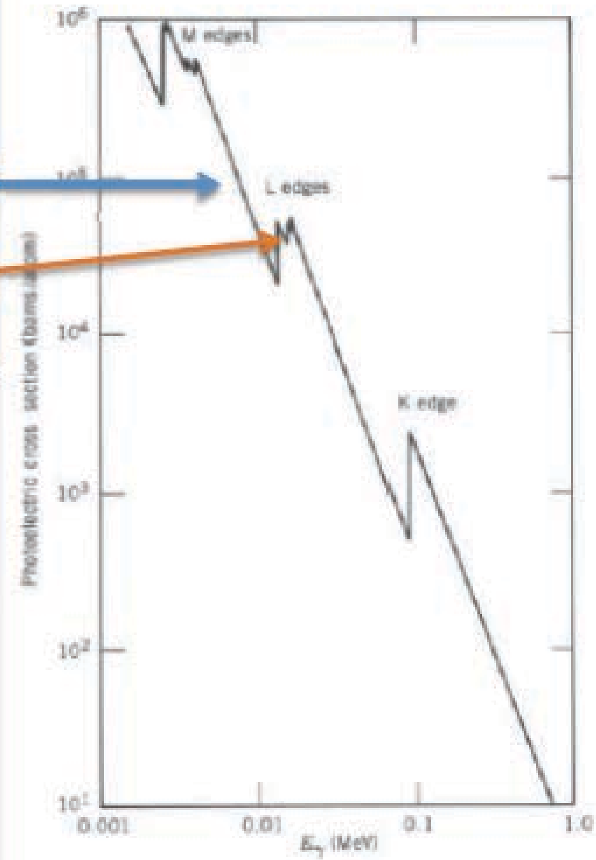

Compton scattering

- scattering off quasi free electrons $\gamma + Atom \rightarrow \gamma' + e^- + Ion$
- cross section

$$\sigma_C \propto Z(1-\varepsilon) \quad \text{für } \varepsilon = \frac{E_\gamma}{m_e c^2} << 1$$

$$\sigma_C \propto Z \frac{1 + 2\ln 2\varepsilon}{\varepsilon} \quad \varepsilon >> 1$$

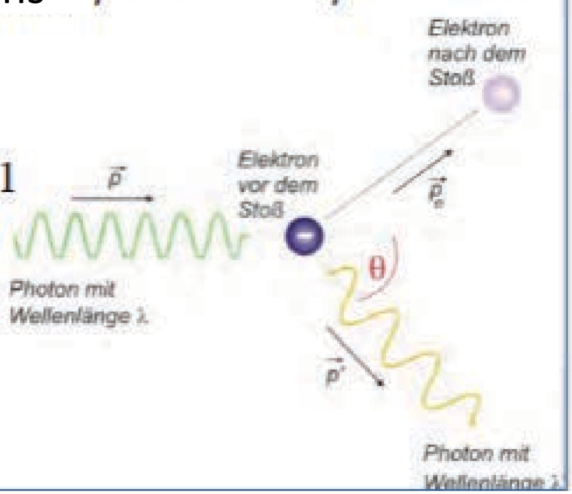

5.1 Photon detection

Distribution of Compton scattered electrons (Klein-Nishina model)

$$\frac{E_{\gamma'}}{E_\gamma} = P(E_\gamma, \theta) = \frac{1}{1 + (E_\gamma / m_e c^2)(1 - \cos\theta)}$$

- maximum energy < energy of incoming γ
- sharp edges for maximal energy γ „ Compton edge"

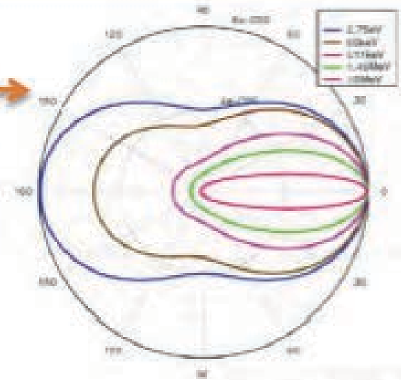

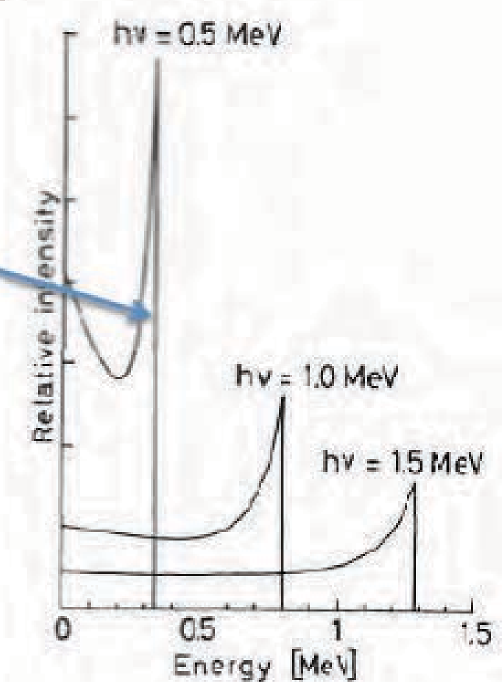

Pair-creation $\gamma + Atom \rightarrow e^- + e^+ + Atom$

$$E > 2m_e = 1.022\,\mathrm{MeV}$$

cross section:

$$\sigma_p \propto Z^2$$

$$\sigma = \frac{7}{9}(A / X_0 N_A)$$

5.1 Photon Detection

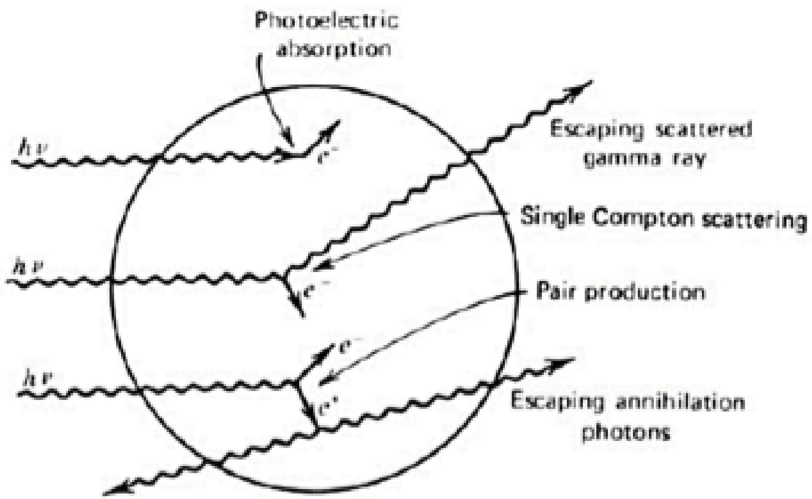

Compton edge: max. momentum transfer through Compton scattering

photo peak: energy fully transferred through photo effect

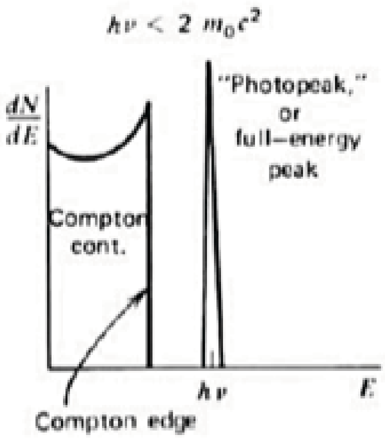

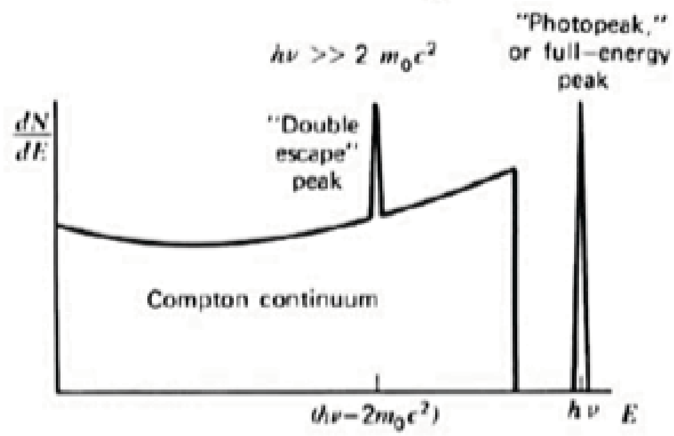

5.1 Application: Compton-Telescope

Goal: Observation of high-energy γ-radiation (0.2 – 10 MeV, e.g. COMPTEL)

⇨ Supernovae, Active Galactic Nuclei, Gamma-Ray Bursts

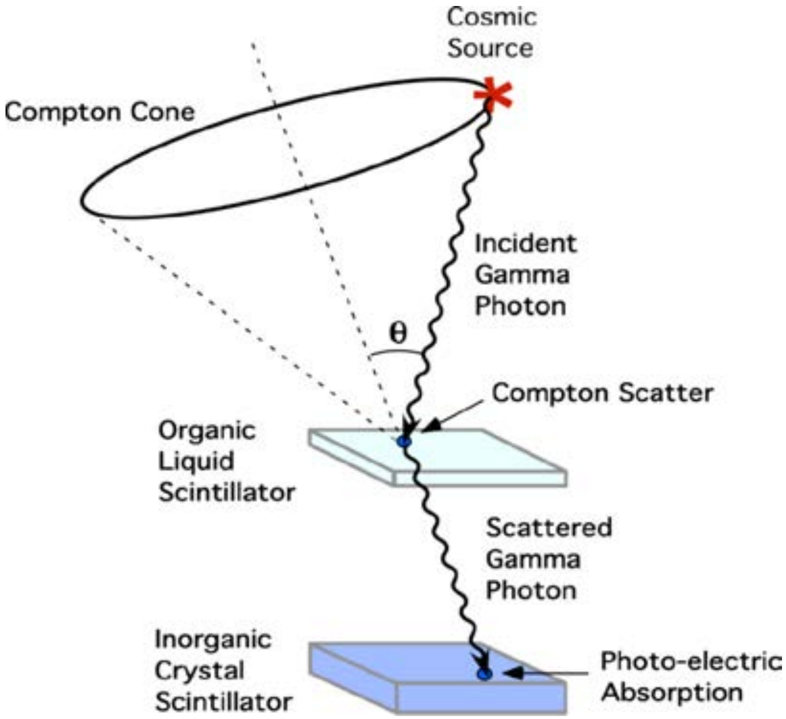

principle: measure

- $E_\gamma - E'_\gamma = E'_e$ (1. detector)
- E'_γ (2. detector)
- position of interaction

kinematic Compton ⇨ determine θ

⇨ determine source on ring

Many events ⇨ point source localisable

only method do determine momentum direction of a photon

Nuclear spectroscopy: AGATA

Total cross section (Frequency of reactions)

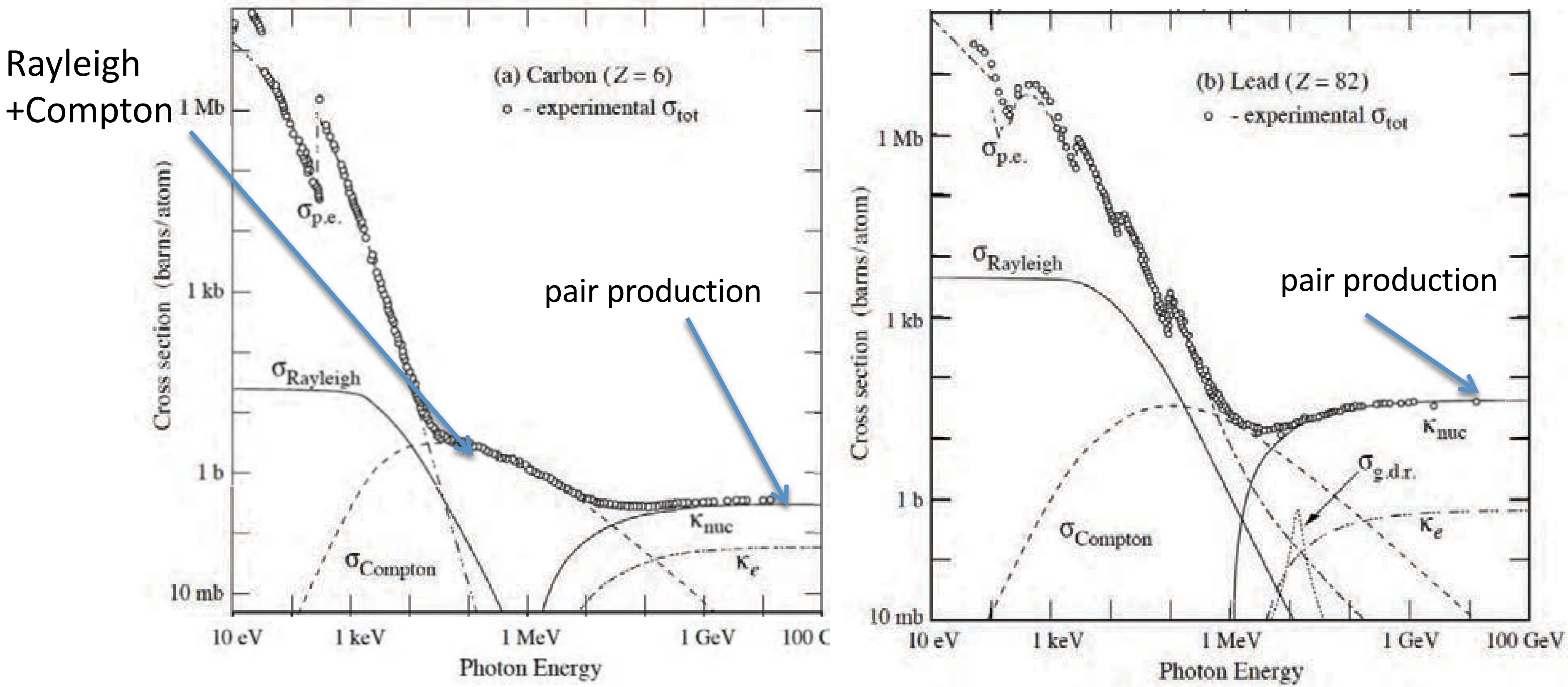

Fig.: PDG 2012

Recapitulation

- What is the semiconductor detector
  - „pn junction with reverse bias -depletion zone "
- What is a fully depleted semiconductor detector ?
  - depletion reaches from n^+ to p^+ zone
- Why do we need to fully deplete
  - largest number of signal ion pairs - lowest thermal noise
- What is a silicon strip detector ?
  - spatially segmented pn-junction with structured „read out"
- What are the processes leading to photo absorption and for which energies are they relevant ?
  - photo effect (E < 0.1 MeV), Compton scattering (0.01 < E<2 MeV), pair creation (E <>1 MeV)
- What is the Compton edge ?
  - electron energy corresponding to the largess possible momentum (energy) transfer in Compton scattering. Cross section vanishes beyond E_{max}

Photomultiplier:

Principle:
- Generate electric signal from photons
- amplification & collection of electrons

Methods:
Gas/solid/vacuum based systems,
e.g. silicon photodioden, APDs, silicon photomultiplier
Example: photomultiplier

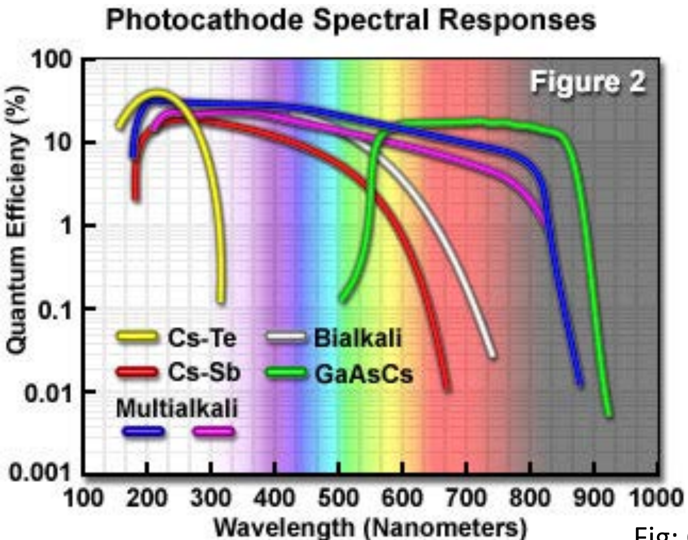

Fig: Olympus

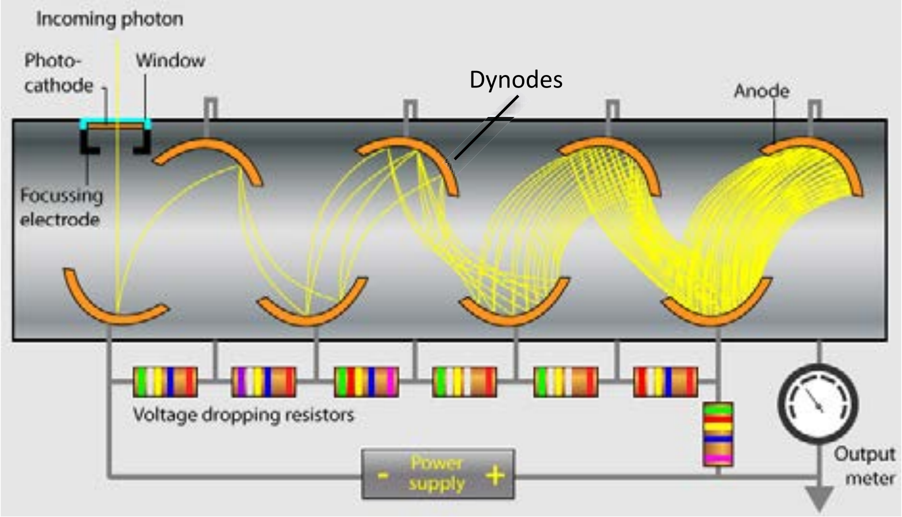

Fig: CHROMacaden

5.3 Silicon Devices: PIN diode

Diodes photodiodes:

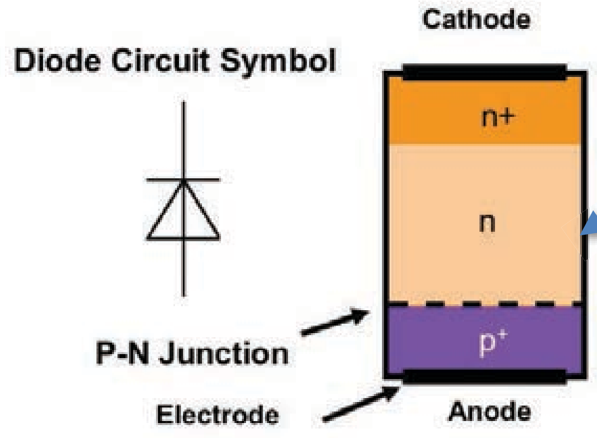

- pn junction operated in reverse bias
- photon absorbed in depletion zone generating charge carriers
- charge carrier collection at anode and cathode
- band gap in silicon: 1.2 eV
- $\lambda_{min} \approx 1100$ nm

Avalanche photodiodes:

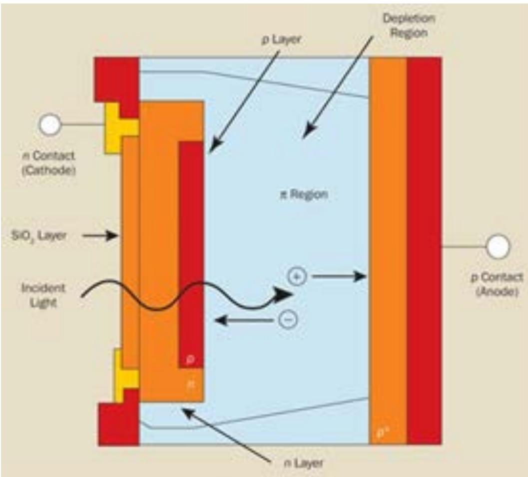

photon absorption in depleted area
electrons drift to avalanche region
high electric field causes amplification

maximum amplification by breakthrough and voltage drop through land resistor

thermal bulk current is also amplified

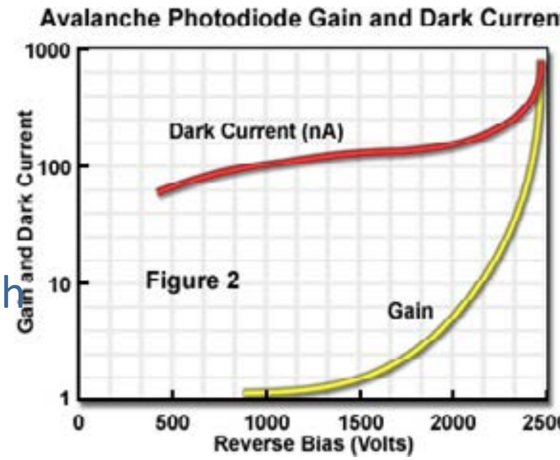

negative temperature profile: (high T → enhanced lattice vibration → energy loss of e$^-$ → increases bias voltage required)

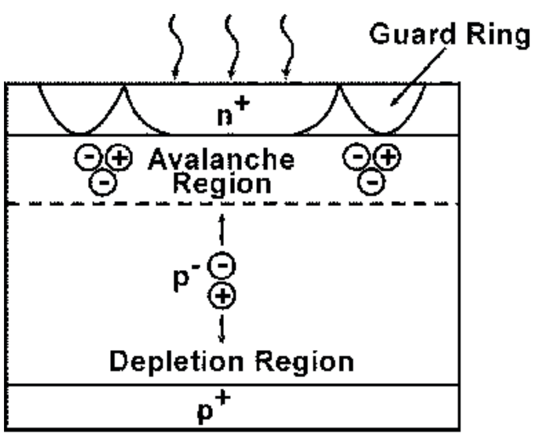

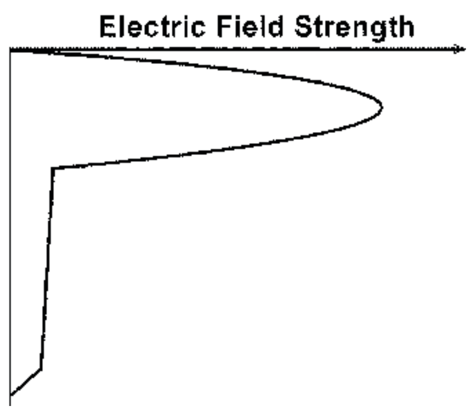

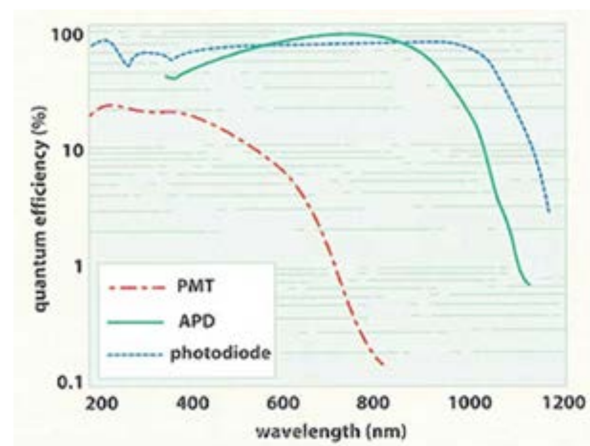

5.4 Silicon Devices: Silicon PMs

Array of many (parallel) avalanche photodiodes: operation in Geiger mode (unit signal height)
Photon energy: pulse height determined by number of APD-cells fired

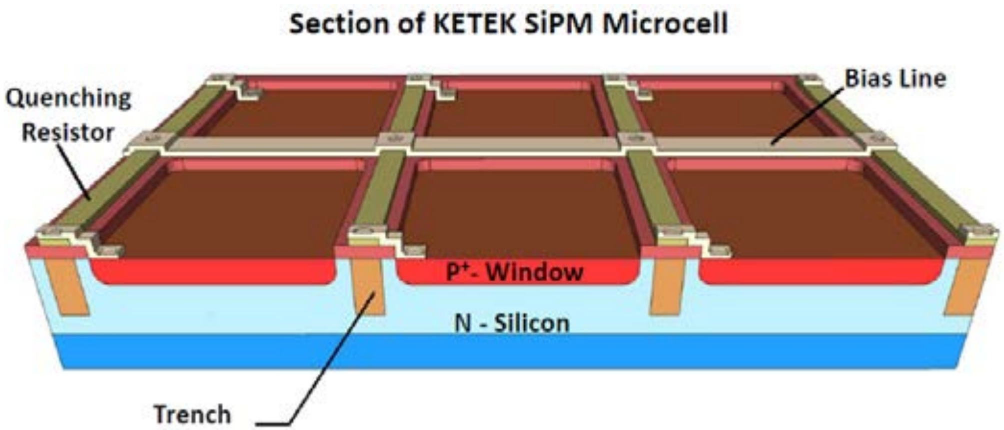

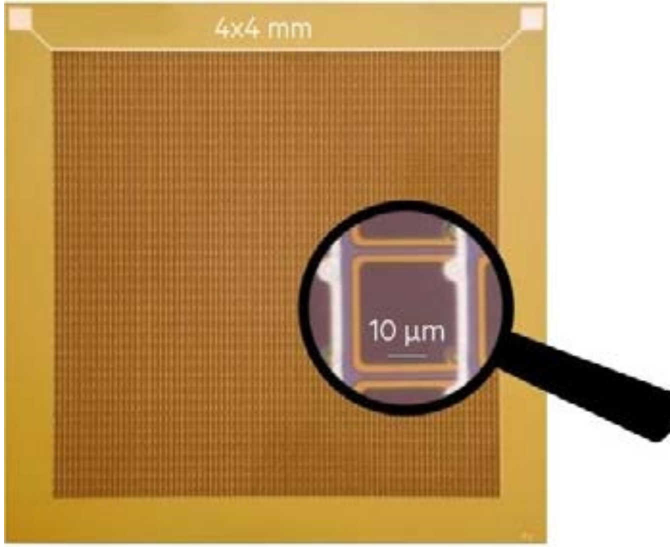

100-1000 APD cells cm^{-2}

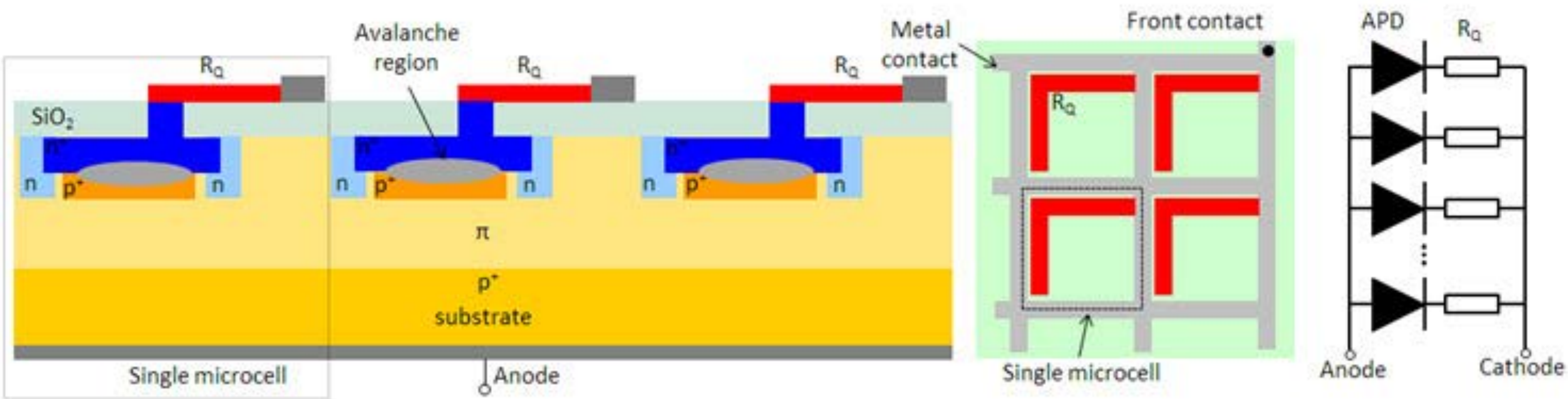

Characteristics:

- dark count rate (thermal charge carriers cause Geiger discharge)
- after pulsing
- gain saturation
- (optical) cross talk: triggered by APD avalanche emitting photons
- photon detection efficiency : Q.E. x fill factor x Geiger probability
  (FF: ~30% to ~80% depending on cell size)
- total size: 1 x 1 mm² to 6 x 6 mm²

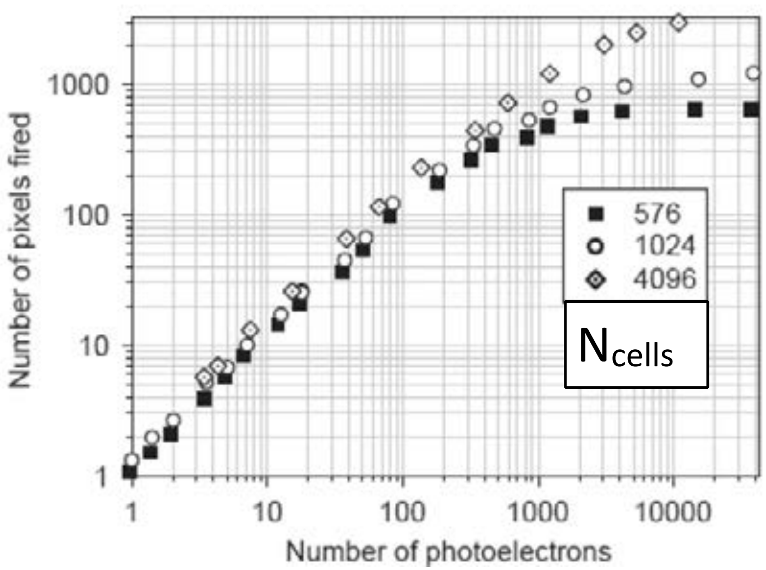

- low light intensity: linear w.r.t. number of photons
- for N_{fired} > 50% N_{cells} deviation from linearity by 20%
- two photons hitting the same cell are indistinguishable

5.4 Silicon Devices: Silicon PMs

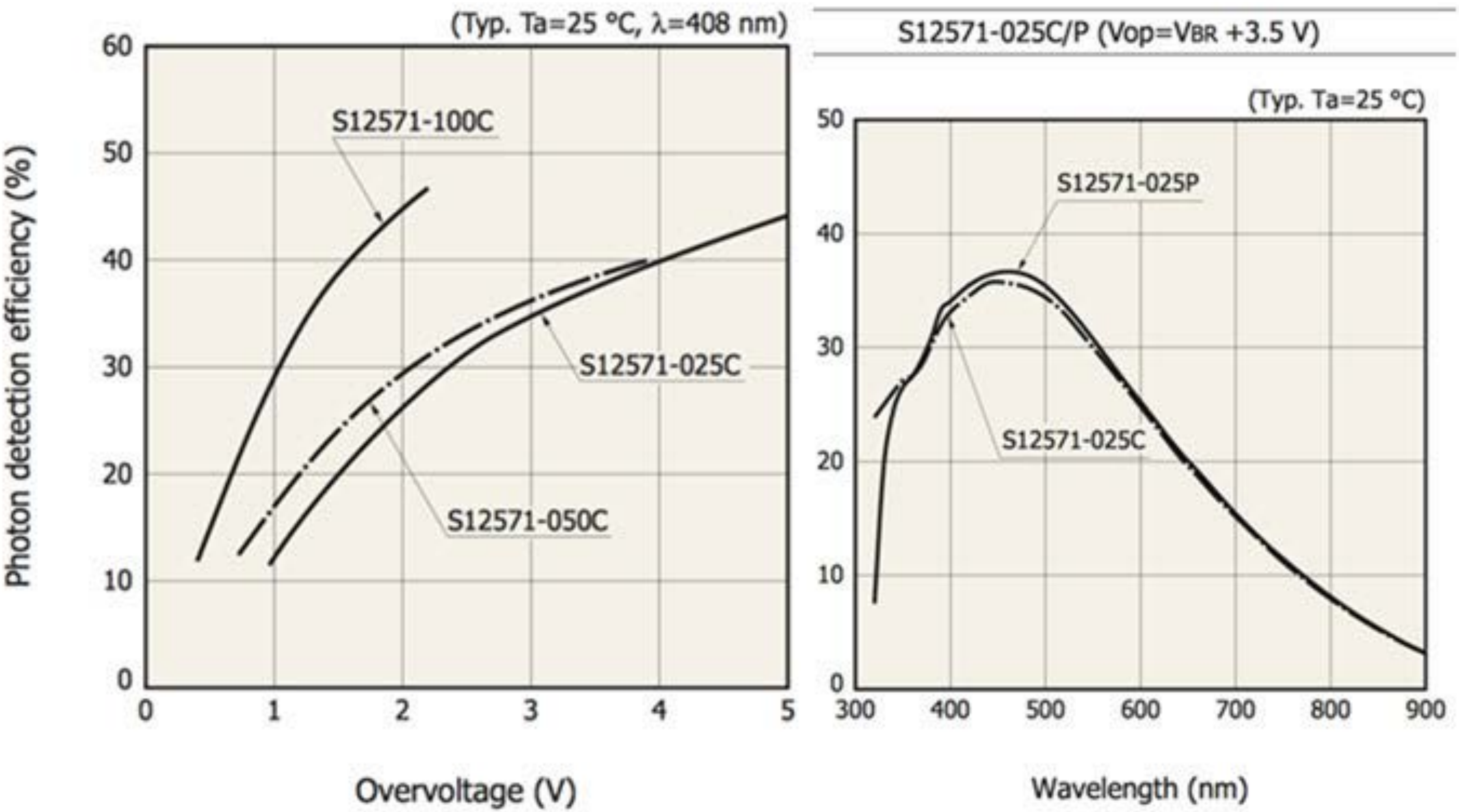

Principle:

- ionising particle looses energy in scintillator → excitation of material
- de-excitation through light emission in scintillator

- detection light sensitive detector

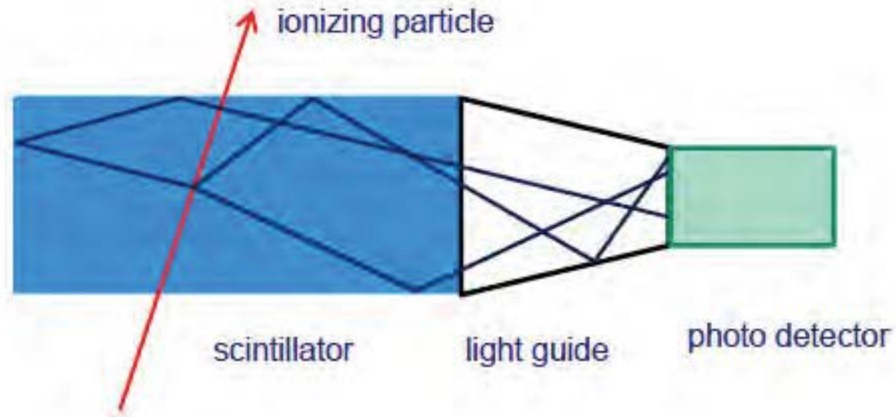

necessary energy deposit:

$C_{14}H_{10}$	60 eV/Photon
Plastik	100 eV/Photon
NaJ	25 eV/Photon
BGO	300 eV/Photon

Emission of UV-optical Licht: luminescence

- "fluorescence“ … time constant $\tau < 10^{-8}$ s
- "phosphorescence" … time constant $\tau > 10^{-8}$ s

possibilities: organic und inorganic scintillators

Inorganic scintillators :

- crystalline structure
- 40000 photons / MeV deposited energy
- high Z
- “slow“ : ~ microsecond decay times

Examples: NaI(Tl), CsI(Tl), BGO, PWO, liquid nobel gases

functional principle:

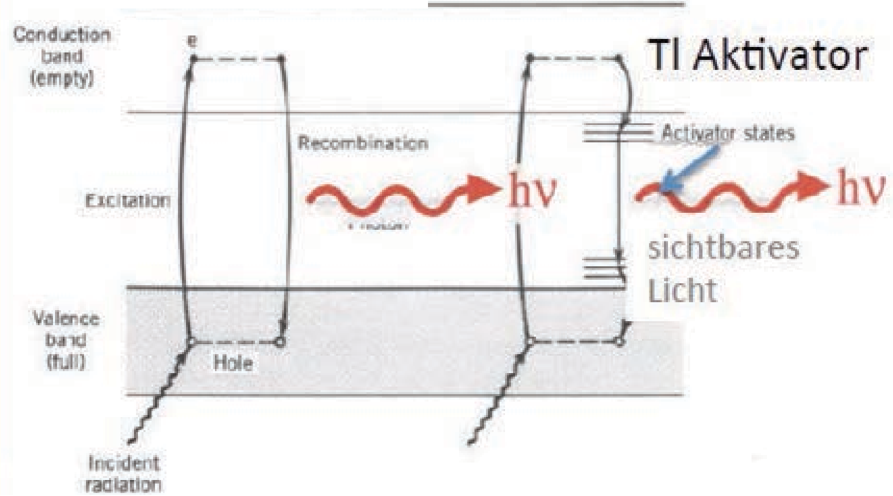

Organic scintillators :

- liquid, solid (plastics)
- polycyclic hydrocarbon (pigments e.g. naphtalene)
- 10000 photons / MeV
- low Z, low density
- „fast“: nanosecond decay time

examples: anthracene, BC400

functional principle:

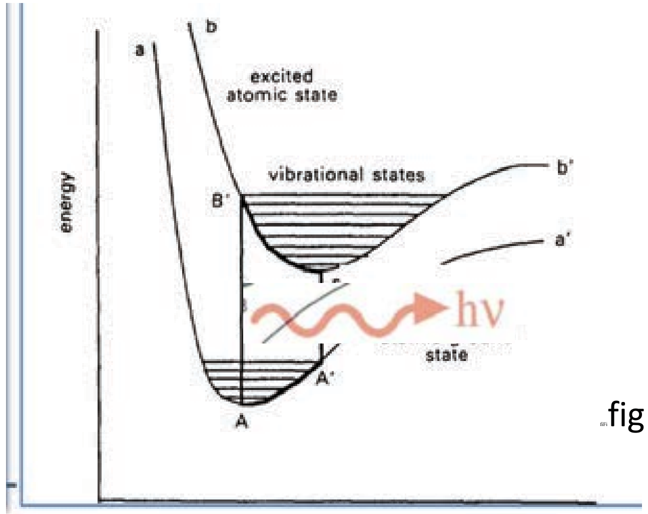

fig: Krane

6. Scintillators - Overview

• Inorganic scintillators

- crystalline structure
- high light yield: up to 40000 ph/MeV
- high Z, varying ρ
- doped & undoped
- mostly slow: decay time ~μs
- expensive (e.g. PWO ~4 €/cm^3)
- good radiation hardness
- applications
  - electromagn. calorimetry
  - medical imaging
  - X-ray spectroscopy

• Organic scintillators

- crystalline, liquid, plastic
- low light yield: up to 10000 ph/MeV
- low Z, ρ ~ 1 g/cm^3
- doped
- fast: decay time ~ns
- relatively inexpensive
- fair radiation hardness (10 kGy/yr)
- applications:
  - trigger, veto
  - time-of-flight
  - tracking
  - sampling calorimeter

The most common inorganic scintillator is sodium iodide activated with a trace amount of thallium [NaI(Tl)].

Energy bands in impurity activated crystal

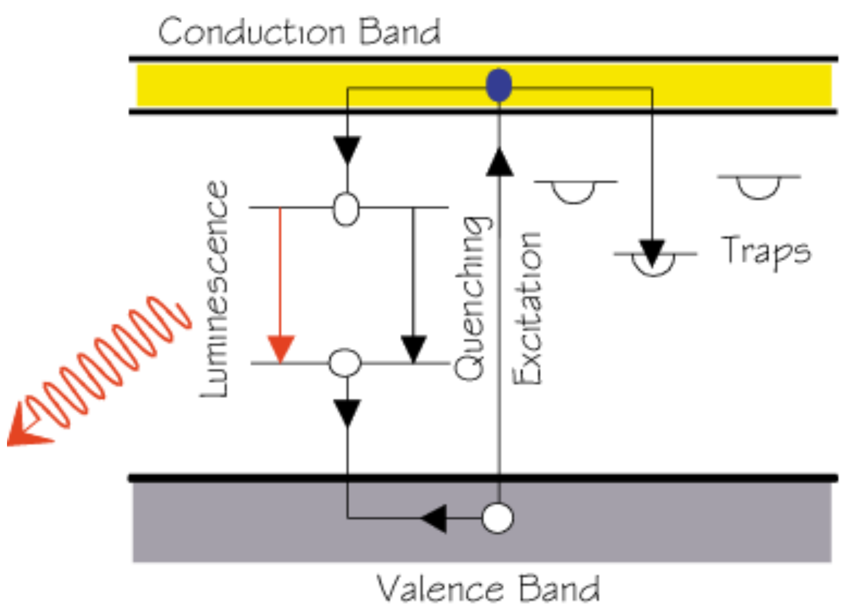

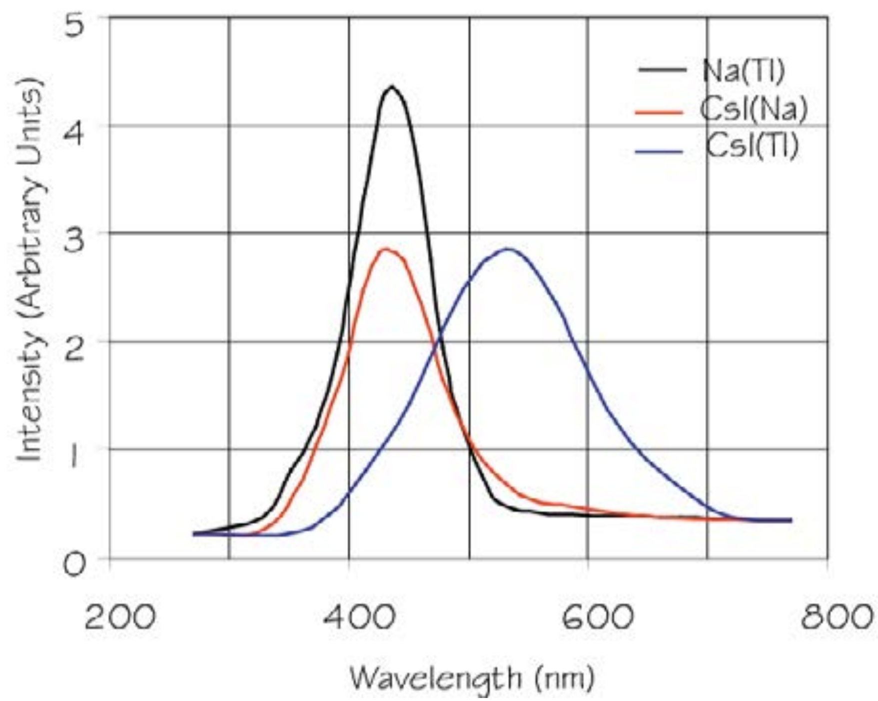

often ≥ 2 time constants:

- fast recombination (ns - µs) from activation center
- delayed recombination due to trapping (100 ms)

6.1 Inorganic Crystalline Scintillators

$PbWO_4$ ingot and final polished CMS ECAL scintillator crystal from Bogoroditsk Techno-Chemical Plant (Russia).

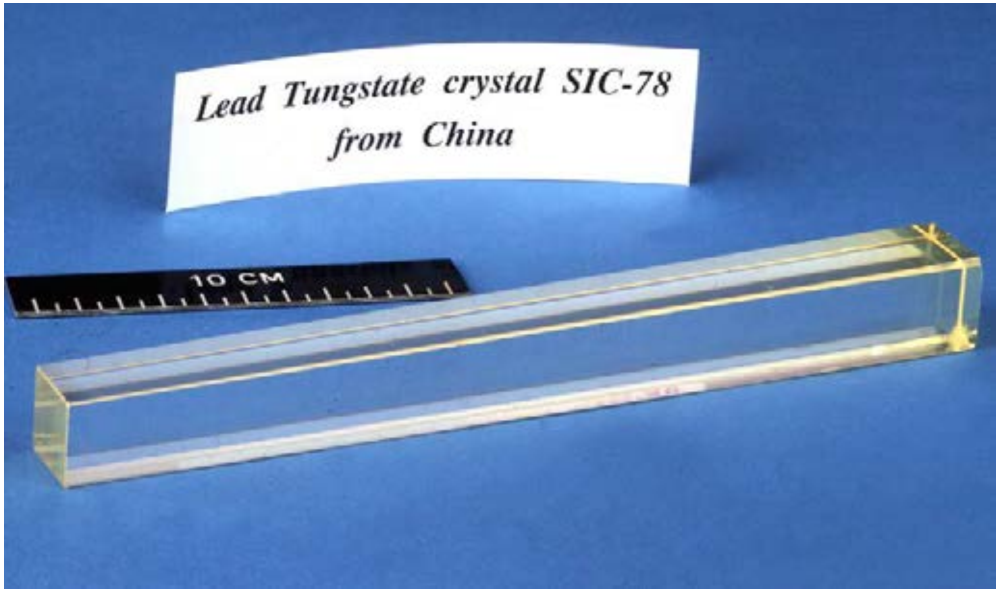

6.3 Liquified Noble Gases: LAr, LXe, LKr

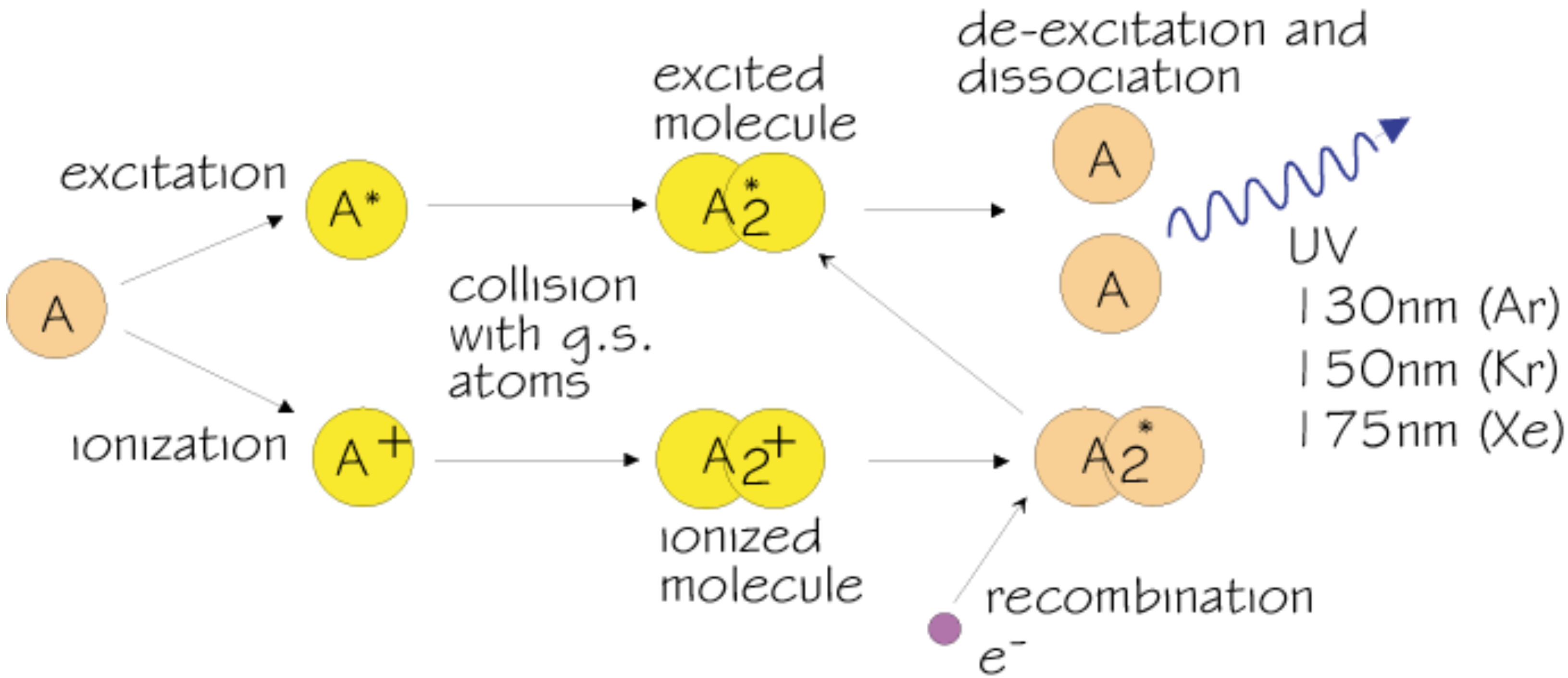

Also here 2 time constants common: from a few ns to 1 s

from C. D'Ambrosio, Academic Training, 2005

6.4 Light Collection

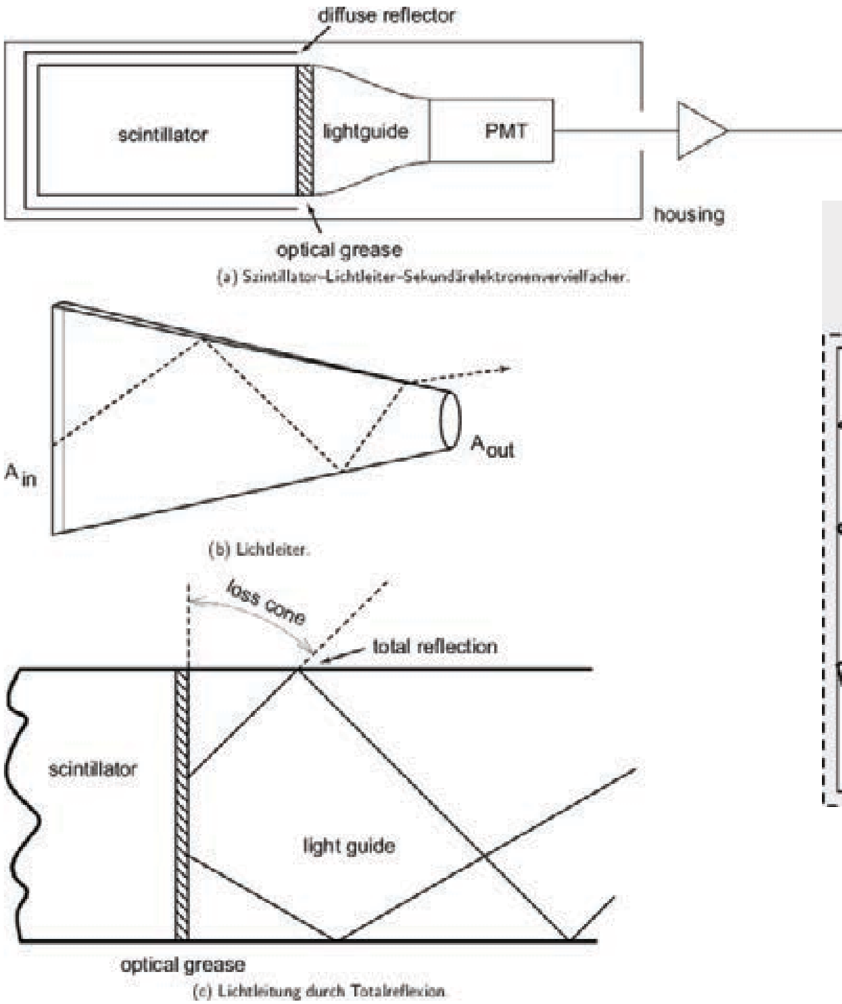

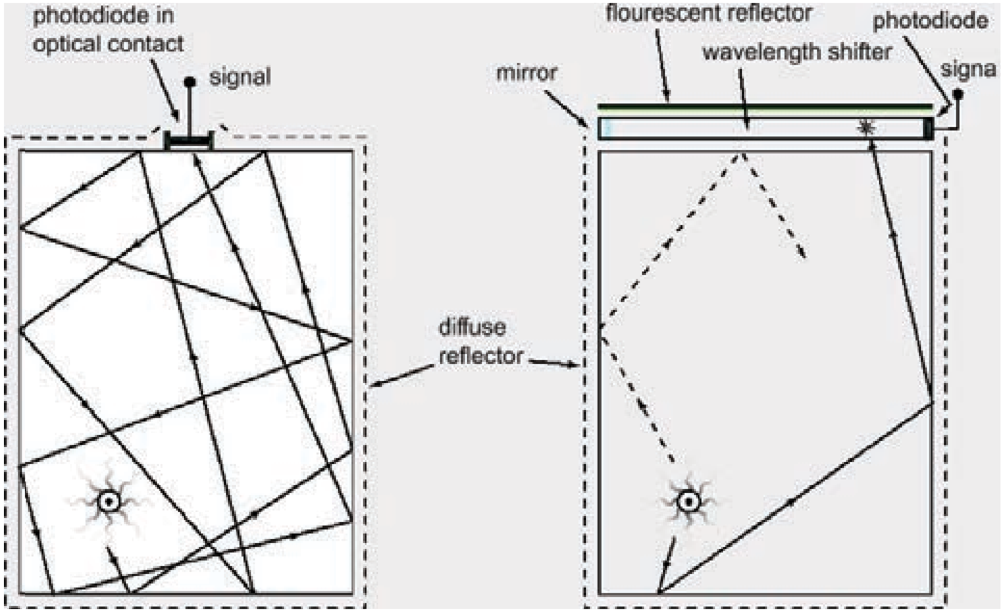

6.4 Light Collection

Geometrical adaptation:

- Light guides: transfer by total internal reflection (+outer reflector)

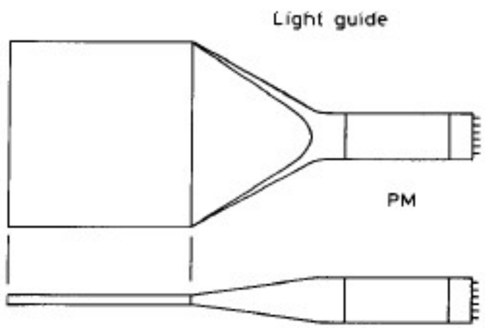

"fish tail"

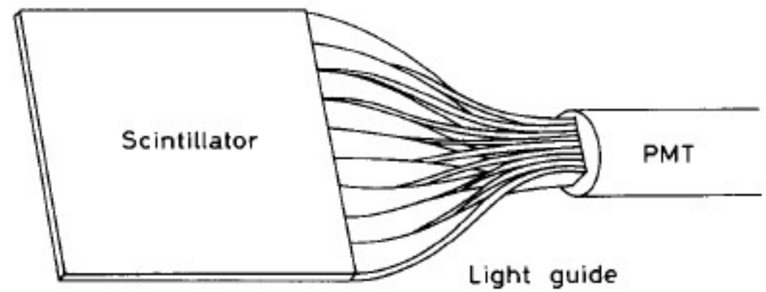

adiabatic

- wavelength shifter (WLS) bars

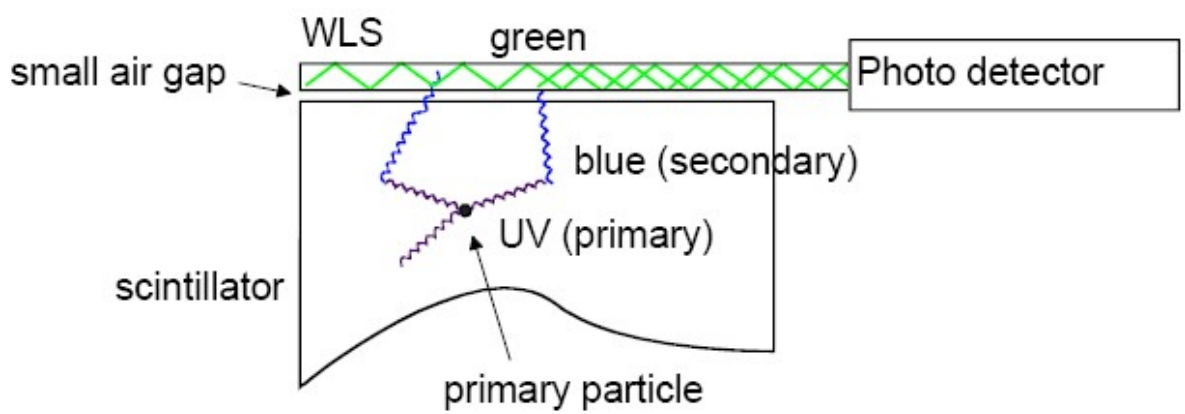

What makes a good scintillator ?

- high conversion efficiency of deposited energy into light

- Transparency for its “own“ (self-emitted) light

- light emission in “useable“ wavelength
  detection of high through light detector (PM or else - later)
- fast decay of emission (high count rates)

time of flight measurement

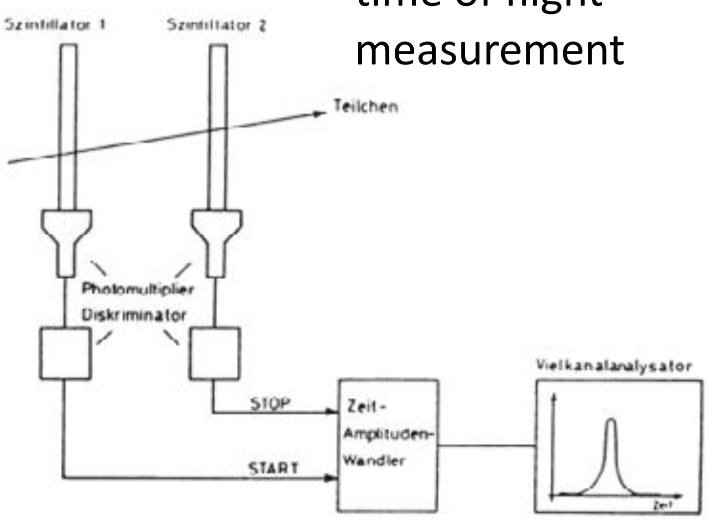

Usage

- Energy measurement:
  amount of light $\propto$ deposited energy
- time measurement
  fast response of scintillators
- particle identification:
  light intensity depends on particle type
  (energy loss according to Bethe-Bloch)

6. Scintillation

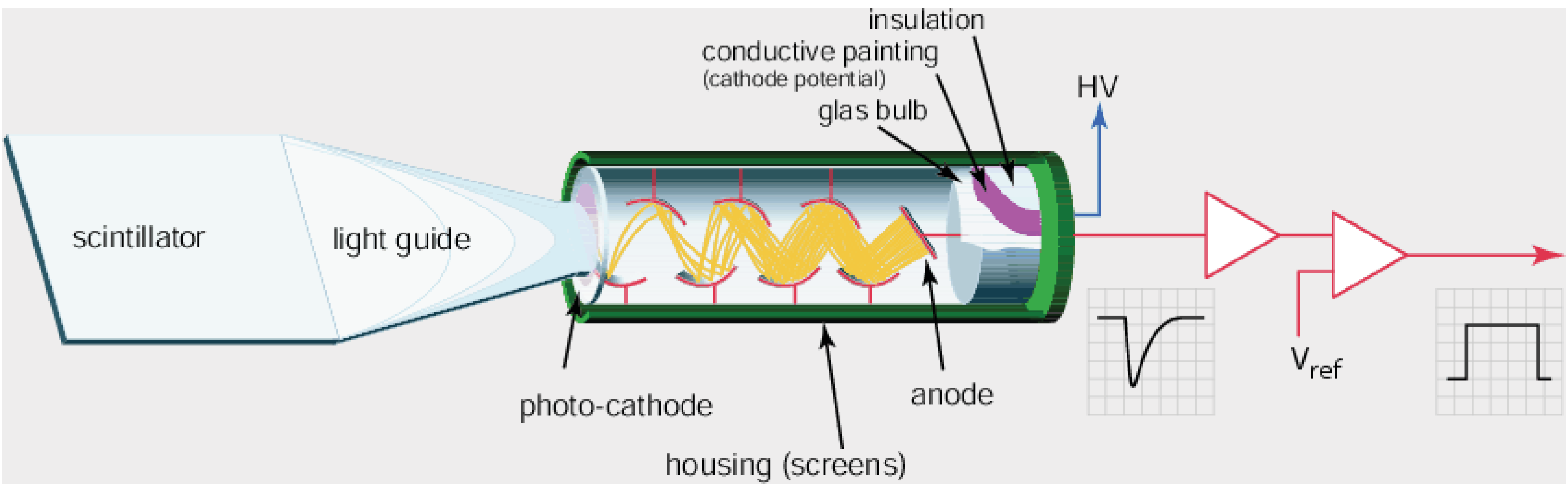

6.5 Scintillating fibre tracking

light transport by total internal reflection

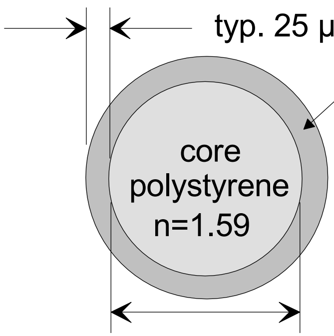

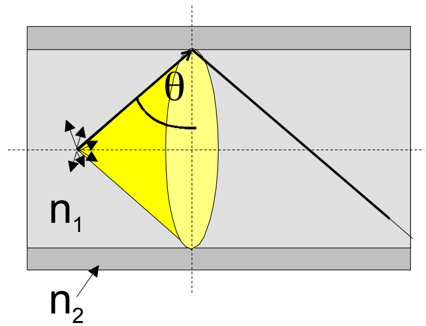

in one direction

$$\theta \geq \arcsin \frac{n_2}{n_1} \approx 69.6^\circ$$

$$\frac{d\Omega}{4\pi} = 3.1\%$$

multi-clad fibres for improved aperture

$$\frac{d\Omega}{4\pi} = 5.3\%$$

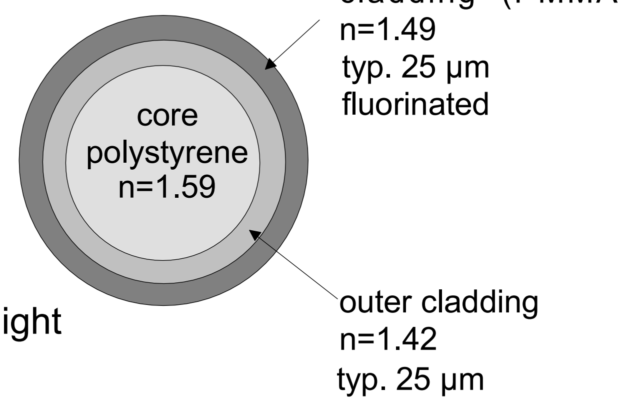

and absorption
length: λ>10 m for visible light

6.5 Scintillating fibre tracking

Exzellenzcluster Universe

Arrangements:

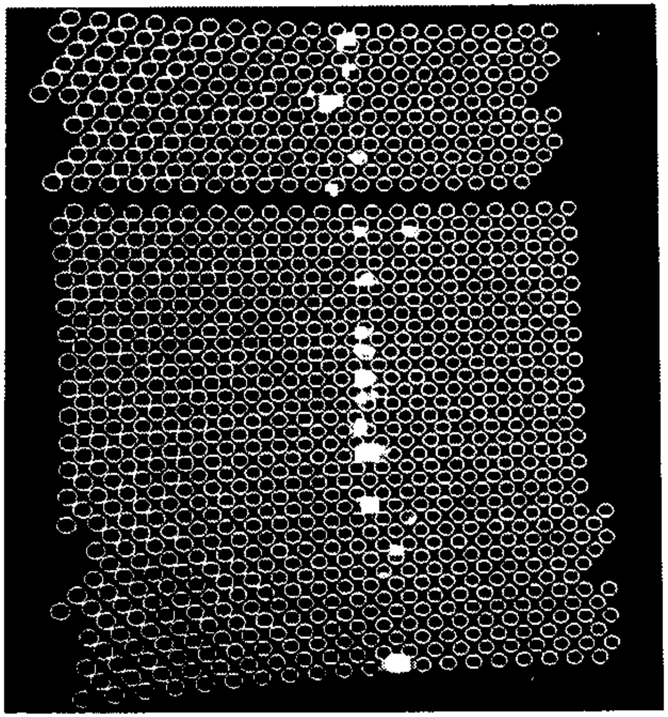

Charged particle passing through stack of scintillating fibres (diam. 1mm)

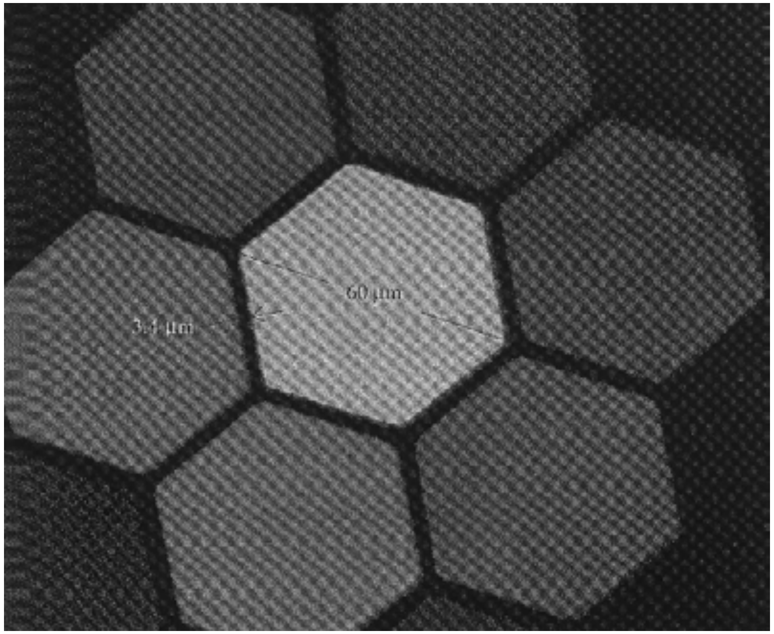

(H. Leutz, NIM A 364 (1995) 422)

Hexagonal fibres with double cladding.

Only central fibre illuminated.

Low cross talk !

6.5 Fibre Tracker for Antimatter Detection in Space

MAPT Technical Overview

- 900-channel active-target spectrometer
- no $\vec{\mathbf{B}}$ field
- scintillating fibers & silicon PM

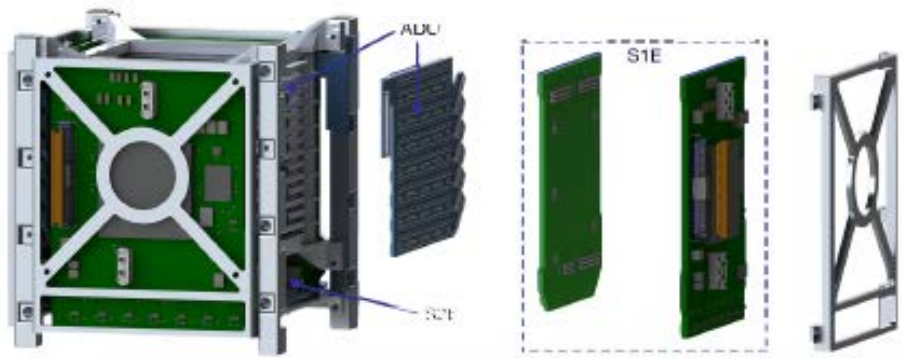

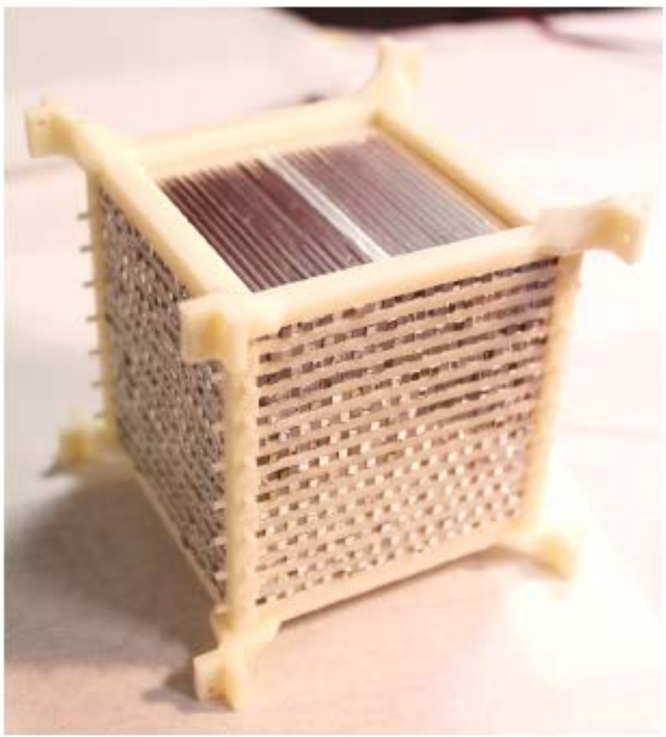

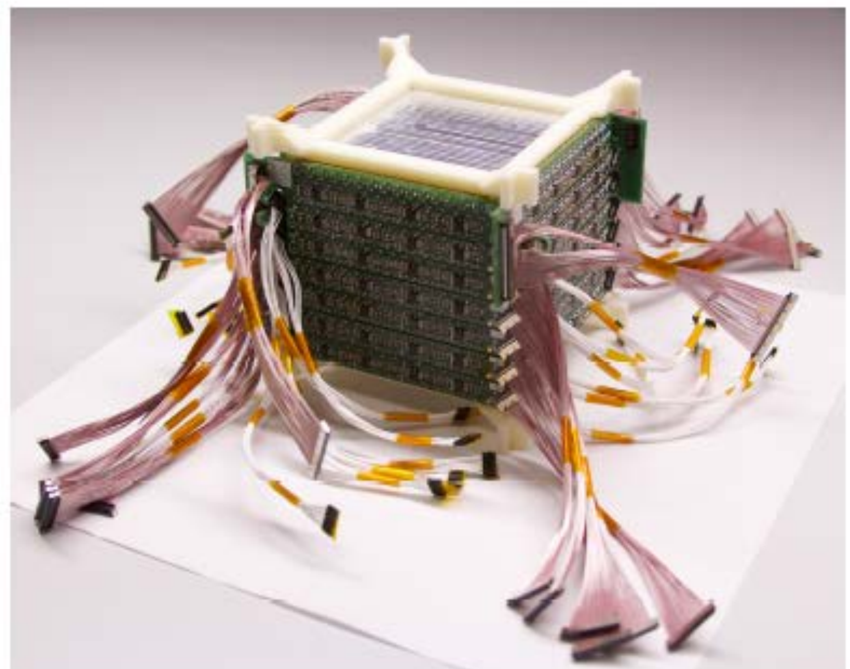

6.6 New Production Methods - 3D Printing

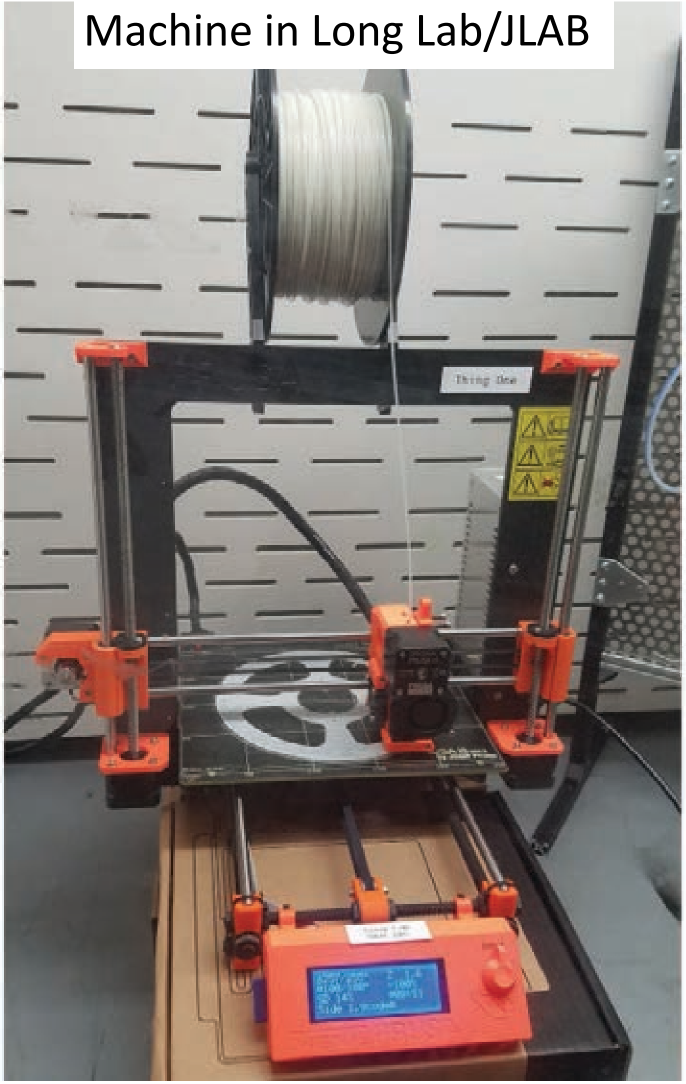

Machine in Long Lab/JLAB

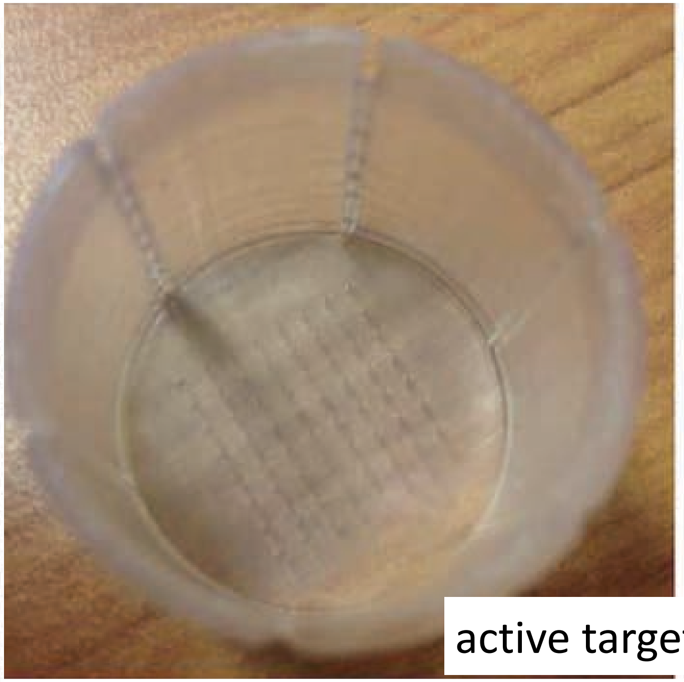

active target cup from A2 experiment

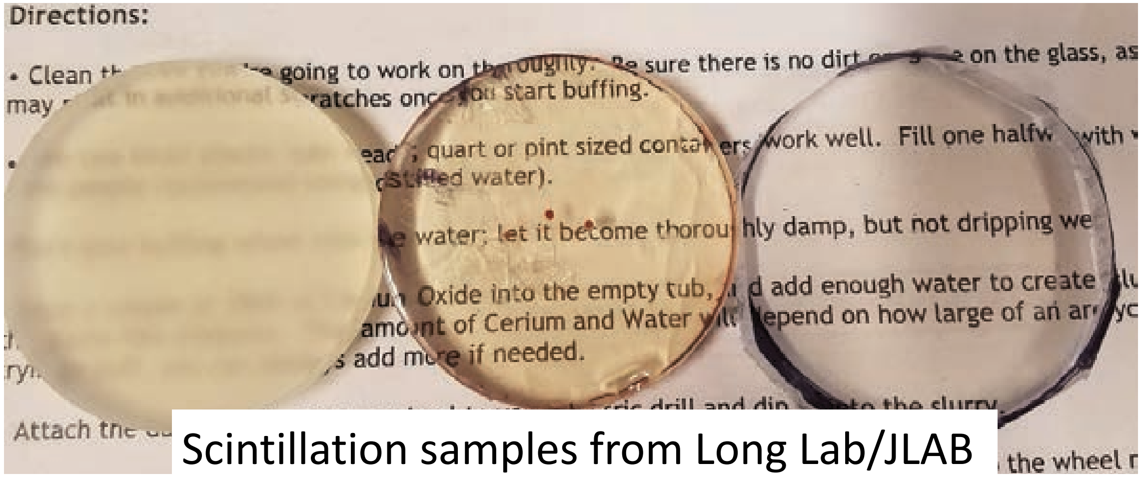

Scintillation samples from Long Lab/JLAB

Recapitulation

- What is an avalanche photo diode ?
  - PIN diode with an extra p+ layer to generate large electric fields for amplifications ($gain_{typ}$: 100)
- What is an organic scintillator and what is it used for ?
  - Polystrene based material with colour centres (e.g. anthracene) and doped with wavelength shifter material for higher transparency
- What is an inorganic scintillator and what is it used for ?
  - Crystalline material typically with doping (e.g. Tl) for higher transparency
- What is a SiPM and what are the benefits ?
  - Matrix arrangement of APDs. Digital readout (# of APDs fired). High quantum efficiency, fast, little noise, cheap, good linearity (scales with APD density)
- How is an optical fibre built-up ?
  - scintillating core with cladding(s) for well defined transitions of refractive index. Light propagation through total internal reflection.

7. Calorimetry

High energy particles form showers

- electromagnetic
- hadronic

important: full deposit (absorption) of energy

For charged and neutral particles:

- $e^{\pm}$ and hadrons
- neutrals particles (n, γ)

conversion of energy into

- **ionisation**
- **excitation of detector material**

Energy determination through detection of ionisation, Cherenkov light, scintillation. Best: proportional to particle energy

7. Calorimetry

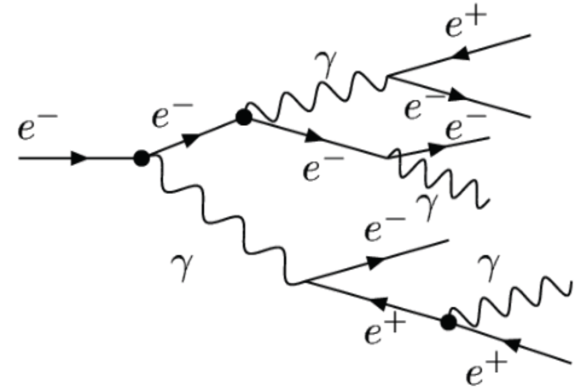

Electromagnetic shower: **Bremsstrahlung** by **e±** and **pair production** → Material with **high charge number Z**

Homogeneous oder stapled set-up of a calorimeter:

Homogen: BGO*, $PbWO_4$**, anorganic scintillators ΔE/E ~ liquid noble gases ΔE/E ~ 10%

path length of all particles is proportional to initial energy E_0

Foto:

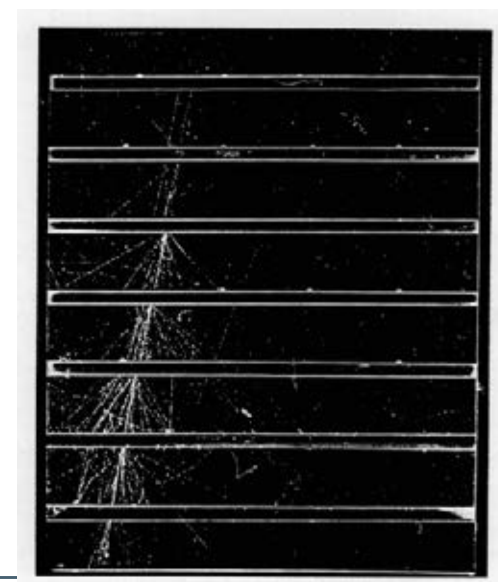

stapled set-up: scintillator - Pb layers

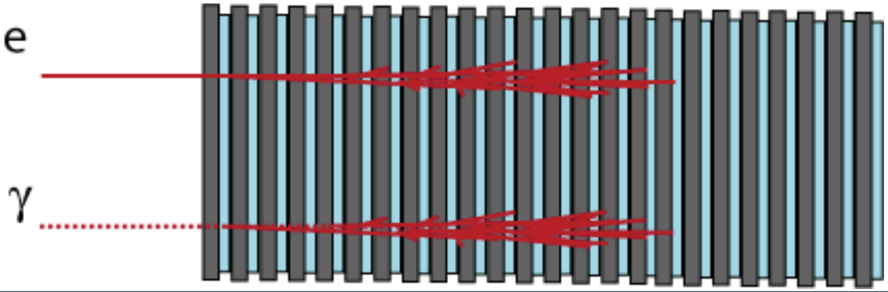

*BGO: Wismut-Germanium-Oxid **$PbWO_4$: Bleiwolframat

Hadronic shower:

- material with large A
- strongly interacting primary particles
- inelastic hadronic interaction

- cascade of pions and nucleons
- pions: 1/3 π^+, 1/3 π^-, 1/3 π^0
- fast electromagnetic component
- slow hadronic component

- hadronic calorimeters are very massive

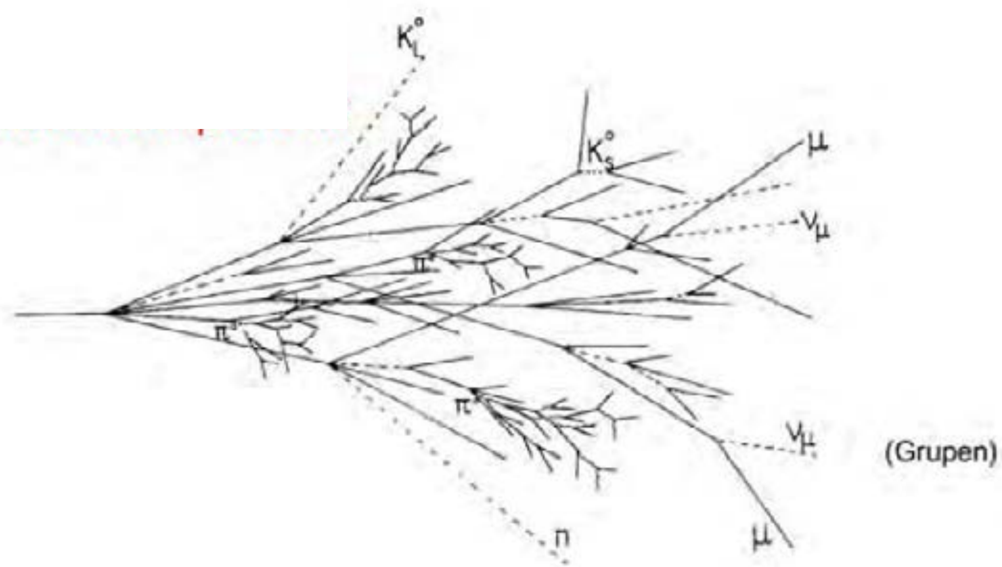

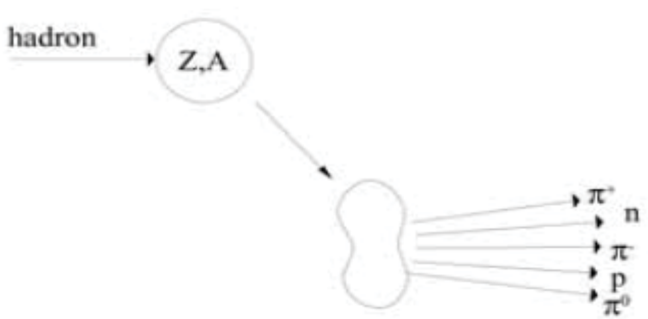

characteristic reaction length

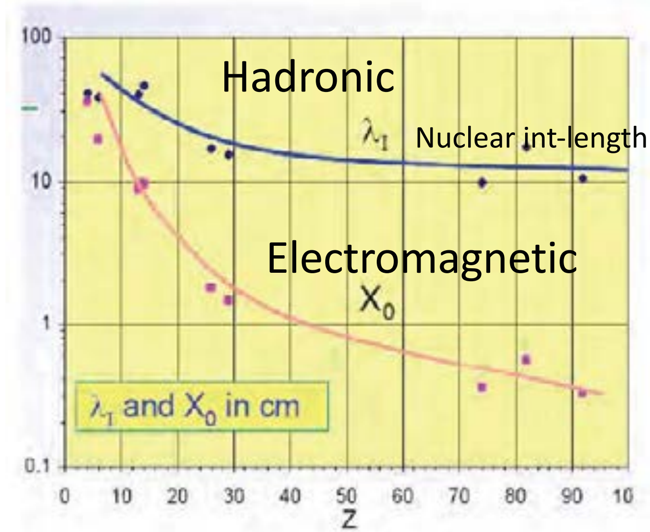

Simple model:

- E > 1 GeV ⇨ processes become ~ energy-independent
- total number of particles after $t\, X_o$ = t radiation lengths: $N \approx 2^t$
- each with energy $\frac{E_0}{2^t} = E(t)$

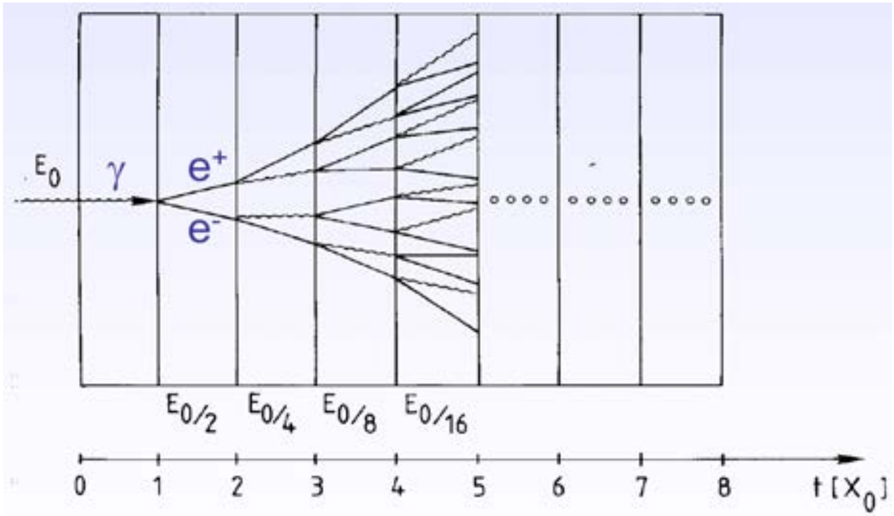

- Shower development stops when $E(t) < E_c$ (energy loss mainly by collisions)

$$E(t_{\max}) = \frac{E_0}{2^{t_{\max}}} \overset{!}{=} E_c \qquad \Rightarrow t_{\max} = \frac{\ln(E_0/E_c)}{\ln 2}$$

i.e. length of calorimeter increases only logarithmically with E_0

- Number of particles in shower maximum: $N_{\max} \approx \frac{E_0}{E_c} \propto E_0$

Quantitative description: Monte Carlo simulations (EGS4, GEANT4)

7.1 Longitudinal Energy Deposition

Empirical parameterization ($t > 1$):

$$\frac{\mathrm{d}E}{\mathrm{d}t} = E_0 b \frac{(bt)^{a-1} e^{-bt}}{\Gamma(a)}$$

with maximum at

$$t_{\max} = \frac{a-1}{b} = \ln \frac{E_0}{E_c} \pm 0.5 \quad \binom{\gamma}{e}$$

a, *b*: material parameters

$b \approx 0.5$

95% of total energy is contained in

$$t_{95\%} \approx t_{\max} + 0.08Z + 9.6$$

Determines length of calorimeter !

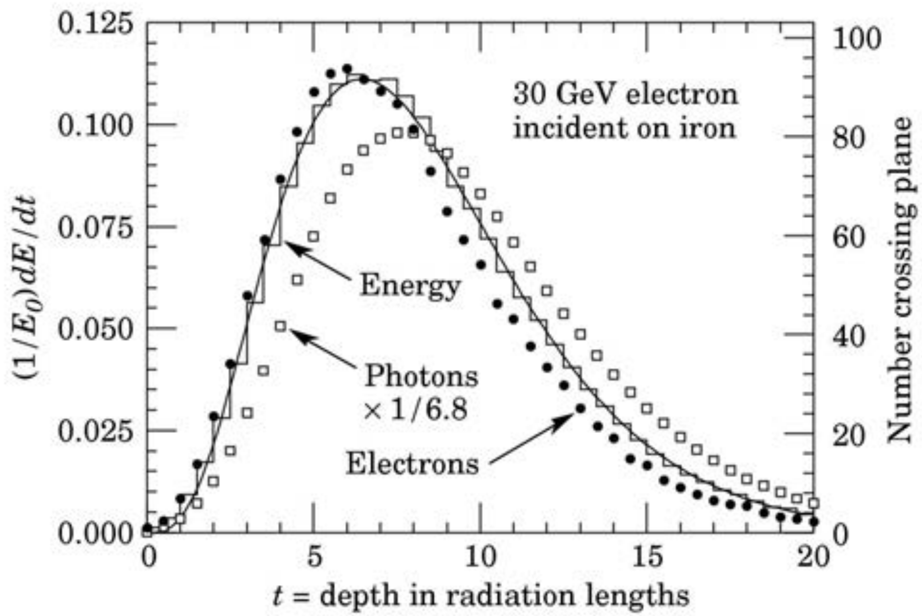

EGS4: 30 GeV electron in Fe

[Particle Data Group, Phys. Lett. B 592, 1 (2004)]

7.1 Transverse Energy Deposition

Increase of lateral dimension with t:

- Multiple scattering of e^- near critical energy
- Finite opening angle between e^- and e^+ from pair production
- Large range of Bremsstrahlung photons

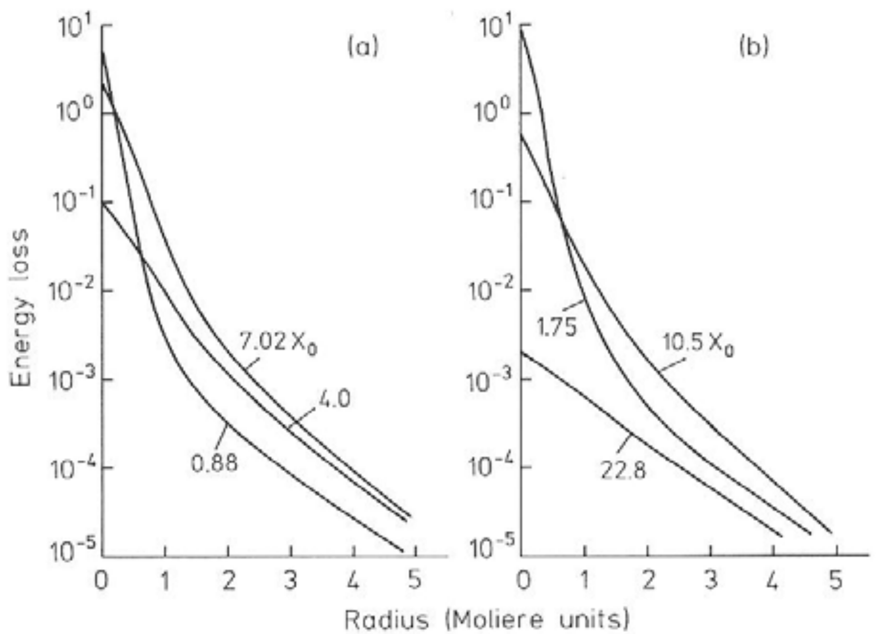

Transverse energy deposition (1 GeV electron in Pb)

In: [W.R. Leo, Techniques for Nuclear and Particle Physics Experiments, Springer (1994)]

Characteristic parameter: Molière radius

$$R_M = \frac{E_s}{E_c} \cdot X_0 \,, \quad E_s = \sqrt{\frac{4\pi}{\alpha}} mc^2 = 21.2\,\mathrm{MeV}$$

Scales as X_0 ⇨ independent of material if expressed in units of X_0

7.1 Transverse Energy Deposition

$$\left.\begin{aligned} X_0 &\propto \frac{A}{Z^2} \\ E_c &\propto Z^{-1} \end{aligned}\right\} \Rightarrow R_M \propto \frac{A}{Z}$$

~90% of shower energy contained in $R < 2R_M$

7.2 Electromagnetic Calorimeters

Challenge:

- Shower containment (20-35 radiation length) : use high Z material
- High energy resolution: reduce shower fluctuations: optimise on active material
- High position resolution - lateral segmentation

Solution:

- Homogeneous calorimeters
  - LySBO, CsI (NaI) crystals, $PbWO_4$: collect scintillation light from charged shower particles
  - Pb-glass : collect Cherenkov light from charged shower particles (fast)
- highly longitudinally segmented structures
  - LAr : collect/count charged particles from shower

Resolution: fluctuations in deposited energy in active sampling layers

- sampling fraction : ratio active / passive material - f_{samp} : sampling fraction for MIPS
- sampling frequency : # sampling elements - d: thickness of active sampling layer

$$\frac{\sigma}{E} = \frac{a}{\sqrt{E}} \text{ with } a = 0.027 \cdot \sqrt{\frac{d}{f_{samp}}}$$

(for non-gaseous calorimeters)

7.2 Electromagnetic Calorimeters

Energy resolution of homogenous electromagnetic calorimeters :

$$\frac{\sigma_E}{E} = \frac{N}{E} + \frac{S}{\sqrt{E}} + C$$

- N: noise term - electronic noise, pile-up
- S: stochastic term - light collection efficiency, stochastic fluctuations of light yield, collection..
- C: constant term - intrinsic non-uniformities, radiation damage - calibration issues

Effect on experiment: Position resolution vs energy resolution: $\text{Higgs} : H_0 \rightarrow \gamma\gamma$

$$M = \sqrt{2E_1E_2(1-\cos\theta_{12})}$$

CMS: excellent energy resolution

ATLAS: excellent position resolution

→ Mass resolution for Higgs about the same for both experiments

ATLAS electromagnetic Calorimeter

Accordion geometry absorbers immersed in Liquid Argon

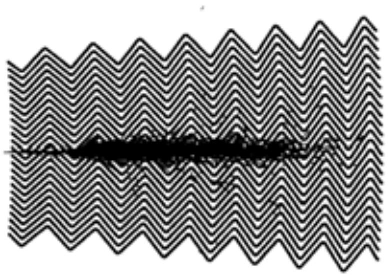

Liquid Argon (90K)

+ lead-steal absorbers (1-2 mm)

+ multilayer copper-polyimide readout boards

→ Ionization chamber.

1 GeV E-deposit → 5 x 10^6 e^-

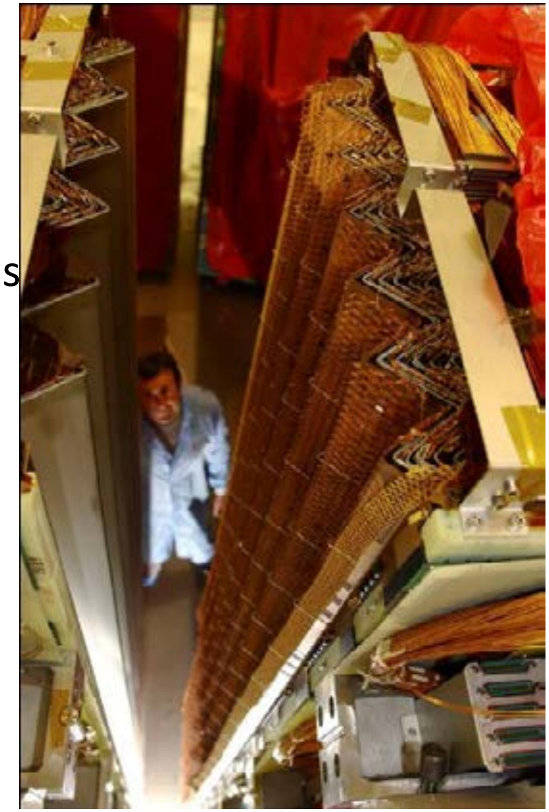

- Accordion geometry minimizes dead zones.
- Liquid Ar is intrinsically radiation hard.
- Readout board allows fine segmentation

Test beam results: $\sigma(E)/E = 9.24\%/\sqrt{E} \oplus 0.23\%$

sampling fraction: $F = \frac{\Delta E_{LAr}}{\Delta E_{LAr} + \Delta E_{Pb}} \simeq 19\%$

7. CMS Electromagnetic Calorimeter

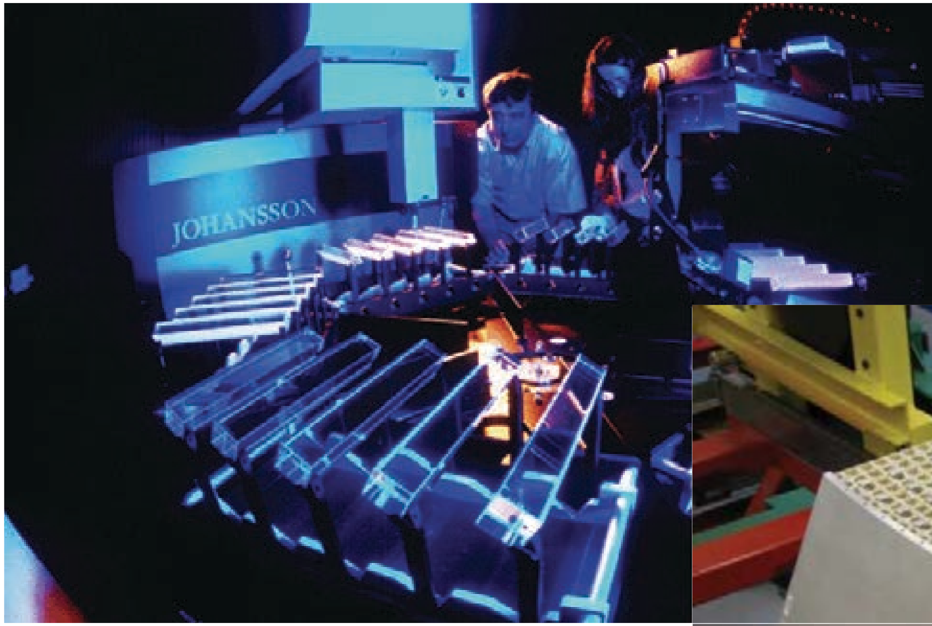

- 61200 lead tungstate ($PbWO_4$) scintillating crystals
  - $X_o = 0.89$ cm; $R_M = 2.19$ cm
- APD readout

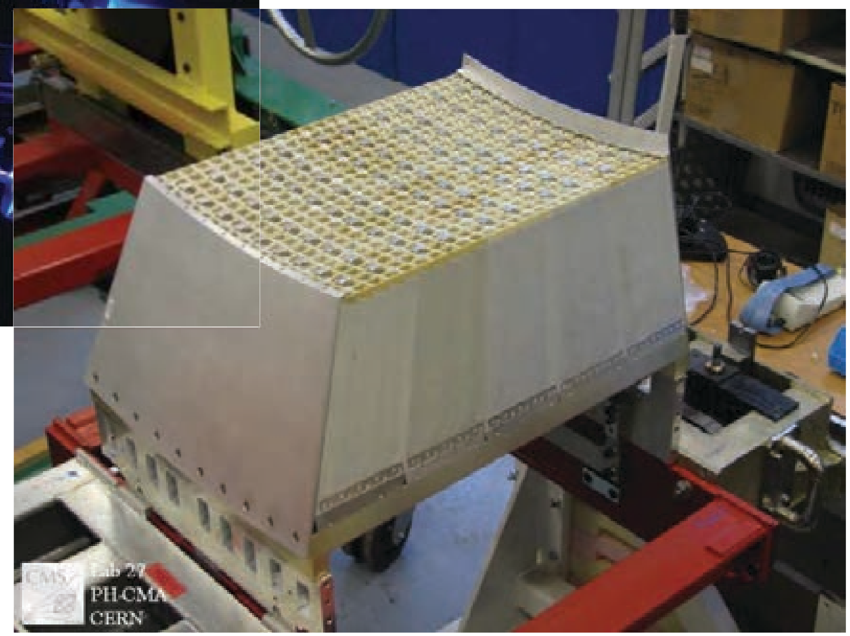

CMS: Test beam results: $\frac{\sigma_E}{E} = \frac{2.8\%}{\sqrt{E[\mathrm{GeV}]}} \oplus \frac{12\%}{E[\mathrm{GeV}]} \oplus 0.3\%$

Shashlik calorimeter: sandwich of W/LYSO crystals with longitudinal WLS fibre readout

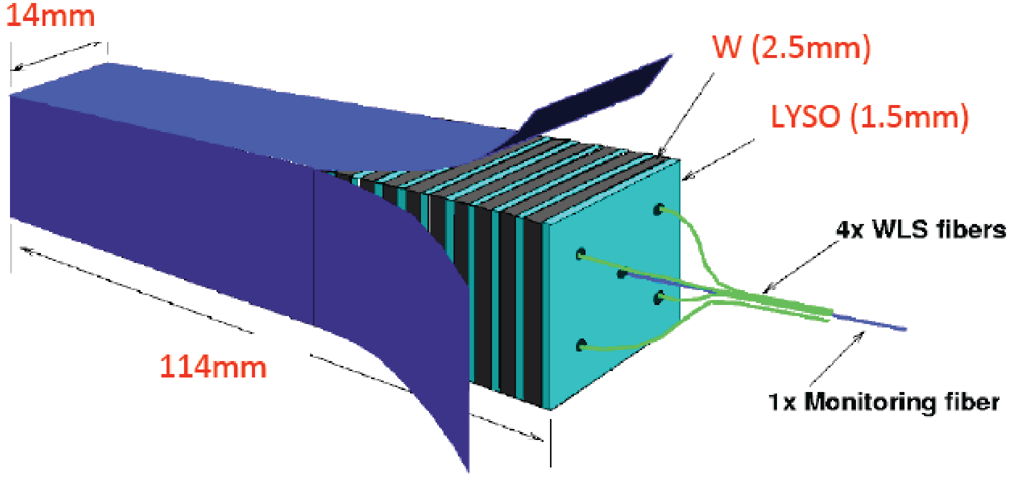

Shower development:

- according to strong interaction : unit is λ_I (scales with mass number A)
- pion production including π^0
- electromagnetic shower component du to $\pi^0, \eta \rightarrow \gamma\gamma$
- nuclear breakups generate neutrons and fragments (may escape detection)
- nuclear binding energy is „lost"
- $\pi^{\pm}$ decay generates ν escaping

large fluctuations in fraction of visible hadronic component
→ sampling calorimeter sufficient

Detector sheet with position resolution:
→ determine shower position from reconstruction

bit: owing to electromagnetic $\pi^0, \eta \rightarrow \gamma\gamma$ component → no typical hadronic shower profile

7.3 Hadronic Calorimeters

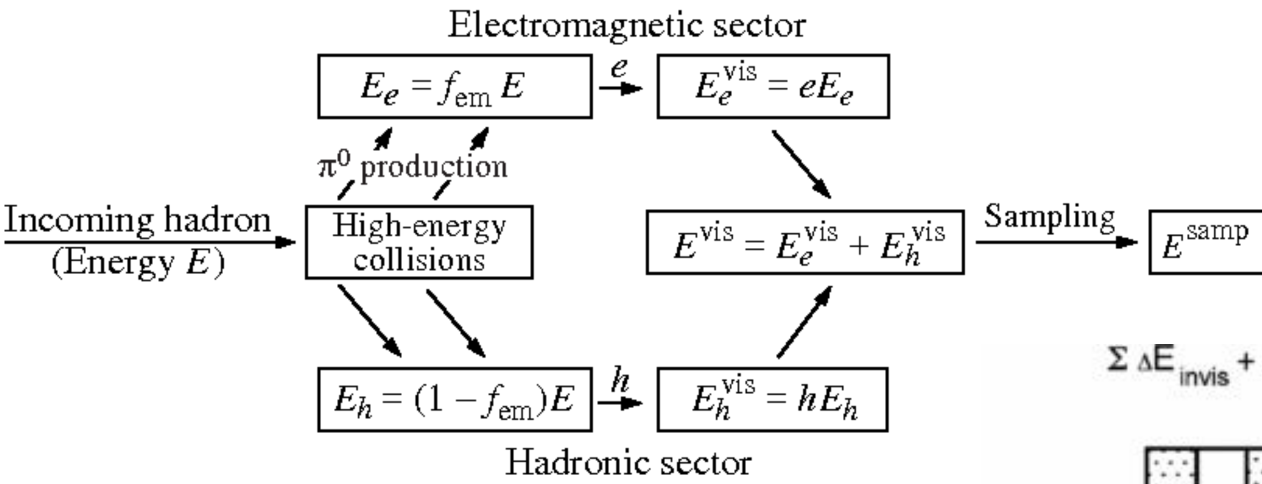

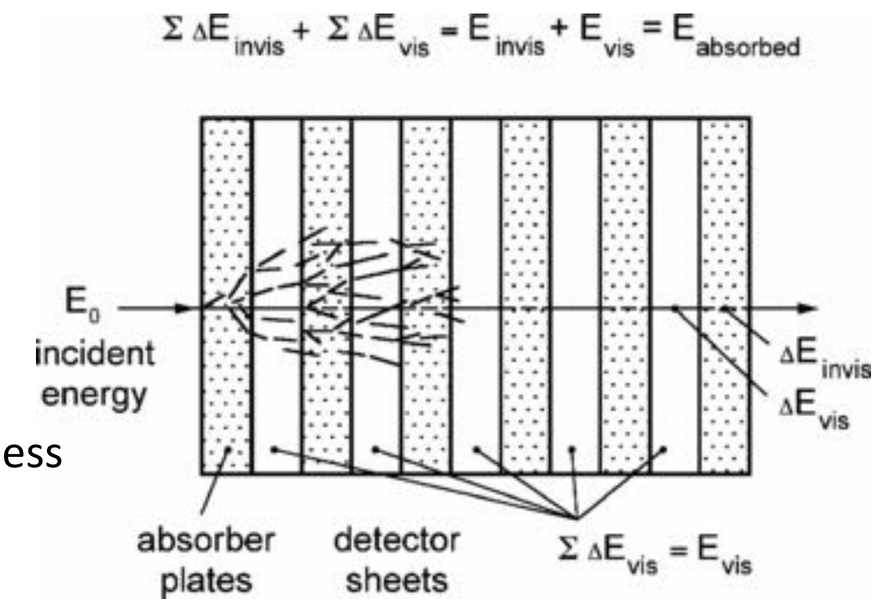

- 99% longitudinal containment requires a thickness
  - 5 λ_I at 20 GeV to 8 λ_I at 150 GeV
- Hadronic energy resolutions of 1% requires
  - longitudinal shower containment at the 99% level
  - lateral containment of 98% or better
- Resolutions: typically

$$\frac{\sigma_E}{E} \approx \frac{(0.7 - 1)}{\sqrt{E}}$$

7.4 Compensating Hadronic Calorimeters

Challenge: Use ONE calorimeter for electromagnetic AND hadronic showers

Problem:

- electromagnetic and hadronic components have different efficiency for signal production ϵ_e and ϵ_{h}
- pions and protons have different signal response functions (e.g. baryon # conservation)
- electromagnetic fraction is energy dependent (and different for π and p)
- large fluctuations in electromagnetic component f_{em}

$$< f_{em} > = 1 - [E/E_0]^{k-1}$$

E_0 is material dependent (0.7-1.3 GeV)
k: 0.82 for pions, smaller for protons

- HCAls become strongly non-linear

CMS foreward cal

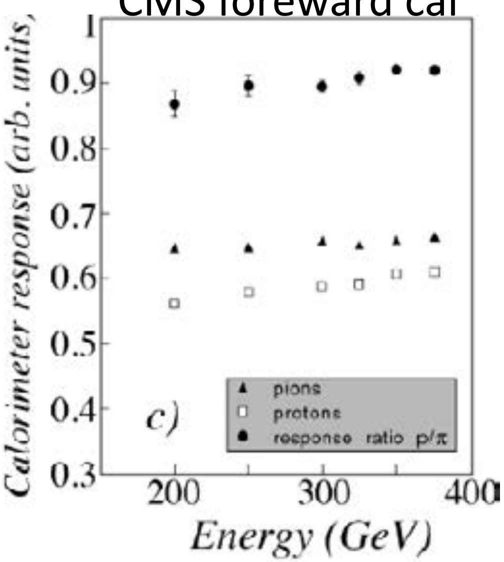

Compensation: $\epsilon_e = \epsilon_h$

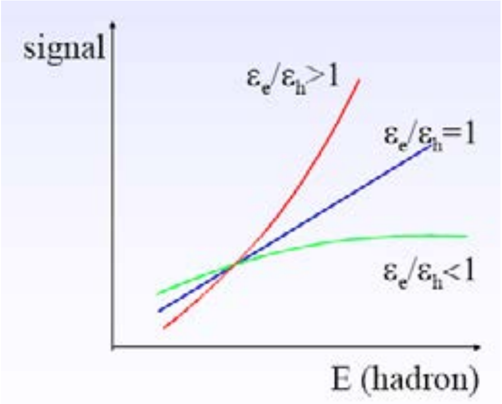

7.4 Compensating Hadronic Calorimeters

ZEUS calorimeter: Uranium scintillator (compensated)

- Uranium has small binding energy (reduced invisible fraction)
- Teflon coating of uranium plates (n-p elastic scattering)

ATLAS calorimeter:

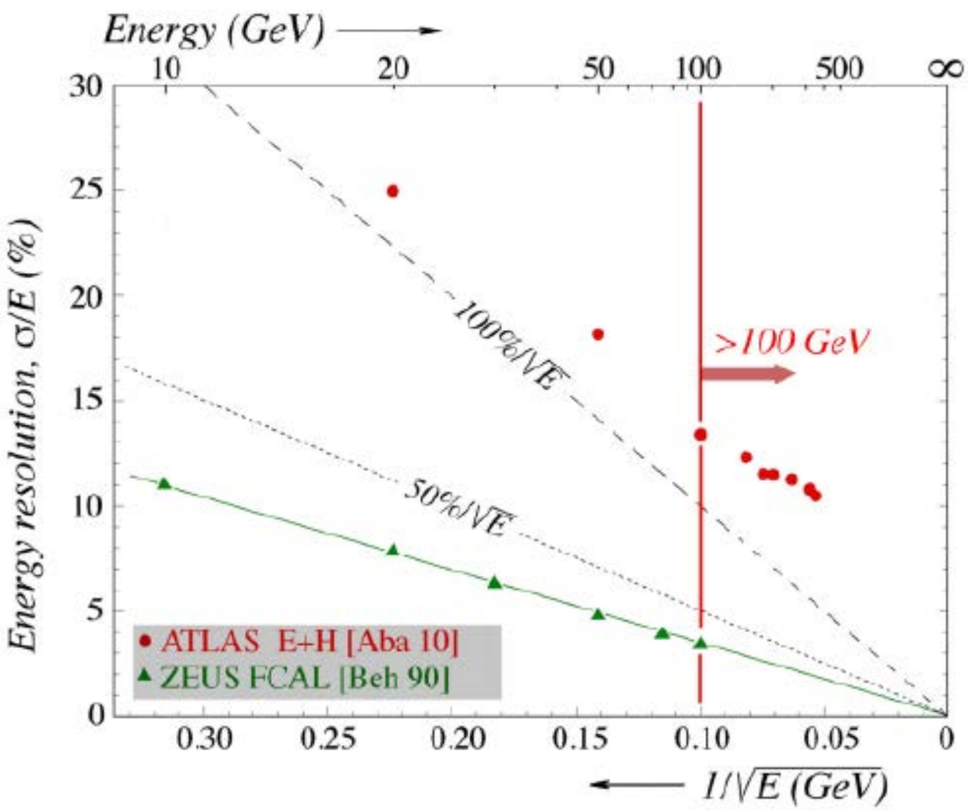

7.4 Compensating Hadronic Calorimeters

How to achieve compensation ?

- enhance response to hadronic shower component
  - catch neutrons through teflon coating of passive material ($n-p$ elastic scattering)
- reduce response to electromagnetic component
  - magic mix: choose ratio of active to passive material to be 1:4
  - use high Z absorber material

Example: SpaCal calorimeter : Pb-scintillating fibre system has excellent hadronic resolution

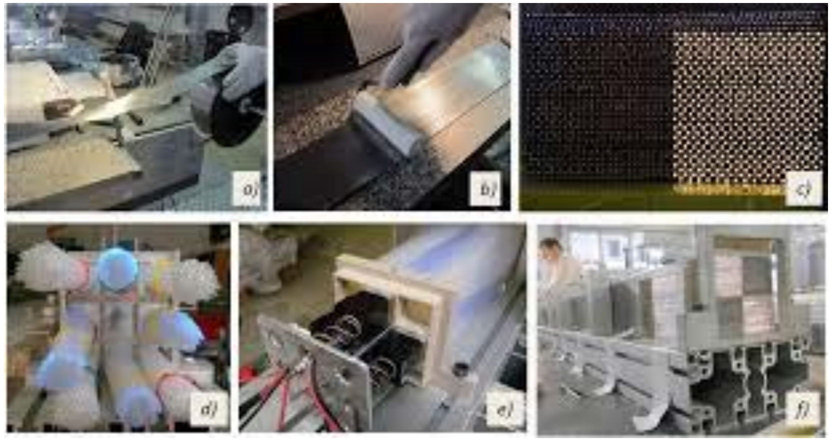

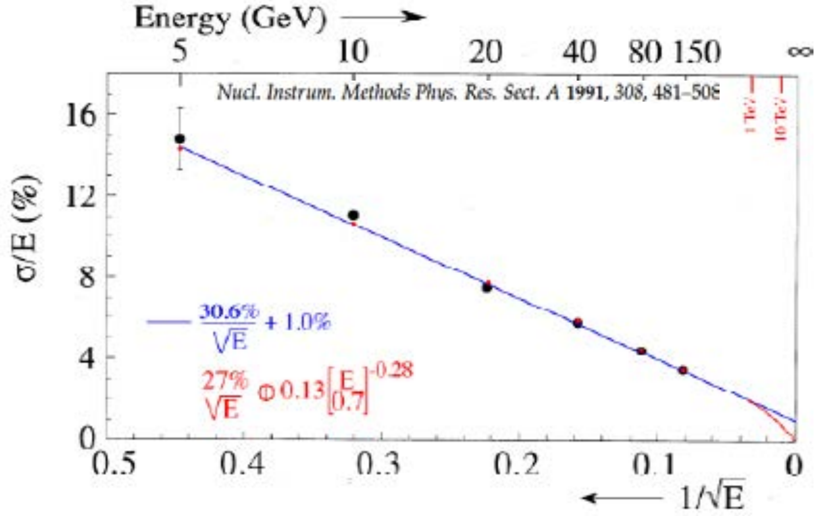

7.4 Combined Calorimeters

Challenge: Use ONE calorimeter electromagnetic AND hadronic showers

Problem:

- Separation of electron and hadron showers (PID)
- saturation due to nuclear fragments (non-MIP)
- shower leakage (longitudinal/lateral)

electron/hadron separation:

- longitudinal segmentation: hadron showers start later (deeper in calorimeter)
- lateral segmentation and dual read-out
    - quartz fibres measure Cherenkov light by electrons/positrons
    - scintillating fibres measure light from any particle
    - ratio and timing give clean indication for e/h separation

Best (test beam) performance so far: DREAM collaboration

- Tungsten/fibre/quartz fibre RO with SiPM
- fully compensating calorimeter
- measure f_{em} (doesn’t work for jets)

7.4 Combined Calorimeters

The DREAM calorimeter

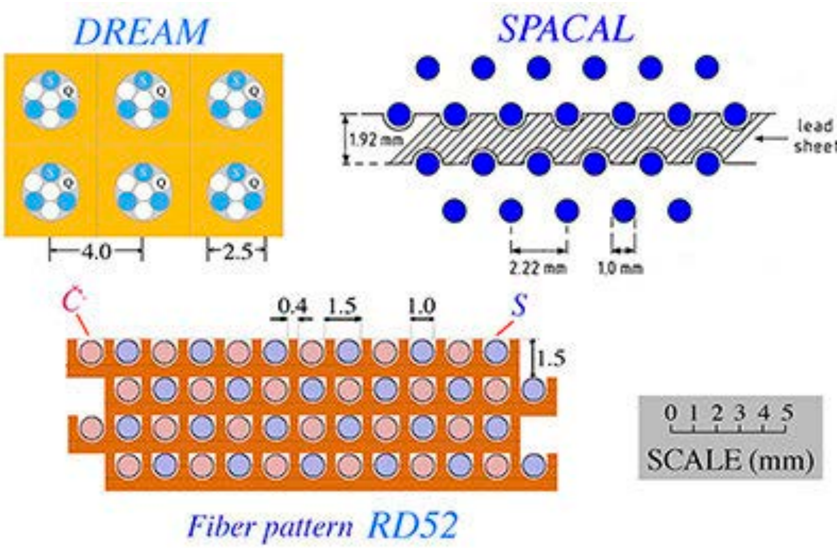

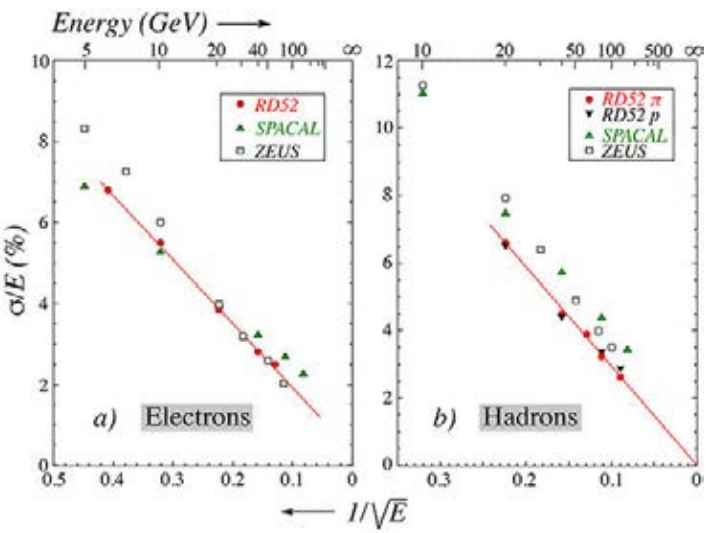

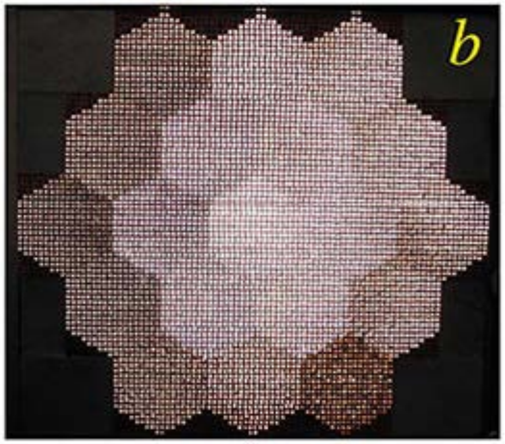

7.5 Calorimeters for Particle Showers

Calice: a particle tracking calorimeter

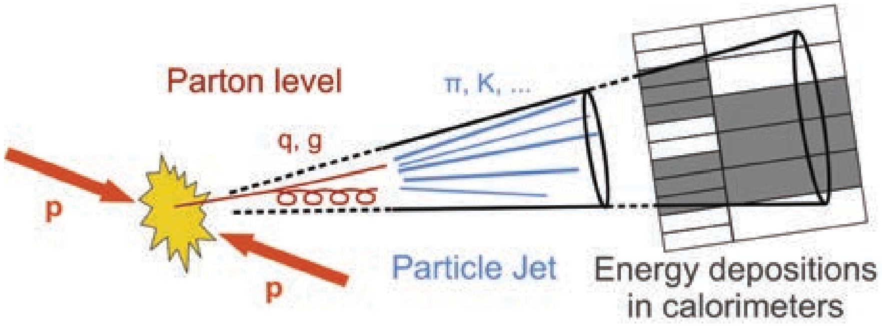

7.6 Technological Developments

Production of large size SpaCal systems:
embed scintillating fibres into a granular tungsten powder and epoxy (fixation)
use SiPM readout

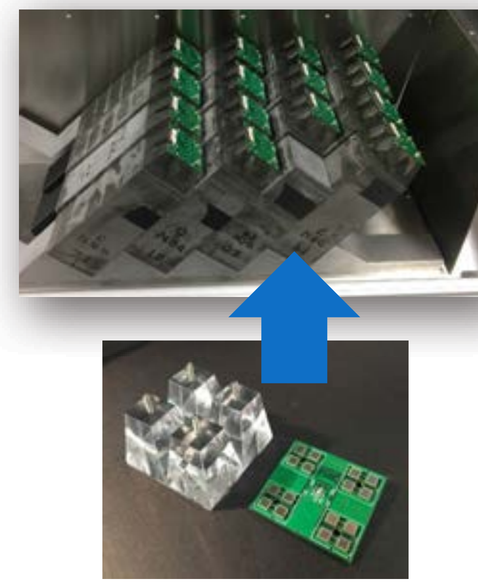

Initial R&D @ UCLA, Prototyping @ UIUC & BNL

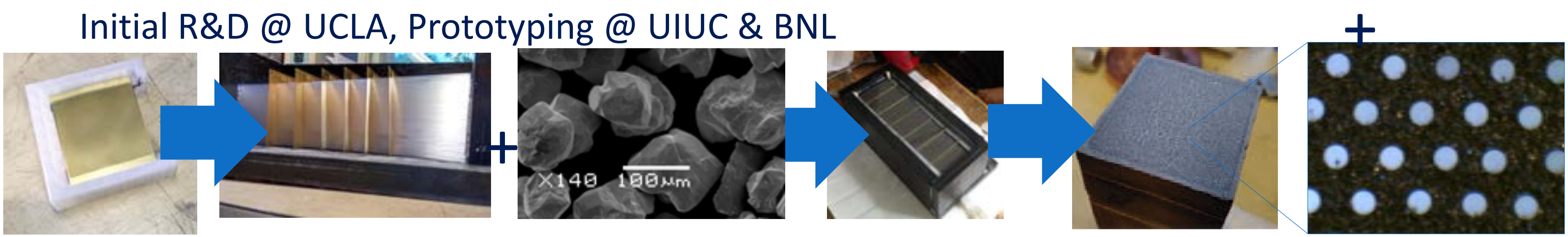

7. Calorimetry - Principle Arrangements

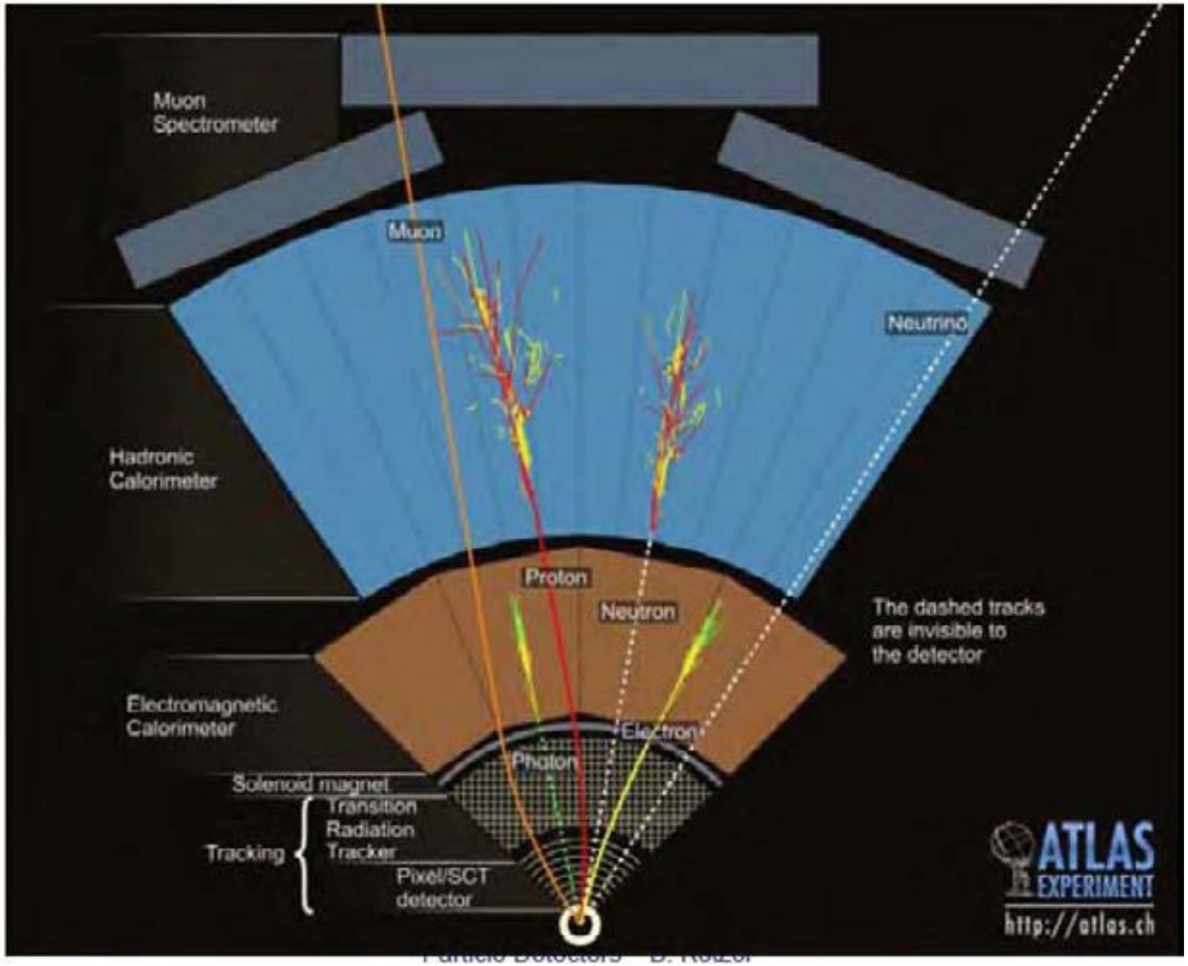

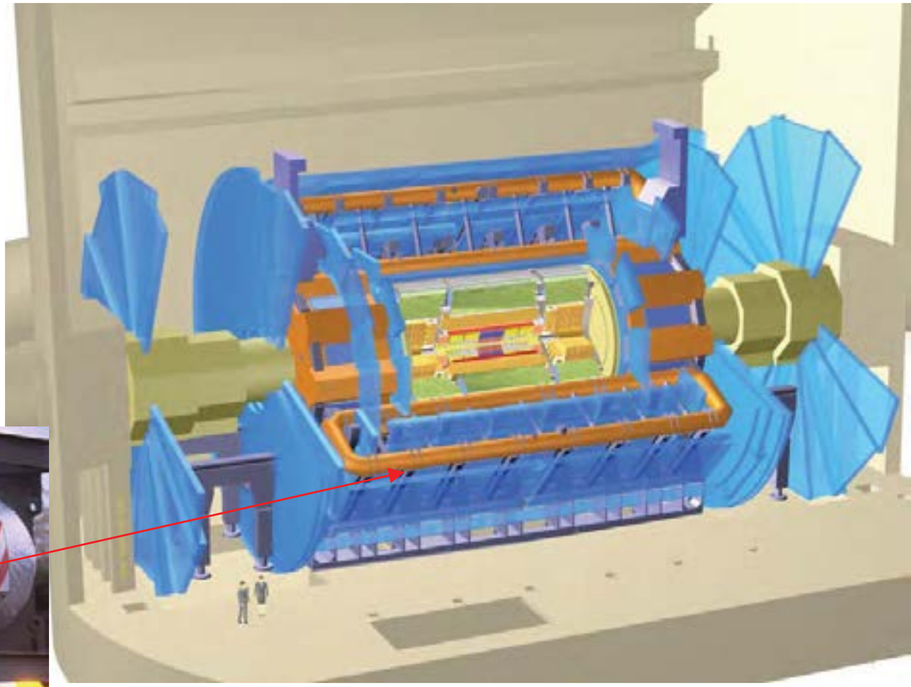

CONVOI EXCEPTIO
8675 BDF

Principle

- Generate supersaturated liquid (expansion of a liquid)
- Ionisation clusters are condensation nuclei → bubbles
- Flashlight illumination and light reflection at bubble surface

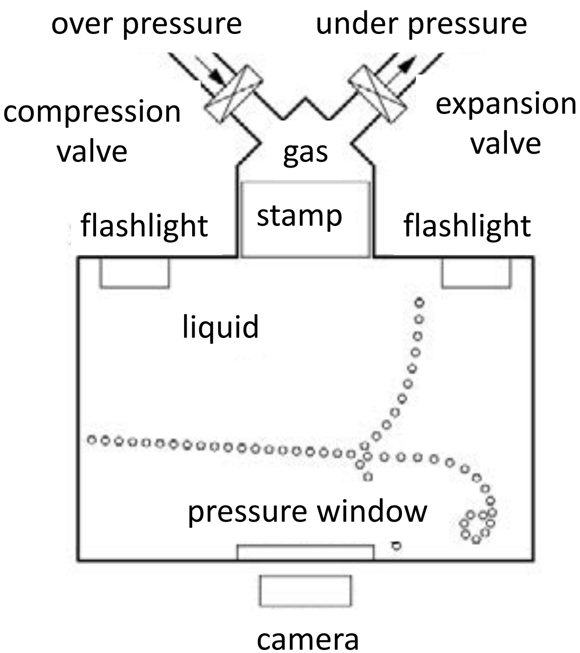

principle

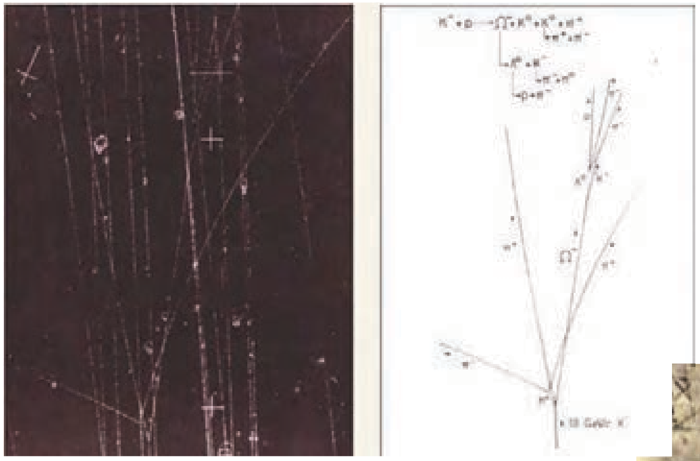

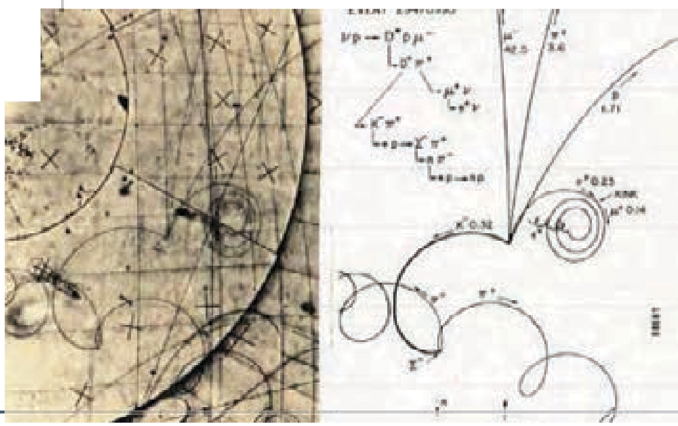

8.0 Bubble Chambers II


Fire alarm at BNL A102I0057
Rights Managed

Foam bath accident at BNL
fire alarm at the hydrogen
bubble chamber

Discovery of Ω^-
80" bubble chamber at
BNL

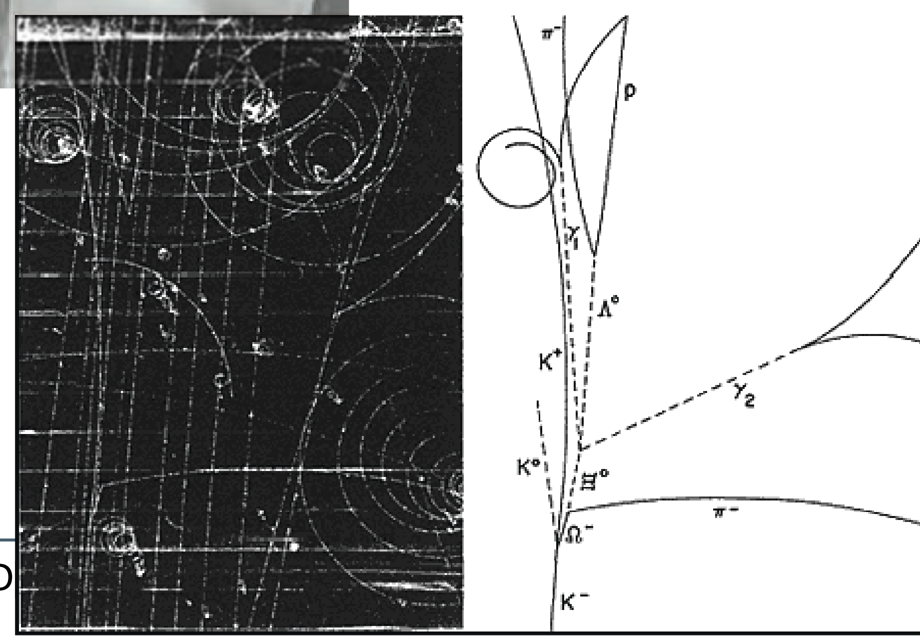

8.0 Inventor of Bubble Chamber

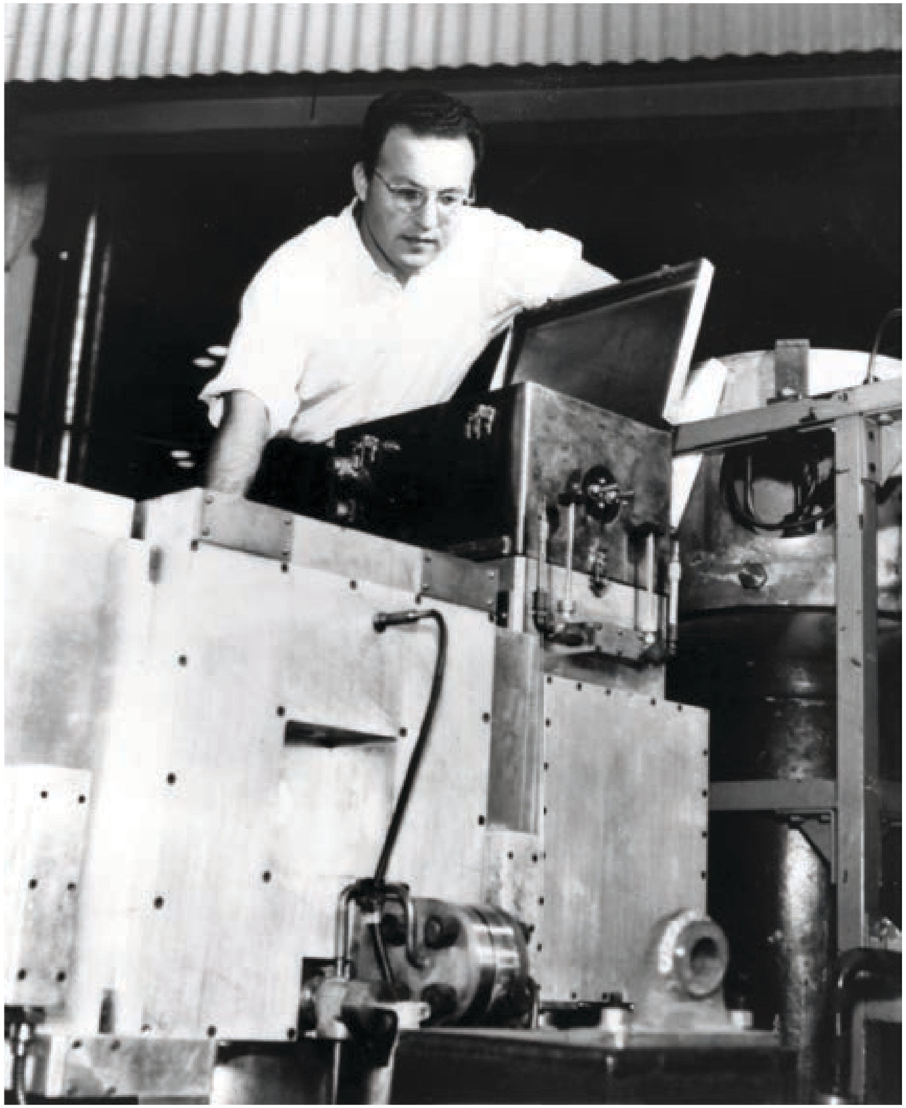

Donald Arthur Glaser (*1926 - † 2013)

- Inventor of bubble chamber 1952
- Nobel prize 1960 (aged 34 years)

Quits particle physics shortly after Nobel prize
and became micro biologies
company start-ups in biotechnology

After selling of companies: neurobiologist

Not covered in these lectures

Further important issues:

Readout electronics

- front-ends
- DAQ

Reconstruction algorithms

- track reconstruction
- shower reconstruction

Trigger

- trigger scheme
- triggerless readout (see DAQ)

……………

Recapitulation

- What is the critical energy
  - energy of an electron at which e-loss through Bremsstrahlung equals e-loss through ionisation
- What is an electromagnetic cascade ?
  - series of alternating processes : bremsstrahlung und pair creation
- How does a hadronic calorimeter work ?
  - Conversion of particle energy to number of loaded particles. Integral measurement of their energy losses yields mass for total energy
- What limits the energy resolution for hcals (intrisically) ?
  - fraction of it's electromagnetic component with large fluctuations and different detection efficiency
- How does a bubble chamber work ?
  - in supersaturated steam: bubble formation at ionisation sites. Stereo flash light image of the bubble distribution in one volume